Orthopädische Klinik und Poliklinik, Universitätsmedizin Rostock

(Direktor: Prof. Dr. med. habil. Wolfram Mittelmeier)

Title:

Gender-Specific Impact of Direct-Coupled Alternating Electric Fields on Human Chondrocytes

Dissertation

to obtain the Academic Degree

“ Doctor medicinae ” (Dr. med.)

at the Medizinische Fakultät, Universität Rostock

submitted by

Zezhong Song

born on 13.12.1989 in Shandong, China

Rostock, June 2024

https://doi.org/10.18453/rosdok_id00005205

Dean: Prof. Dr. med. Emil C. Reisinger

First Reviewer: Prof. Dr. med. Dipl.-Ing. Rainer Bader, Forschungslabor für Biomechanik und Implantattechnologie, Universitätsmedizin Rostock

Second Reviewer: Prof. Dr. rer. nat. Jessica Bertrand, Orthopädische Universitätsklinik mit Endoprothetikzentrum, Universitätsklinik Magdeburg

Third Reviewer: Priv.-Doz. Dr. rer. nat. et med. habil. Kirsten Peters, Center for Medical Research (ZEMFO), Institute of Cell Biology, Universitätsmedizin Rostock

Year of submission: 2024

Year of oral defense: 2025

Table of Content

1 Introduction

1.1 Articular Human Cartilage

1.1.1 Characteristics of Cartilaginous Tissue and Cells

The cartilage within the human body is categorized into elastic, fibro-cartilage, fibro-elastic, and hyaline cartilage, differentiated by the varied composition of their extracellular matrix (ECM) [1, 2]. Hyaline cartilage is particularly noted for its lack of blood vessels, lymphatics, and neural pathways, which results in its inherently limited regenerative abilities [3, 4]. Articular human cartilage, a tissue ranging from 2 to 4 mm in thickness, comprises a dense ECM peppered sparsely with the sole cell type present, the chondrocytes. The matrix-to-cell volume ratio is substantial, as chondrocytes constitute only about 10% of the wet weight of articular cartilage [5, 6]. This type of cartilage is essential for the smooth functioning of joints, offering a slick, well-lubricated surface that minimizes friction and cushions the joints against external forces during movement [7].

Articular cartilage is composed of two primary components: a fluid phase, made up of water and electrolytes, and a solid phase, consisting of collagen fibrils, chondrocytes, proteoglycans, and various glycoproteins [8]. The fluid phase constitutes 60-80% of the cartilage's total wet weight, while the solid phase makes up the remaining 20-40%. Within the solid phase, collagen fibers account for roughly 50-75%, chondrocytes for less than 5-10%, and the balance is formed by proteoglycans and other glycoproteins [2, 9]. Each chondrocyte, along with its adjacent pericellular matrix, is often regarded as a singular entity termed a chondron [10] (Figure 1). Despite its seemingly simple composition, cartilage displays significant heterogeneity in the orientation of its collagen fibrils and in the variation and arrangement of its cells (Figure 1). For example, electron microscopy shows that the different orientations of collagen fibrils define four distinct layers within the cartilage: the superficial, transitional, deep, and calcified zones [11]. Each layer displays unique matrix compositions and exhibits distinct cellular, metabolic, and mechanical properties [12-17]. The intricate architecture of articular cartilage is depicted in Figure 1.

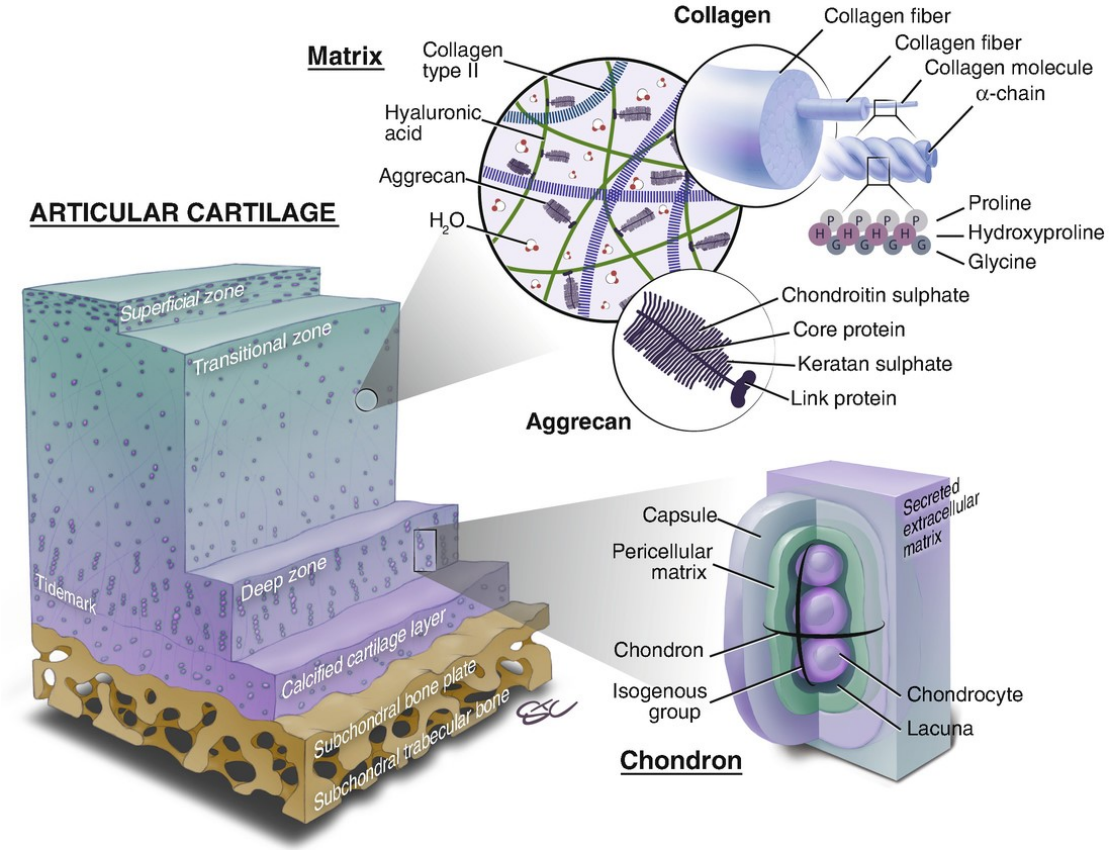

Figure 1. Structure of human articular cartilage and the components of extracellular matrix and chondron according to C.A. Baumann et al (https://link.springer.com/chapter/10.1007/978-3-030-01491-9_1). Articular cartilage consists of extracellular matrix and chondrocytes. The ECM primarily comprises water, collagen, and proteoglycans, with trace amounts of other proteins, glycoproteins, and lipids. Including the extracellular matrix surrounding the chondrocytes, it is referred to as the chondron. Articular cartilage exhibits low chondrocyte cellularity, with chondrocytes encapsulated within a dense matrix.

1.1.2 Characteristics and Phenotypes of Human Chondrocytes

By the fifth week of gestation, a cluster of mesenchymal cells converges to form a blastema. These blastema cells transform into chondroblasts, which actively secrete the ECM that eventually surrounds them [2]. These chondrocytes are sparsely distributed throughout the matrix. Each chondrocyte is surrounded by a thin layer of ECM known as the pericellular matrix (PCM), a crucial interface that enables communication between the chondrocyte and its external surroundings [13]. Chondrocytes, which are isolated and lack direct interactions with other cells, obtain their nutrients from capillaries located in the synovium. These nutrients diffuse into the synovial fluid and then move through a dual diffusion barrier to penetrate the cartilage matrix. Chondrocytes regulate the synthesis and proteolytic breakdown of ECM

components, maintaining a precise balance between the creation of collagen fibers, proteoglycan aggregates, and the enzymes that degrade these structures [18-20]. Despite their high individual metabolic activity, the overall metabolic activity of chondrocytes remains relatively low due to their low density [21]. In response to this limitation,, chondrocytes have adapted to thrive in hypoxic conditions, relying on anaerobic metabolism to sustain their vital functions [2, 22]. Based on the type of collagen they produce, chondrocytes have been classified into distinct phenotypes [23]. Prechondrogenic mesenchymal cells predominantly express collagens 1, 3, and 5 [24], while differentiated chondroprogenitor cells exhibit a higher expression of the alternative splice variant of collagen 2, type 2A procollagen [25] . Mature or activated chondrocytes synthesize collagens 2, 9 and 11 with collagen 2 constituting the majority of the matrix, forming heteropolymers with collagen 9 and collagen 11 (approximately 1% collagen 9, 3% collagen 11, and over 90% collagen 2) [26]. Hypertrophic chondrocytes, located in the calcified layer of articular cartilage and the terminal differentiation stage of the growth plate, are characterized by their expression of collagen 10. In vitro studies have revealed the existence of post-hypertrophic or transdifferentiated chondrocytes, which exhibit the simultaneous secretion of collagen 1 and collagen 10 [27, 28]. Finally, another chondrocyte phenotype, identified in vitro, manifests as a fibroblast-like cell secreting collagen 1 and collagen 3, named the de-differentiated chondrocyte [29].

1.2 Cartilage Lesions

Both direct trauma, such as intraarticular fracture, or indirect trauma, such as joint instability following ligament injury, can lead to articular cartilage lesions [30-32]. Cartilage lesions will result in compromised joint function, pain, and ultimately osteoarthritis [33].

1.2.1 Classification of cartilage lesions

According to the depth of the lesion, articular cartilage defects can be generally divided into two categories, partial and full-thickness defects. Partial-thickness defects are limited to the cartilage; while full thickness cartilage defects extend to the subchondral bone [34, 35]. The detailed classification of the lesions that occur in the injured articular cartilage is essential in the procedures of understanding and describing what happens to the articular cartilage, what the prognosis is as well as how it should be treated [36]. Outerbridge's classification system and International Cartilage Repair Society (ICRS) cartilage lesion classification system are the most widely used systems. Based on direct visualization of the joint, either under arthroscope or open, the Outerbridge classification system assigns a grade of 0 through IV to the chondral area of interest [37] (Table 1). The ICRS classification system characterizes cartilage injury on the

basis of lesion area and depth [38] (Table 2).

Table 1. Outerbridge classification system. In 1961, the Outerbridge classification system was initially devised by R.E. Outerbridge [37]. Based on direct visualization of the joint, this system assigns a grade of 0 through IV to the chondral area of interest. Grade 0 signifies normal cartilage. Grade I chondral lesions are characterized by softening and swelling. A Grade II lesion describes a partial-thickness defect with fissures not exceeding 0.5 inches in diameter or reaching the subchondral bone. Grade III involves fissuring of the cartilage with a diameter greater than 0.5 inches, extending to the subchondral bone. The most severe, Grade IV, includes erosion of the articular cartilage, exposing the subchondral bone.

Grade	Description	Size of defect
0	Normal cartilage	
I	Softening and swelling	
II	Fragmentation and fissuring	< 1/2 inch
III	Fragmentation and fissuring	> 1/2 inch
IV	Erosion down to subchondral bone	

Table 2. International Cartilage Repair Society (ICRS) cartilage lesion classification system [38] is an enhanced version of the Outerbridge classification, recommended by the International Cartilage Repair Society for clinical assessment of tissue condition. It ranges from healthy cartilage (ICRS grade 0) to complete absence of cartilage with exposed subchondral bone (ICRS grade 4). Each grade in the ICRS score is further detailed based on the area and depth of the injury, providing a more precise classification.

Grade	Description	Grade Subgroup
0	Normal cartilage	
1	Cartilage with intact surface but fibrillation and/or softening is present	Grade1A—fibrillation and/or slight softening is present Grade1B—additional superficial lacerations and fissures
2	Defects that extend deeper but involve <50% of the cartilage thickness	
3	Lesions that extend through >50% of the cartilage thickness	Grade3A—defect > 50% but not down to the calcified layer Grade3B—defects down to the calcified layer Grade3C—defects down to but not through the subchondral bone plate Grade3D—defects with blisters
4	Full-thickness osteochondral injuries	Grade4A—defect included the superficial subchondral bone plate Grade4B—defect down to deep subchondral bone

1.2.2 Therapeutic Approaches

Treatment of articular cartilage lesions has always been a focus in the field of orthopedics [32, 39, 40]. The therapeutic approaches include biologic therapies and surgical therapies.

Biological Therapies

1) **Platelet-Rich-Plasma (PRP)**: PRP is obtained by centrifuging autologous blood to produce a higher concentration of platelets than average. Variety of growth factors, coagulation factors, adhesion molecules, cytokines, chemokines and integrins are stored in platelets [41, 42]. Multiple studies have reported positive effects of PRP for improvement in pain and function in patients with cartilage lesions [43-45].
2) **Mesenchymal stem cells (MSCs)**: MSCs can differentiate into cells of chondrogenic lineage, produce proteins conducive to cartilage regeneration. Meanwhile, the anti-inflammatory effects of MSC has been reported [46, 47].
3) **Bone marrow aspirate concentrate (BMAC)**: BMAC is most commonly harvested from iliac or tibial bone marrow and unprocessed BMA has been used as a source of bone marrow-derived MSCs [48]. Moreover, BMAC also contains multiple growth factors [49]. Positive results with functional improvement has been reported after injection of BMAC [50].

Surgical Therapies

1) **Debridement:** Debridement involves removing loose fragments such as unstable chondral flaps and osteophytes, superfluous synovia, degenerated menisci, and torn ligaments [51]. The aim of this method is to mitigate mechanical symptoms and irritation as well as to prevent the spread of the cartilage lesion resulting from any mechanical strain on the unstable flap [52].
2) **Microfracture:** The procedure of microfracture consists of debridement of the injured or degraded cartilage for the exposure of the subchondral bone, and drilling V-shape microfractures to the vascularized subchondral area. The bleeding due to piercing leads to the formation of clot with multipotent stem cells, platelets, and growth factors and hence mediating the fibrocartilage-based repair tissue formation [53].
3) **Osteochondral Autogenic Transplant:** This therapeutic approach involves procuring an osteochondral plug from a non-weight-bearing region of the knee, usually the peripheral aspect of the medial or lateral trochlea or intercondylar notch, and subsequently relocating it to a weight-bearing chondral lesion [54]. The plug provides a hyaline cartilage surface supported by underlying subchondral

bone, facilitating the healing process [52].

4) **Osteochondral Allogenic Transplant:** This approach involves debriding the cartilage lesion and subchondral bone until reaching a stable, healthy rim and then establish a press-fit fixation of the allograft with specialized instrumentation [55].

5) **Autologous Chondrocyte Implantation (ACI) / Matrix-Induced Autologous Chondrocyte Implantation (MACI):** ACI was first utilized in human patients in 1987, with the initial pilot study emerging in 1994 [38]. By 2010, ACI had been administered to over 35,000 patients globally [56]. ACI/MACI showed favorable postoperative outcomes for cartilage lesions [57], attracting growing attention [58-60].

1.3 Autologous Chondrocyte Implantation (ACI) / Matrix-Induced Autologous Chondrocyte Implantation (MACI)

1.3.1 Evolution of ACI / MACI

Autologous Chondrocyte Implantation (ACI) involves three steps: harvesting chondrocytes from a non-weight-bearing cartilage region, cultivating and proliferating them in vitro, followed by the surgical implantation of these cells (Figure 2). The first generation of ACI involved implanting monolayer expanded chondrocytes under a periosteal patch which is secured with resorbable sutures. Complications associated with the periosteum were reported [61]. Second and third generations of ACI were introduced since the 1980s. Periosteum was replaced by membrane composed of collagen 1 and collagen 3, which resulted in a better quality of tissue repair [62, 63]. The latest advancement, the third generation ACI, known as Matrix-induced ACI, involves embedding the expanded chondrocytes within a biodegradable and hydrated matrix to promote cell growth and maturation [58]. Clinical outcomes have shown marked enhancements with Matrix-Induced Autologous Chondrocyte Implantation (MACI), significantly reducing the failure rate from 33% to 10.7% [64-66].

1.3.2 Challenge in ACI / MACI

A critical challenge of ACI is obtaining enough chondrocytes, since these cells are harvested from only a small biopsy of the patient's own cartilage. In vitro expansion is crucial to meet the demand for large numbers of chondrocytes required for effective cartilage repair. Currently, the predominant commercial method for chondrocyte expansion employs a monolayer 2D culture system, efficiently generating a substantial count of viable cells. Companies specializing in ACI provide patients with between 4 to 12 million viable cells for the implantation process. However, this method of in vitro expansion often leads to the formation of fibrocartilage with inferior mechanical properties [67]. Recently, ACI research has pivoted towards enhancing the

chondrocyte phenotype by transitioning the cells to a 3D matrix supplemented with biomolecules designed to increase the chances of hyaline cartilage formation [68]. Current biomolecule cocktails include L-ascorbic acid-2-phosphate, dexamethasone, transforming growth factor 3 (TGF-3), and insulin transferrin-selenium (ITS) [67]. Nevertheless, this procedure still produces inconsistent results, accompanies with the formation of fibrous, fibrous-hyaline, and hyaline cartilage. This inconsistency arises from chondrocyte de-differentiation, which diminishes their ability to regenerate hyaline articular cartilage when expanded in vitro [29].

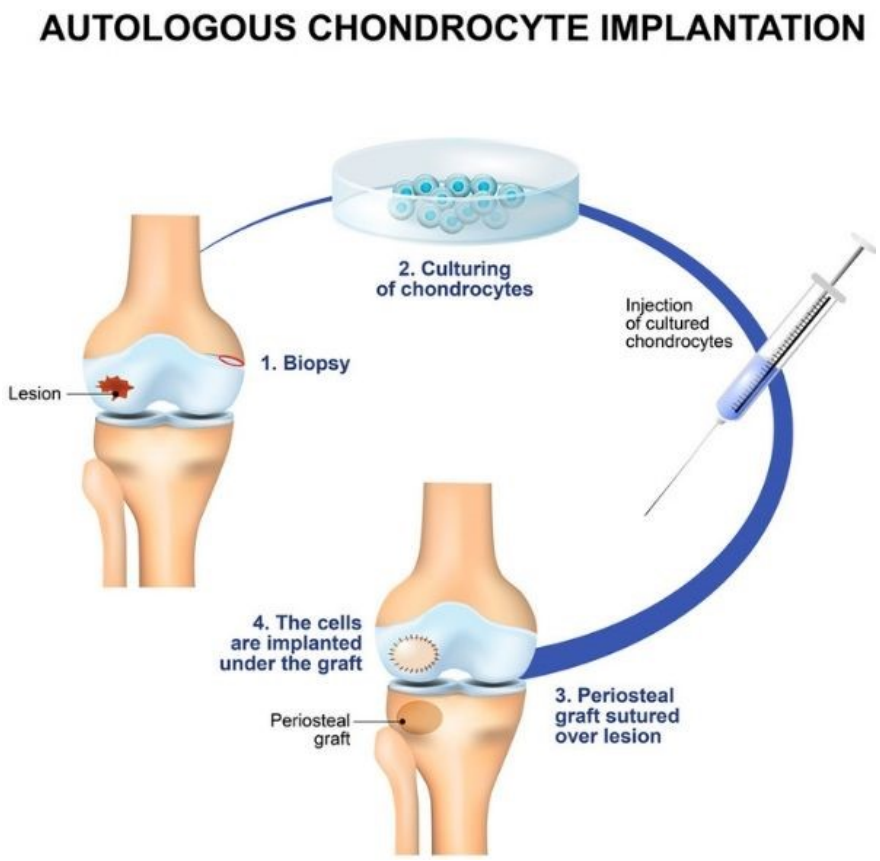

Figure 2. The three steps of autologous chondrocyte implantation: chondrocytes are harveste d from non-weight-bearing cartilage regions, cultured and expanded in vitro, and then surgical ly implanted into damaged cartilage (Figure link: https://caringmedical.com/prolotherapy-news /knee-articular-cartilage-repair-without-surgery/).

1.4 De-differentiation of Chondrocytes

1.4.1 Shift in Chondrocyte Phenotype

In the 1960s, significant morphological transformations were identified in chondrocytes extracted from their matrix and cultured in vitro in a monolayer [69]. Observations made using bright field microscopy showed that the typically rounded chondrocytes adopted a more flattened, elongated shape, resembling fibroblasts [70]. This change was later

termed "de-differentiation". De-differentiation in chondrocytes is defined by a shift from the chondrogenic phenotype to a fibroblast-like cell phenotype [70, 71], involving a morphological transition from a rounded, cobblestone appearance to an elongated, slender fibroblastic morphology [72]. This morphological shift in de-differentiated chondrocytes is accompanied by a significant alteration in their protein synthesis profile, described as biphasic, involving the upregulation and downregulation of specific genes [73]. Over the years, researchers have endeavored to track the genes and proteins associated with this de-differentiation process [74-77]. One potential reason for this phenotypic transition is that the monolayer culture environment in vitro lacks the 3D structure and properties of native articular cartilage, presenting a notably different environment [78]. Furthermore, it has been noted that chondrocytes within their PCM exhibit considerably higher levels of SOX9, collagen 2, aggrecan, COMP, and collagen 10, and lower levels of RUNX2 compared to chondrocytes that have lost their PCM and adhere to the tissue culture plastic surface [79]. These findings underscore the adaptation that human chondrocytes undergo to adhere to tissue culture plastic, and the crucial role of PCM's geometric constraints in preserving the chondrocyte phenotype. The adherence of chondrocytes to the culturing surface following the loss of the PCM highlights de-differentiation as an adaptive response to a new environmental [79].

1.4.2 Collagen Imbalance

The structural integrity and physicochemical characteristics of articular cartilage are largely attributable to its collagen fibrils, which are mainly composed of collagen 2, alongside lesser quantities of other collagen types [26, 80]. Research from the mid-1970s indicated a significant shift in collagen synthesis during the monolayer culture of human articular or septal chondrocytes. Instead of producing collagen 2, these cells began synthesizing collagen 1 and collagen 3 [70, 81, 82], transitioning towards a fibroblastic-like phenotype. This change was particularly noted in rabbit articular chondrocytes, which exhibited a de-differentiated phenotype, characterized by a composition of 41% collagen 1, 25% X2Y, 20% type I trimer, 13% collagen 3, and only 1% of collagen 2 [82]. These initial observations have been reinforced by numerous subsequent studies, including those focused on differential gene expression [71, 75]. In line with these findings, the Col2/Col1 ratio has been suggested as a definitive marker of the de-differentiation process [83, 84]. Remarkably, this ratio was found to decrease from 15-fold to over 1800-fold after just 10 days in a monolayer culture environment [83, 84]. This phenomenon poses a significant challenge in the context of ACI, where the implantation of de-differentiated chondrocytes typically results in the formation of fibrocartilage [85]. This fibrocartilage, possessing inferior mechanical properties compared to hyaline cartilage, often leads to unsuccessful cartilage repair

endeavors.

1.4.3 Chondrocyte De-differentiation and Osteoarthritis

Chondrocyte phenotypic changes play a crucial role in the disruption of homeostasis within osteoarthritic cartilage [23]. A hallmark of osteoarthritis (OA) is the hypertrophy of chondrocytes, a process significantly contributing to the progression of the disease. In OA-afflicted cartilage, markers indicative of hypertrophic chondrocytes, such as collagen 10, MMP-13, osteocalcin, and alkaline phosphatase, are notably elevated. These markers are closely associated with the calcification and degradation of the matrix as well as chondrocyte de-differentiation [86]. Furthermore, there is a similarity in gene expression patterns observed between the de-differentiation of chondrocytes and experimental models of OA [87]. It has been reported that the upregulation of markers associated with de-differentiated chondrocytes is potentially linked to the fibrosis or aging processes inherent in OA cartilage [88]. Moreover, it was reported that certain harmful substances related to OA can accelerate the process of de-differentiation [11]. Significantly, the in vitro-induced transition of chondrocytes to a de-differentiated fibroblast phenotype has also been observed to occur naturally within OA cartilage [11]. This underscores the interplay between chondrocyte de-differentiation and the pathophysiological development of OA [11, 23, 77].

1.4.4 Strategies to Mitigate De-differentiation of Cultured Chondrocytes

Extensive researches have focused on countering the de-differentiation of chondrocytes in vitro cultures. Strategies such as high-density cell seeding [89], limiting the number of cell passages [90], and cultivating cells in a low-oxygen environment [91] have been reported effective in decelerating chondrocyte de-differentiation. Maintaining a low-temperature environment, specifically at 32.2°C, has been found to significantly slow the de-differentiation of chondrocytes in monolayer cultures [92]. Additionally, employing specific substrates like collagen 2, poly(L-lactic acid), and polyamide amine dendritic polymers, as well as certain chemicals including insulin, ferritin selenium, and FGF-2, have demonstrated efficacy in keeping chondrocyte from de-differentiation [90, 93-95]. Furthermore, coating the culture surface with collagen 1 and aggrecan was observed to reverse de-differentiation alterations in the gene expression of chondrocytes [96].

1.4.5 Approaches to Induce Re-differentiation of Human Chondrocytes

1) **3D Cultures with Scaffolds**: 3D cultures are gaining attention as they offer a more realistic extracellular environment compared to 2D cultures [97]. Chondrocytes in 3D cultures have been observed to regain their spherical shape and re-express cartilage-specific markers [98].

2) **Growth Factors**: Factors such as Fibroblast Growth Factor 2 (FGF-2), Epidermal Growth Factor (EGF), Transforming Growth Factor Beta (TGF-β), and Platelet-Derived Growth Factor BB (PDGF-BB) are known to support the re-differentiation process. These factors play a crucial role in cell proliferation, ECM synthesis, phenotype maintenance, and cartilage formation [99-102]. Extensive studies have examined various combinations of factors to identify the most effective duo for reversing chondrocyte de-differentiation, with BMP-2 and insulin emerging as a particularly potent combination [103].
3) **Platelet Derivatives**: Products like platelet-rich-plasma, hyperacute serum (HAS), platelet lysate (PL), and low-molecular-weight fractions of human serum albumin have been employed to counteract the de-differentiation of chondrocytes caused by in vitro expansion [104, 105].
4) **Mechanical Stimulation**: Mechanical stimulation has been reported effective in encouraging the re-differentiation of chondrocytes [106-108].
5) **Co-Culture with Stem Cells**: Hiemer et al. [7] highlighted the induction effects of MSC co-culture on chondrocyte re-differentiation in vitro. At the same time, culturing chondrocytes alongside sphincter-derived stem cells has also been found to enhance chondrocyte re-differentiation [109].
6) **Electrical Stimulation**: Recent studies exploring the impact of electrical stimulation on cartilage tissue and chondrocytes have uncovered several beneficial effects. These include an increase in chondrocyte proliferation, enhanced formation of the ECM, and a reduction in matrix degradation [110, 111]. Such findings highlight the potential of electrical stimulation as a therapeutic strategy, particularly in the context of ACI, where it could facilitate the re-differentiation of chondrocytes during their expansion phase [7, 110, 112, 113].

The strategies to mitigate chondrocyte de-differentiation and to promote re-differentiation are comprehensively summarized in Figure 3.

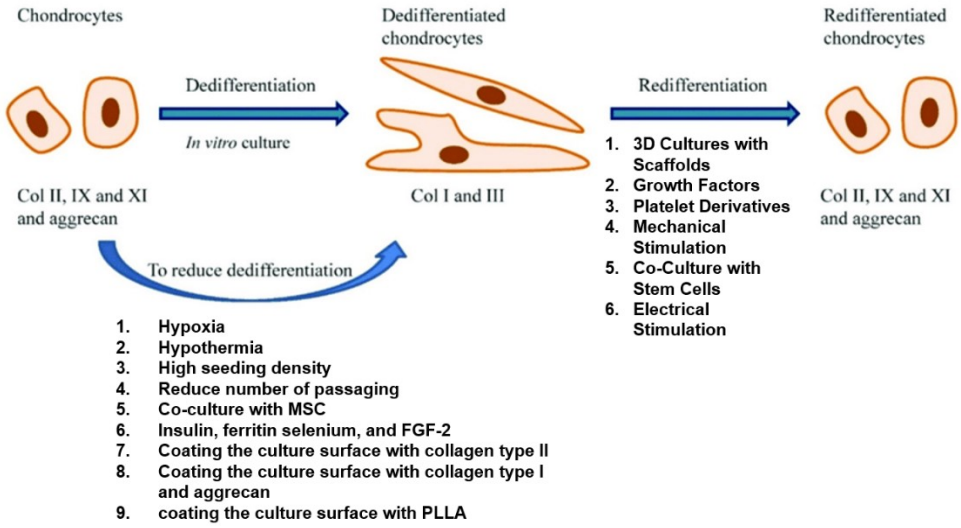

Figure 3. Approaches to reduce de-differentiation and induce re-differentiation of chondrocyte in vitro. The original figure was created by L. Liau et al. (https://www.researchgate.net/figure/Factors-that-affect-chondrocyte-dedifferentiation-and-redifferentiation-in-vitro_fig2_348847638). Modifications were made in the approaches to mitigate de-differentiation and promote re-differentiation in the figure.

1.5 Endogenous Electric Field in Articular Cartilage

The structural and functional attributes of hyaline cartilage are largely determined by its extracellular matrix, chiefly composed of collagen and proteoglycans. The ECM, together with chondrocytes which are responsible for its formation, exhibits unique characteristics across the different layers of hyaline cartilage. In the superficial layer of the cartilage, there is a dense arrangement of collagen fibers oriented parallel to the articular surface, with this region having relatively low proteoglycan content and low fluid permeability. Under compression, this collagen network demonstrates increased resistance to fluid flow [114, 115]. The intermediate or transitional zone features larger, radially arranged collagen fibers [116, 117]. The proteoglycan content in this zone rises from 10% to 25% (dry weight basis), leading to high swelling pressures and increased water content [118]. In the deepest layer, closest to the calcified cartilage and subchondral bone interface, the collagen fibers are larger and form bundles that are perpendicular to the calcified/bone interface [119]. Here, the proteoglycan content decreases, but the aggregates are larger and more saturated with aggrecan than in the superficial or intermediate zones [120]. When an external load is applied to the joint, the cartilage deforms to increase contact areas and enhance joint compatibility [121]. This results in various stresses – tensile, shear, and compressive – within the cartilage, with a spatial variation across the joint and through the cartilage thickness [122]. The response of articular cartilage to these stresses is influenced by its

specialized composition and structural organization, exhibiting viscoelastic properties. This includes shear stresses from interstitial fluid flow through a porous and permeable matrix, and deformation of solid macromolecules over time. The inherent electrical properties of articular cartilage, combined with the electrolytes present in the interstitial fluid, result in cartilage displaying intricate electrochemical characteristics alongside its mechanical reactions [123]. The electrochemical behavior results from the movement of unbound cations (like Na+, Ca2+) against fixed negative charges in the proteoglycans, leading to phenomena such as streaming and diffusion potentials, and charge-dependent osmotic swelling pressures. These electrochemical properties generate external electric signals, which are then translated into intracellular signals [123]. Meanwhile, the signal transduction mechanism is amplified by inherent heterogeneity of cartilage [124].

Empirical research has proved that fluid flow within tissues can generate electrical potentials and these electric fields are integral to numerous physiological processes such as embryogenesis, wound healing, tissue repair and remodeling, as well as the general growth of organisms [125-127]. Disturbances in these endogenous electric fields can lead to various abnormalities [128], which indicates that electrical signals are essential in conveying information to chondrocytes [129, 130].

1.6 Exogenous Electrical Stimulation for Articular Cartilage

The use of exogenous electrical stimulation in cartilage repair and regeneration has been an area of interest since 1974, when Baker et al. [131] successfully utilized direct current (DC) generated by a bimetallic platinum electrochemical device to enhance the recovery of full-thickness articular cartilage injuries in experimental animals, noting a 71% increase in ECM production. This pioneering study set the stage for further research into the effects of electrical and electromagnetic stimuli on various cellular activities. Subsequent studies have demonstrated that electric fields (EFs) and electromagnetic fields (EMFs) can significantly influence cell migration [111, 132], differentiation [111, 133, 134], morphology [10, 111, 135-137], proliferation [111, 138-140], and gene expression in chondrocytes [111, 141-150]. These studies have explored a range of electrical stimulation modalities [151], including:

1) **Direct Current Electrical Stimulation (DCES)**: Involves the application of a constant, unidirectional electric current.
2) **Pulsed Electrical Stimulation (PES)**: Utilizes intermittent bursts of electrical current.
3) **Alternating Current Electrical Stimulation (ACES)**: Utilizes a current that changes direction periodically.
4) **Oscillating Magnetic Flux-Induced Electrical Stimulation**: Involves the use of

fluctuating magnetic fields to induce electrical currents.

The method of applying the electric field can vary, including direct coupling, capacitive coupling, semi-capacitive coupling, and inductive coupling [151] (Figure 4). Among these, capacitive coupling and direct coupling are the most commonly used methods in cell experiments in vitro.

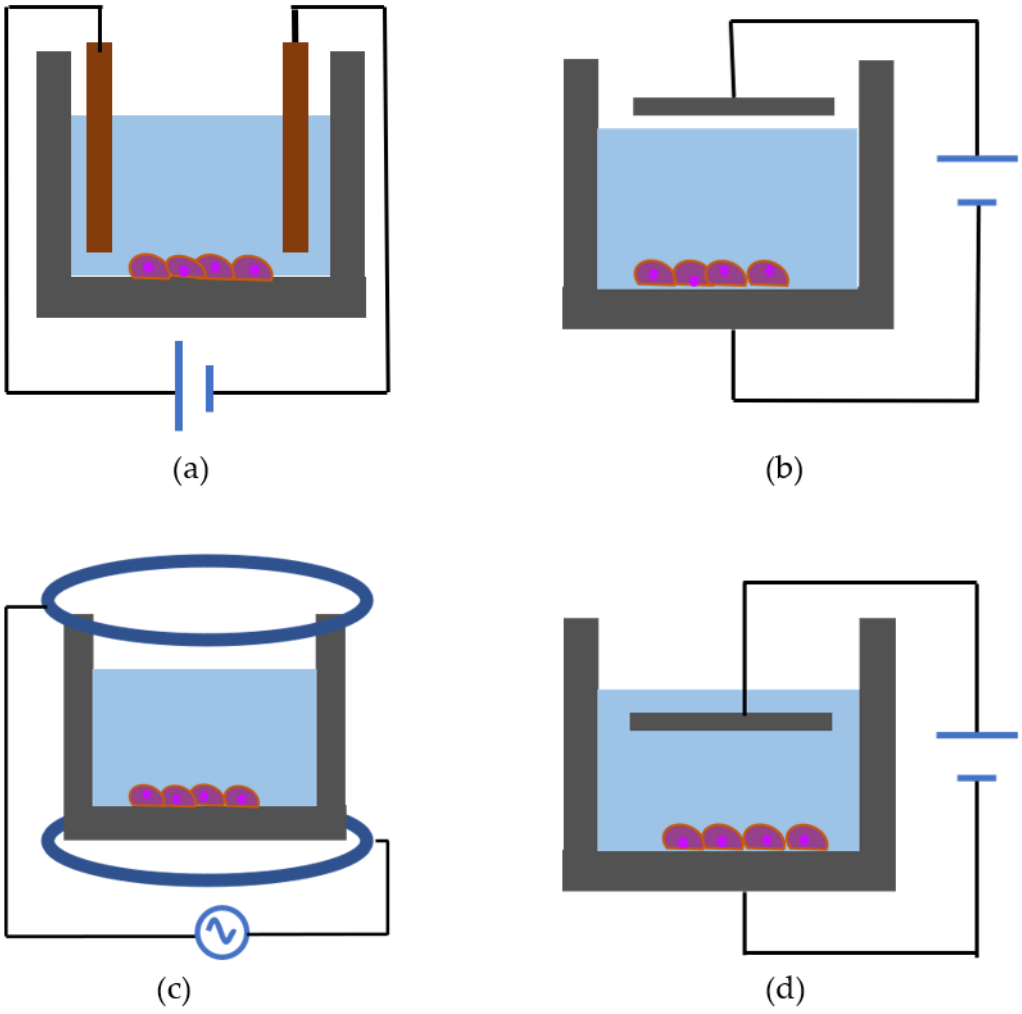

Figure 4. Schematic representation showing approaches for electric field application in in vitro. (a) Direct coupling: two parallel electrodes immersed into the culture medium and connected to power source; (b) Capacitive coupling: two metallic/conducting plates placed above and below the cell culture dishes without contact with the culture medium; (c) Inductive coupling uses Helmholtz coils to create electric fields from oscillating electromagnetic fields generated by alternating current (AC); (d) Semi-capacitive coupling: one of the plates (usually the top plate) is immersed into the culture medium while the other without contact with the medium.

1.6.1 Constant Direct Current

Korpan et al. [152] reported an increase of collagen in the cartilage after exposure to a direct current (DC) intensity of 0.2 mA/cm^2. Okihana et al. [153] reported that constant DC increased syntheses of both proteoglycans and DNA when l μA calculated current density of l μA/cm^2 was applied for three days on cartilage cells. Conversely, Akanji et al. [147]. reported that chondrocyte constructs embedded in 4% ultra-low gelling agarose and exposed to current densities of 2, 4, and 24 mA/cm² for 12 hours showed no significant differences in protein synthesis, cell proliferation, or mRNA expression levels.

1.6.2 Pulsed Direct Current

Baker et al. [154] applied voltages ranging from 15 to 500 mV using a direct current (DC) battery-operated device to treat full-thickness defects in rat articular cartilage. This study, which reported successful hyaline cartilage repair, laid the groundwork for using electrical therapy in joint pathologies and inspired further research into in vivo electrical stimulations. Subsequent studies have primarily focused on pulsed DC for electrical stimulation. Farr et al. [154] used a transcutaneous electric stimulator on 288 patients with OA, generating 0-12 V at 1 Hz electric fields for periods ranging from 16 to over 600 days. This treatment resulted in pain relief and reduced anti-inflammatory drug usage. Similarly, Lipiello et al. [155] applied a pulsed DC field to osteochondral defects in rabbit knees, observing an increase in cartilaginous healing. The applied electric fields in the tissue were between 20-60 mV/cm² with a peak current of 2 μA at 100 Hz. Another study by Ciombor et al. [136] reported that pulsing DC applied to osteoarthritic cartilage in guinea pigs suppressed the synthesis of matrix-degrading enzymes.

In vitro applications of pulsed DC have also been explored. Capacitive coupling, involving external parallel electrodes connected to a power supply, is a common method for delivering DC-generated electric fields to cell cultures [156, 157]. Another study by Nakasuji et al. [158] observed increased cell proliferation and proteoglycan synthesis in chondrocytes exposed to pulsed electric fields of 5 and 25 V/m.

1.6.3 Alternating Current (AC)

Capacitive coupling

In this setup, two electrodes are placed parallel to each other without contact with the medium (Figure .4b). One significant advantage of this method is the avoidance of direct electrode-electrolyte contact, thereby preventing electrochemical effects that might alter the cell environment (e.g., pH, temperature, metal ion dissolution) [151]. Capacitive coupling is an effective method for applying AC to monolayer chondrocytes,

cartilage explants, and 3D cartilage constructs [110, 113, 139, 156, 159].

Brighton et al. [159] conducted a study using a 60 kHz sine wave capacitive coupled signal of various voltages (10, 100, 250, and 1,000 V peak-to-peak) to stimulate bovine knee articular cartilage for 24 hours. The results indicated that 10 V and 1000 V reduced cell proliferation and 250 V enhanced GAG synthesis. Other studies subjected chondrocytes to electric fields of multiple amplitudes (1.5, 2.25, 3, and 4.5 V/m) at 60 kHz, observing an increase in cell population at 1.5 and 3.0 V/m electric fields and a 66% increase in GAG synthesis at 4.5 V/m electric field [139, 156]. Subsequent research by Brighton et al. [140] found that an electric field of 2 V/m at 60 kHz increased cell proliferation by 47%. Wang et al. [113] applied a similar 60 kHz sine wave signal to bovine cartilage, producing an electric field of 2 V/m, and reported increased levels of collagen 2 and aggrecan synthesis. Capacitive coupled electric signals have also been used to stimulate cartilage explants and 3D constructs. Szasz et al. [146] stimulated calf femoral condyle cartilage chondrocytes seeded in agarose gels as a 3D construct and observed significant increases in collagen and GAG synthesis following electrical stimulation in the 10 Hz to 10 kHz range. Brighton et al. [112] applied a 60 kHz, 2 V/m electric field to bovine full-thickness articular cartilage explants, noting upregulation in total proteoglycan and collagen production, as well as matrix gene expression. Brighton et al. [110] used the same parameters to stimulate human osteoarthritic cartilage explants, resulting in upregulation of cartilage matrix protein expression and production, and concurrently inhibited the stimulatory effect of IL-1b on metalloproteinase expression. Vaca-González et al [157] reported that electric fields of 0.4 V/m applied for 30 minutes promoted chondrocyte proliferation, while electric fields of 0.8 V/m applied for five hours maintained stable GAG synthesis. Krueger et al. [160] reported a frequency dependent trend for downregulation of collagen 1 following stimulation at 0.3 – 2.5 V/m and 0.004–0.040V/m. Subsequent study by Krueger et al. [161] used small electric field strengths of 5.2×10^{-6} V/m 5.2×10^{-5} V/m for stimulation, observing reduction of metabolic activity after electrical stimulation and increased synthesis rates of collagen 2, glycosaminoglycans (GAG), and collagen 1 protein following stimulation.

Direct coupling

Direct coupling is a method where electrodes are inserted directly into the culture medium to deliver electrical stimulation (Figure 4a). This approach is favored for its simplicity and ease of operation. Unlike capacitive coupling, direct coupling doesn't require high energy input to achieve the desired electric field strength. However, it has certain drawbacks, such as potential biocompatibility issues with the electrodes, pH changes in the medium, and the formation of hydrogen peroxide and reactive oxygen

species, which are harmful to exposed cells [162].

Dauben et al. [163] designed an in vitro direct coupling system using AC for electrical stimulation. By switching from DC to AC, harmful electrochemical reactions can be reduced [163]. Initially, this system was used to apply a 20 Hz AC signal to human osteoblasts. The results indicated a substantial increase in osteocalcin mRNA synthesis rate following stimulation with 1.4 V_{RMS}. Additionally, an increase in collagen 1 synthesis was observed when stimulated with 0.2 V_{RMS}, but this effect decreased with stimulation at 1.4 V_{RMS} [163]. Further experiments by Hiemer et al. [7] involved stimulating human chondrocytes using this system. Human chondrocytes and bone marrow-derived mesenchymal stem cells (BM-MSCs) were seeded onto a collagen-based scaffold either separately or as a co-culture. After three days of incubation with growth factors, the cells were exposed to 20-25 V/m electric field for more than seven days under both hypoxic and normoxic culture conditions. Under hypoxic conditions, there was an increased expression and synthesis of collagen 2 and aggrecan in human chondrocytes. A similar but less pronounced effect was observed in BM-MSCs and the co-culture of chondrocytes and BM-MSCs. Various studies of using alternating current electric field for in vitro chondrocyte stimulation are illustrated in Table 3.

Table 3. Alternating electric fields for chondrocyte stimulation in vitro.

Frequency	Voltage	Field strength	Stimulation time	Effect on cell viability, proliferation and Matrix synthesis	Reference
60 kHz	(5-13, 5-33,7-85) V_{RMS}	0.7, 2, 5, 12.6 V/m	24h	Increase in proliferation under an electric field of 2 V/m	Brighton et al. [140]
60 kHz	13, 5 V_{RMS}	2 V/m	24h	The cycles in an output signal (100%, 25%, 2%, and 0.25%) are no relevant parameters, hence changes in cell proliferation and matrix synthesis were not found.	Brighton et al. [140]
60 kHz	10,100, 250, and 1000 V_{RMS}	_	24h	voltages of 10 and 1000V decreased cell proliferation while voltage of 250V increased the GAG synthesis.	Brighton et al. [159]

60 kHz	500 V_{RMS}	_	48h	An increased production of cAMP was observed after 2.5 and 5.0min of signal application	Brighton et al. [139]
60 kHz	10, 100, 250, 500, 750, 1,000, and 1,500 V_{RMS}	1.5, 2.25, 3, and 4.5 V/m	24h	An increase in cell population was observed when exposed to electric fields of 1.5, 2.25, and 3V/m. An increase in GAGs synthesis (66%) was obtained after stimulation with electric field of 4.5 V/m.	Armstrong et a. [156]
60 kHz	_	2 V/m	6h	Increased levels of collagen 2 and aggrecan with an electric field of 2 V/m during 30 minutes	Wang et al. [113]
60 kHz	_	2.V/m	1 hour and 30 minutes each for 6 hours	Significant up-regulation of total proteoglycan and collagen production as well as matrix gene expression	Brighton et al. [164]
60 kHz	_	2 V/m	14days	1.4- and 1.5-fold increase in PG and collagen 2, respectively	Brighton et al. [110]
60 kHz	50 V_{RMS} 100 V_{RMS}	0.4 and 0.8 V/m	30 minutes, 1 and 5 hours during 1 week	Increase of proliferation with an electric field of 4 V/m	Vaca-González et al. [157]
10 Hz-10 kHz	–	–	–	Increased collagen and GAG synthesis	Szasz et al. [146]
1 kHz	0.1 V_{RMS} 1 V_{RMS}	5.2×10^{-6} V/m 5.2×10^{-5} V/m	45 minutes each time, 3 times each day for 7 days	Reduction of metabolic activity after electrical stimulation and increased synthesis rates of collagen 2, glycosaminoglycans (GAG), and collagen 1 protein following stimulation with 0.1Vrms was observed.	Krueger et al. [161]

1 kHz	0.7 V_{RMS}	20-35 V/m	45 minutes each time, 3 times each day for 7 days	No cell viability changes after stimulation. Increased synthesis of collagen 2 and aggrecan in human chondrocytes and the co-culture of chondrocytes and BM-MSCs was observed under hypoxic culture conditions were observed	Bettina et al. [7]
1 kHz and 60 kHz	5 V_{RMS} 10 V_{RMS} 20 V_{RMS} 30 V_{RMS}	0.3 – 2.5 V/m 0.004– 0.040V/m	45 minutes each time, 3 times each day for 7 days	No metabolic activity difference was observed after stimulation while a frequency dependent trend for downregulation of collagen 1 was noticed.	Krueger et al. [160]

1.7 Electric Field Strength

To date, the absence of a universally accepted standard for comparison and description of electric fields remains a limitation in related research. Factors like current density and electrode material were recommended for comparison [165]. Simultaneously, there is a push for using measured current and voltage in electrical stimulation experiments to estimate strength of the electric field and current density. This approach aids in experimental calibration [166]. However, the predominant method in literature reviews is the use of electric field strength as a key metric for contrasting various electric fields (EFs) [167, 168].

As early as 1985, Gundersen and Greenebaum proposed three methods for measuring electric fields [169], emphasizing their suitability for relatively homogeneous fields. Typically, the uniformity of an electric field is mainly influenced by the geometry and arrangement of electrodes, as well as the properties of the medium [170]. Generally, capacitive coupling often uses parallel plate electrodes. What's more, the electric field usually exists within an insulating medium with more uniform dielectric properties in capacity coupling. Therefore, it is more likely to generate a relatively uniform electric field. Analytical formulas can be applied to estimate the strength of such a field [139, 156, 159]. Dauben et al. [163] introduced an in vitro electrical stimulation setup utilizing AC with direct coupling for stimulation. The cylindrical electrodes and the dielectric irregularities of medium contribute to the inhomogeneity of its electric field. For such non-uniform electric field, it is necessary to construct a simulation model to determine the electric field strengths. The development of the simulation model was parallel to the creation and subsequent improvements of this stimulation setup. Zimmermann et al. [171] has established the latest simulation model for this electric field. To verify the accuracy of this simulation model, experimental validation is essential.

What's more, additional elements integral to the electrical stimulation experiment, such as electrodes and generators, may have effect on the generation of the electric field. Since it is common to use multiple electrodes and several generators in a single experiment, the consistency between different electrodes and generators plays a crucial role in the outcomes of these experiments. However, in all the literatures related to electrical stimulation, there is no mention of analyzing the influence of different electrodes and generators.

1.8 Aim of the Work

The experimental study is based on a well-established in vitro setup for direct-coupled AC electrical stimulation [7]. It consists two distinct phases: firstly, verification of the accuracy of constructed simulation model as well as assessment of the influence of varying generator and electrodes and secondly, electrically stimulate chondrocytes from male and female donors with a range of biologically relevant electric field strengths by direct coupling. Subsequently, assess the re-differentiation potential of human chondrocytes.

1.8.1 Verification of the Accuracy of Constructed Simulation Model and Assessment of the Influence of Varying Generators and Electrodes during In Vitro Stimulation

In our cellular electrical stimulation experiment, based on the electrical stimulation setup [7], a simulation model was developed [171]. The purpose of this model is to determine the distribution of electric field strength in the medium given a specific input voltage and frequency. The first phase involves verification the accuracy of the simulation model by conducting a comparative analysis between simulated and measured local voltages. During this process, utilizing the voltage-slope method introduced by Gundersen and Greenebaum [169] and developed by Zimmermann [171], the electric field strength by calculating the gradient of the measured local voltages is to determine. Meanwhile, our cellular electrical stimulation experiment requires the simultaneous use of multiple electrodes and generators, the other aspect is to assess potential influence of electrodes and generators by comparing the measured local voltages.

1.8.2 Electrical Stimulation of Human Chondrocytes from Male and Female Donors

Building upon the achievement of the aforementioned objectives, the second objective of this work is to use varying electric field strengths to administer electrical stimulation to human chondrocytes from both male and female donors. Afterwards, assess the effects of direct-coupled alternating electric fields on the metabolic activity as well as the synthesis of collagen2 and collagen1 of chondrocytes. Concurrently, we aim to numerically analyze morphology changes in chondrocytes using CellProfiler, an open-

source image analysis software. Through this comprehensive approach, the study endeavors to uncover the potential impact of varying electric field strengths on chondrocyte re-differentiation. Additionally, comparisons between both sexes are made to explore whether there are differences in the tendency for re-differentiation between chondrocytes from male and female donors when cultured in vitro

2. Materials and Methods

Comprehensive details of all materials, equipment, software used in both the experimental and evaluative phases of this study are meticulously documented in a tabular format, appended to the thesis (refer to Chapter 10.1, page 74).

2.1 Verification of the Accuracy of Constructed Simulation Model and Assessment of the Influence of Varying Generators and Electrodes during In Vitro Stimulation

2.1.1 Experimental Setup for Electrical Stimulation

The experimental setup is based on a well-established setup by Hiemer et al. [7] (Figure 5). The cylindrical electrodes, constructed from pure titanium, exhibited dimensions of 14 mm in length and 5 mm in diameter. A 5 mm-long insulator made of polyetherether ketone (PEEK) separated the electrodes. The electrode holders, also crafted from PEEK, ensured a 3 mm gap between the electrodes and the well bottom. The contact rods, measuring 35 mm in length, were composed of titanium. The lid of the 6-well plate had pre-drilled holes for the contact rods. Chondrocytes were seeded and cultured at the central region of the well bottom beneath the electrodes with 5ml medium added.

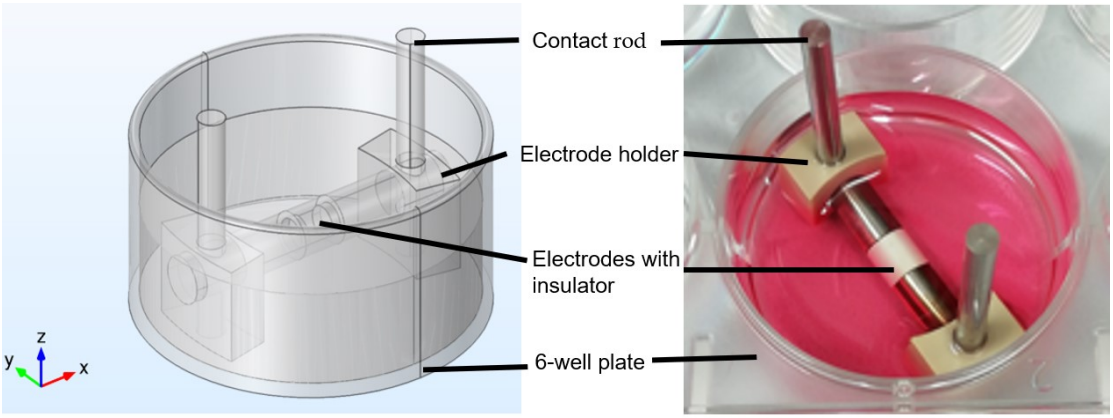

Figure 5. (a) 3D model of the stimulation chamber; (b) actual image of the stimulation chamber, modified from Hiemer et al.(https://www.spandidos-publications.com/10.3892/mmr.2018.9174).

2.1.2 Simulation Model

The simulation model was primarily developed by J. Zimmermann and is detailed extensively in the relevant paper [171]. For the finite method model construction, first of all, the geometry for model was prepared using the OCCT kernel in NGSolve for computer-aided design (CAD) modelling. Meanwhile, the dielectric properties used in this work are summarized in Table 4. With all these dielectric properties incorporated to the finite element model, computations were performed using the FEM library

NGSolve [172] with NETGEN as the mesher [173]. The impedance of the electro-electrolyte interface (EEI) can be integrated into the finite element model through Robin boundary conditions [174]. Utilizing this finite element model, for a specific voltage applied to the electrode, the anticipated voltage distribution can be computed from the benchmark simulation results through shifting and scaling. Subsequently, the simulated electric field strength can be estimated by calculating the gradient of simulated voltages. However, this model has a limitation: the electrode is solely utilized for stimulation at a single frequency. Therefore, the frequency-dependent changes in impedance of the EEI cannot be derived from the stimulation signal.

Table 4 [171]**.** The dielectric properties of materials used in simulation model.

Domain	Conductivity/ Sm^{-1}	Permittivity
DMEM at 37◦C	1.84	80
Plastic	10^{-14}	2
Air	10^{-14}	1

2.1.3 Measurement Setup

The schematic illustration in Figure 6a depicts the experimental arrangement and circuit connections of measurement setup. A frequency generator Metrix GX310 or Metrix MTX 3240 (both from Chauvin Arnoux Ltd, France) was used to provide the voltage, amplified by a factor of 10 using an F30PV linear amplifier (FLC, Gothenburg, Sweden). At the same time, the voltage drops across the shunt resistor (1 Ω), the applied voltage and the voltage across the measurement probe were recorded. Data were acquired using a Rigol MSO5104 oscilloscope (Batronix GmbH, Prez, Germany) with additional amplification as required (using an F10A, FLC, Gothenburg, Sweden, gain 10 or an Agilent 33502a, Santa Clara, CA, United States, gain 5). The local voltages at the coordinate points on the grid (Figure 6b) were measured using a customized unipolar platinum-iridium microprobe with a diameter of 370 µm and an uninsulated metal tip extending a few micrometers (PI2PT33.0B10, Microprobes, Gaithersburg, MD, United States). Channel 1 records the input voltage and frequency, Channel 2 monitors the current, and Channel 3 records the local voltages within the medium on the grid (Figure 6b). To prevent electrode displacement during the experiment, a lid was customized for the 6-well plate to secure the contact rods (Figure 7). In addition, to simulate the incubator environment, an enclosed temperature control box was constructed to maintain a constant temperature of 37°C throughout the entire measurement process (Figure 8). The overall measurement setup is shown in Figure 6c. The measurement setup in the temperature control box is shown in Figure 6d.

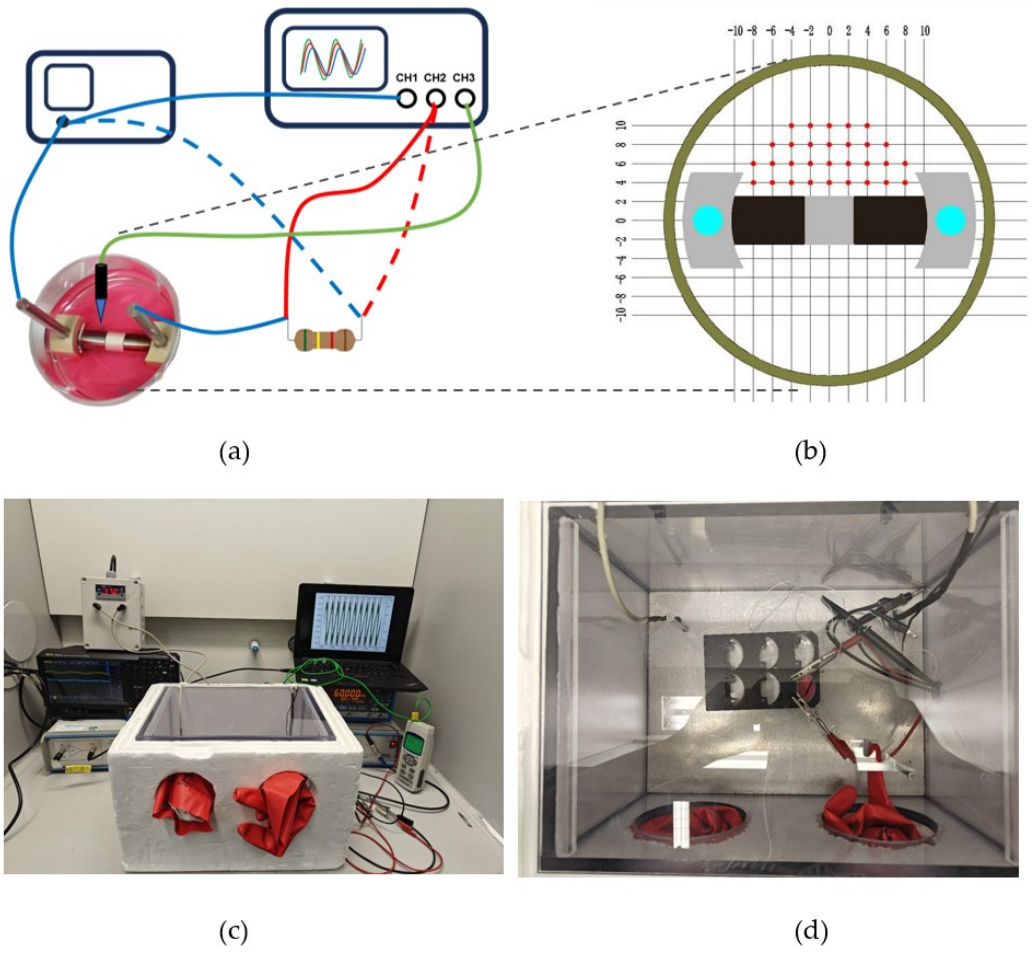

Figure 6. (a) Depiction of the experimental arrangement and circuit connections of measurement setup, modified from J. Zimmermann et al. (https://www.sciencedirect.com/science/article/pii/S1567539423000324?via%3Dihub). (b) Top view of coordinate system for measurements. Red dots indicate the coordinates where measurements for verification were executed. (c) The overall measurement setup. (d) Top view of the measurement setup in the temperature control box.

2.1.4 Three-Dimensional Printing of the Lid

To ensure the stability of the electrode's contact rods during experimentation, a custom-made lid was crafted for the 6-well plate (Figure 7a). The detailed dimensions are described in the Supplementary Material (Figure S1). The 3D model (Figure 7b) was designed with the aid of SOLIDWORKS (Dassault Systèmes SolidWorks Corporation, 175 Wyman Street, Waltham, MA, United States, available at https://www.salome-platform.org/). It is transformed into a physical form through 3D printing, using acrylonitrile butadiene styrene (ABS) as the material. One of the distinctive features of this lid is its fixed-spacing small holes. These holes are crucial for securely positioning the contact rods of the electrodes, thereby preventing any

potential displacement during the measurement procedures. Another feature of this lid is that the hollowed-out portion reserves space for measurement.

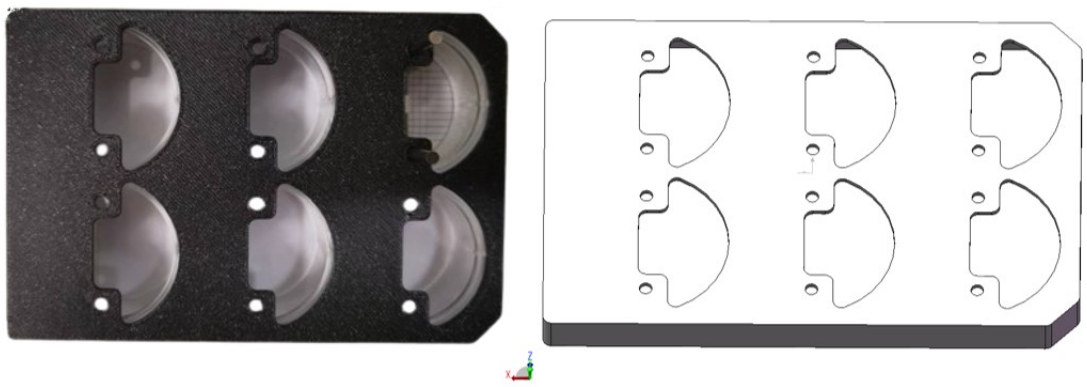

Figure 7. (a) Physical picture of the lid; (b) 3D structural schematic of the lid. The small holes are used to secure the contact rods, preventing electrode displacement during the measurement process, while the hollowed-out sections provide space for measurement.

2.1.5 Construction of Temperature Control Box

The temperature control box (Figure 8a), constructed from acrylic board, is designed to replicate the incubator conditions, providing an ideal environment for all measurements. The 3D structural model was built using SOLIDWORKS (Dassault Systèmes SolidWorks Corporation, 175 Wyman Street, Waltham, MA, United States, available at https://www.salome-platform.org) (Figure 8b). The box incorporates a hot water bath system, maintained at a constant temperature through the JUMO eTRON M controller (JUMO GmbH & Co. KG Fulda, Germany). The synergy of a heating coil and an aluminum alloy plate within the box ensures optimal heat distribution. A type K temperature sensor, interfaced with a PCE-T390 thermometer (PCE Germany GmbH, Meschede, Germany), is strategically positioned within the box to meticulously monitor and regulate the temperature. The precise dimensions of the box are detailed in the Supplementary Material (Figure S2). For construction, the acrylic panels are securely bonded with a robust adhesive Acrifix 1S 0116 (Röhm GmbH, Stadt, Bundesstaat, United States), while an L-shaped plate ensures their vertical alignment during fabrication. The acrylic case is then encased within a polystyrene foam shell for enhanced insulation. A pair of Solvex® 37-900 chemical protective gloves (Ansell GmbH, Brussels, Belgium) were sealed and affixed for operation. This setup guarantees a controlled temperature, ample space, and unobstructed visibility for manual measurements.

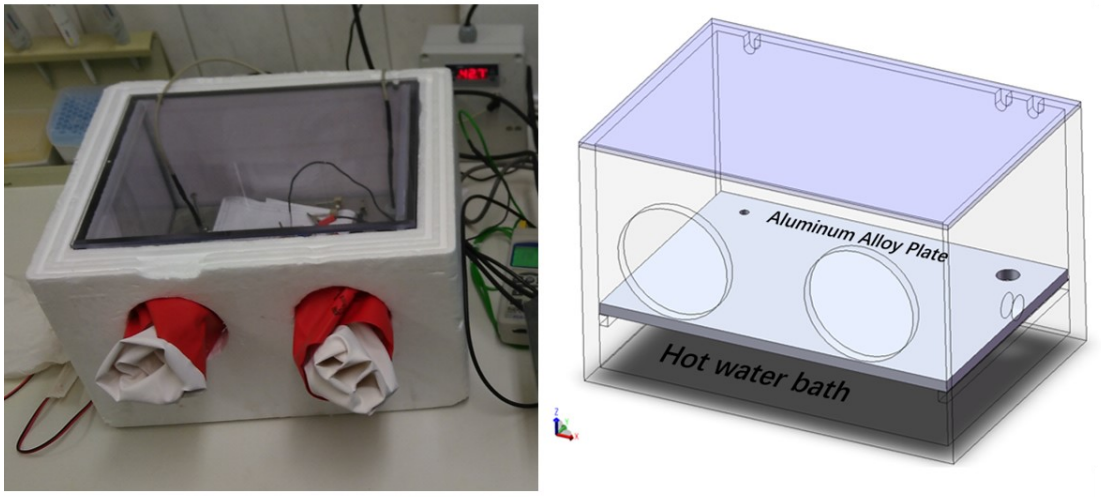

(a) (b)

Figure 8. (a) Physical picture of the temperature control box (b) 3D structural schematic of the temperature control box. This temperature control box simulates the incubator environment, providing a closed space with a constant temperature of 37°C, where all measurements are conducted.

2.1.6 Local Voltage Measurement

During local voltage measurements, 5 ml DMEM was added into the well. The probe tip was precisely positioned at grid coordinate points and the local voltage at each coordinate point was recorded. A noteworthy observation from our preliminary experiments is that any deviation in the verticalness of the probe leads to a consequential alteration in the measurement value, resulting in a notable deviation from the anticipated value [171]. Consequently, it is imperative for the measurement probe to retain vertical alignment throughout the assessment, rendering manual measurement directly under the electrode unfeasible. To ensure accuracy, each data point is measured four times to calculate the average value. To ensure experimental integrity, both the input voltage and current were consistently monitored to maintain stable conditions. All measurements were carried out in temperature-controlled box at 37 ± 0.5 °C. All resultant data were automatically archived to a laptop computer interconnected to the oscilloscope as YAML files, and Python scripts are available from Github [1]. The measured voltages, input amplitude, and current were extracted using automated Python scripts. For comparison purposes, the experiment uses two different generators- Metrix GX310 and Metrix MTX 3240, both from Chauvin Arnoux Ltd, France, along with two electrodes varying in usage status: one nearly new and one has been in use for one year. The usage frequency of the electrode is 135 minutes each day, three days per month. The electrodes were cleaned with 10% acetic acid and ultrasound before using. Three frequencies and two input voltages, which were

previously used for the in vitro stimulation of chondrocytes, osteoblasts, or mesenchymal stem cells and proven to have biological relevance, were employed as the frequencies and voltages for local voltage measurement (Table 5).

Table 5. Biologically relevant frequencies and voltages selected for measurement.

Frequencies	Biological relevance
20 Hz	This frequency was reported for its relevance in bone regeneration [163, 175]. It has also been used for human osteoblast stimulation, resulting in enhanced osteocalcin mRNA and collagen I synthesis [163].
1 kHz	This frequency was used for the stimulation of chondrocytes and mesenchymal stem cells [7]. It has been extensively studied for cartilage regeneration in multiple research studies[148, 176, 177].
60 kHz	This frequency was widely investigated in the context of articular cartilage [140, 157, 164], It has also been explored in studies involving bone cells [178].
Voltages	**Biological relevance**
0.2 V_{RMS}	This voltage was applied in studies involving bone cells and bacteria [163]. Meanwhile, it was also used in osseointegration in titanium implants [179].
1.4 V_{RMS}	This voltage was used in the research on bone cells and bacteria [163]. It has been reported in studies on neuron activity and stem cells as well [151, 180].

2.1.7 Data Acquisition, Visualization and Analysis

The voltages expected at the measuring points were derived from the simulation model. To assess the conformity between expected and measured voltages at the measurement points on the grid, absolute and relative differences were computed and visualized using Matplotlib [171, 181]. Additionally, the differences of the measured voltages between different generators and different electrodes were also computed and visualized using Matplotlib. The electric field strengths were determined by calculating the gradient of local voltages.

2.2 Electrical Stimulation of Human Chondrocytes In Vitro

2.2.1 Cell Isolation and Cultivation

Human chondrocytes were sourced from six patients undergoing primary total knee replacement, with an equal distribution of male (n=3, average age 64.3±2.1 years) and female (n=3, average age 72.7±2.6 years) participants. This study was conducted with the approval of the Local Ethical Committee of the University of Rostock (registration no. A2011 138).

The process of isolating primary chondrocytes involved removing the cartilage from the bone, cutting it into small pieces, and washing it in phosphate-buffered saline (PBS) (PAA, Cölbe, Germany). The cartilage, with an approximate wet weight of 3 grams, was then treated with 1% Trypsin/EDTA (Gibco® Invitrogen, Darmstadt, Germany) at 37°C for 20 minutes, followed by overnight incubation with 0.2% collagenase A (Roche, Mannheim, Germany) in Dulbecco's modified eagle medium (DMEM) (Gibco®, Thermo Fisher Scientific Inc., Waltham, MA, United States) supplemented with 10% fetal calf serum (FCS) (Pan Biotech, Aidenbach, Germany), 1% amphotericin B, and 1% penicillin/streptomycin (Gibco® Invitrogen, Darmstadt, German) at 37°C. The resultant cell suspension was filtered through a 70 µm cell strainer (Nunc, Wiesbaden, Germany) and centrifuged at 118 × g for 10 minutes. The cell pellet was resuspended in DMEM with the aforementioned supplements and ascorbic acid. The freshly isolated chondrocytes were seeded in a 25-cm^2 culture flask containing 8 ml of supplemented culture medium. Chondrocytes were expanded at 37 °C, 5% CO_2, and 21% O_2 and cryopreserved at passage two. For all experimental procedures, cryo-conserved chondrocytes were used. Upon thawing, chondrocytes were cultivated in Dulbecco's Modified Eagle Medium (DMEM, Gibco®, Thermo Fisher Scientific Inc., Waltham, MA, United States) with 10% fetal bovine serum (Pan Biotech, Aidenbach, Germany), 1% penicillin/streptomycin (Thermo Scientific, Waltham, MA, United States), 1% amphotericin B (Biochrom GmbH, Berlin, Germany), and 50 µg/mL ascorbic acid (Sigma-Aldrich, Merck KGaA, Darmstadt, Germany) in a 75 cm^2 cell culture flask at 37 °C, 5% CO_2, and 21% O_2 for seven days to reach a confluency of nearly 90%. Chondrocytes in passage four were used for electrical stimulation.

2.2.2 Field Strengths for Cell Stimulation

Electric field strengths (Table 6) in cell exposure area within the stimulation chamber (Figure 5) were determined by calculating the gradient of measured local voltages at different frequencies. Of them, three electric fields strengths which were previously used for the in vitro stimulation of chondrocytes, osteoblasts, or mesenchymal stem cells and proven to have biological relevance, were selected for later electrical stimulation experiments. Their biological relevance is illustrated in Table 7.

Table 6. Electric field strengths in cell exposure area within the stimulation chamber at different applied voltages and frequencies. The field strengths were determined by calculating the gradient of measured local voltages

	1.4 V_{RMS}	**0.2 V_{RMS}**
60 kHz	100-140 V/m	15-20 V/m
1 kHz	60-80 V/m	8-12 V/m
20 Hz	8-12 V/m	0.8-1.2 V/m

Table 7. Biological relevance of the electric field strengths selected for the electrical stimulation experiments.

EF strength	**Frequency**	**Voltage**	**Biological relevance**
100-140 V/m	60 kHz	1.4 V_{RMS}	This electric field strength has been used in studies involving brain cells [182]. It has also been explored in the context of implants for bone regeneration [183]. Electromagnetic fields (EMF) with a comparable density were applied to the bone surface to stimulate new bone formation [184]. A similar electric field of 80-90 V/m was employed in the investigation of bone cells and bacteria [163].
15-20 V/m	60 kHz	0.2 V_{RMS}	This electric field strength has been employed in studies related to the conductivity of bone regeneration [185]. An electric field of 13.2V/m was applied to the proximal tibia of rabbits [186]. Electromagnetic fields (EMF) with a similar density were also applied for bone healing in conjunction with mechanical loading [187]. An electric field with a strength of 20-35 V/m was applied to human chondrocytes and mesenchymal stem cells, no alterations in collagen 1 and collagen 2 were observed under normoxic conditions. However, under hypoxic conditions, an increase in the synthesis of collagen 2 was noted [7].
0.8-1.2 V/m	20 Hz	0.2 V_{RMS}	Various electric fields with strengths at this level (1.5, 2.25, 3, and 4.5 V/m) have been used for Chondrocytes electrical stimulation by Brighton et al., increased cell proliferation was observed after exposure to electric field of 1.5 to 3.0 V/m. Meanwhile, increased cAMP was observed after short time exposure to 1.5V/m electric field [139, 140, 156]. Concurrently, 2 V/m electric field was widely used in stimulation for bovine articular chondrocytes [113], bovine articular cartilage explants [112] as well as human osteoarthritic cartilage explants [110], significantly elevated production of collagen and proteoglycan, and up-regulated collagen 2 and aggrecan mRNA expression in vitro was observed. Vaca-González et al. [157] utilized 0.4 V/m and 0.8 V/m electrical stimulation on chondrocytes in vitro, observing increase of proliferation with an electric field of 0.4 V/m during 30 mins.

2.2.3 Electrical Stimulation

From passage four, 20,000 chondrocytes in 200 µL of medium were seeded in a 6-well plate, positioned in the center of the well. Following an initial adherence period of 45 minutes, each well was filled with 5 mL DMEM containing 1% Pen/Strep, 1% Amphotericin B, 1% insulin-transferrin-selenium (ITS+TM Premix, BD Biosciences, Franklin Lakes, NJ, United States), 50 µg/mL ascorbic acid, and 100 nM dexamethasone (Sigma-Aldrich, Merck KGaA, Darmstadt, Germany). After 24 hours of incubation, the electrical stimulation started. The complete electrical stimulation unit (Figure 5), consisting of the electrodes, holder, and contact rods, was placed in the well. Alternating current as a sinusoidal signal was applied to the stimulation chamber for three days using a Metrix GX 310 function generator (Chauvin Arnoux Ltd, France), with combinations of voltages and frequencies set at 1.4 V_{RMS} at 60 kHz, 0.2 V_{RMS} at 60 kHz, and 0.2 V_{RMS} at 20 Hz. Chondrocytes underwent stimulation three times per day for 45 minutes each, with 225-minute breaks between stimulations. Throughout electrical stimulation, chondrocytes were cultured at 37˚C under 5% CO_2, and 21% O_2. For the unstimulated control, chondrocytes were similarly cultured in the presence of the electrode system but without a connection to the function generator.

2.2.4 Cell Staining and Microscopy

Upon removal of the medium, 1ml solution comprising Calcein AM (Thermo Fisher Scientific, Inc., Waltham, MA, United States) and PBS at the ratio of 1:4000 was added each well and incubated at room temperature for 10 min. Calcein AM (Ex/Em 494/515 nm) can selectively cross the cell membrane of living cells and be hydrolyzed by esterase in living cells to produce green fluorescence. The stained samples were captured at 10x magnification using the Nikon Eclipse 120 fluorescence microscope (Nikon Instruments, Tokyo, Japan). FITC- filter was used for imaging. A total of four images were acquired each well. Image acquisition settings for the microscope were configured with a 250 ms exposure time.

2.2.5 Image Analysis

Prior to analysis, preprocessing was done using ImageJ 1.53 (National Institutes of Health, Bethesda, MD, United States, available at https://imagej.net/ij/). The Bright/Contrast of the images was adjusted, with a minimum displayed value of 0 and a maximum displayed value of 60. Subsequently, chondrocytes in contact with each other were manually separated. The analysis was then performed using CellProfiler (version 4.2.1; Broad Institute, Cambridge, MA, United States, available at https://cellprofiler.org/citations). The CellProfiler image analysis process is shown as a pipeline in Supplementary Material (Figure S3). The associated image transformation of images after processing is depicted in Figure 9. Chondrocytes were classified

according to their shape as either rounded or elongated, with the form factor used as criteria. Form factor is a dimensionless quantity used to de-scribe the shape of cell. Form Factor= 4π×Area / Perimeter^2, where π is the mathematical constant ~3.14, Perimeter is cell perimeter, and Area is cell area [188]. The form factor has a value of 1 when the cell's outline is a perfect circle and decreases as the cell elongates [189]. It is noteworthy that the number of chondrocytes classified as elongated is adjusted by subtracting three for each image, accounting for the fixed scale bar in the lower right corner identified as three elongated chondrocytes.

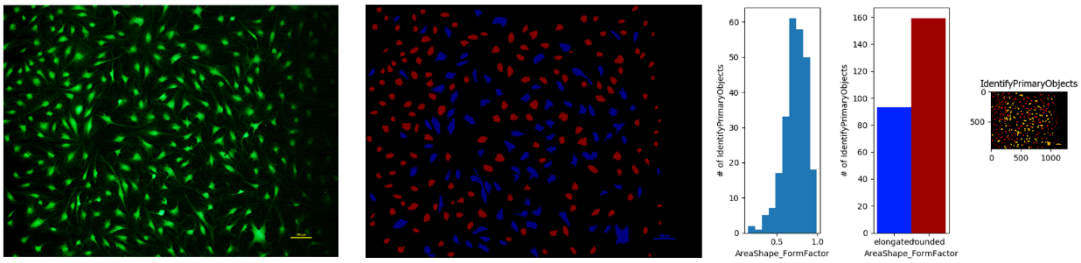

Figure 9. The transformation of staining images after processing through ImageJ and CellProfiler. (a). The image after Bright/Contrast adjustment by ImageJ (scale bar, 100μm). (b). Identification of rounded and elongated chondrocytes following the "Identify Primary Objects" step. Blue cells were recognized as elongated chondrocytes and red were recognized as rounded chondrocytes. (c). From left to right, histograms of the formfactor distribution of all chondrocytes, histograms of chondrocytes classified as elongated and rounded, and a reduced version of image (b).

2.2.6 Protein Synthesis Assessment

Collagens are primarily found in the form of collagen fibrils, which are essential for various structural and functional purposes in the body. To form these complex structures, collagen molecules are initially synthesized as procollagens. Procollagen peptidases, enzymes critical in this process, cleave the carboxy-terminal and amino-terminal ends of the procollagen molecules. This enzymatic action is crucial for the maturation and integration of the collagen proteins into the fibrillar structures. The measurement of the liberated amino-terminal and carboxy-terminal ends of procollagen molecules can be employed as an indicator of the rate of collagen synthesis. In this study, 700μL of supernatant was collected from each well, amounting to a total of 1400μL of medium per group. This collected medium was then stored at -20˚C for further analysis.

2.2.6.1 Collagen 1 Synthesis Assessment

For assessing collagen 1 synthesis, specifically the concentration of Type I C-terminal

collagen propeptide (CICP), the MicroVue CICP ELISA kit from Quidel, San Diego, CA, United States, was used according to the manufacturer's guidelines.

The process began with thawing of the supernatants. 100 µl of the standard solution, control, and each diluted supernatants were added to wells coated with purified murine monoclonal anti-CICP antibody. This was followed by an incubation period of 120 minutes at a controlled temperature of 25°C. Subsequently, the wells were washed three times with the wash buffer and then dried using green cloths. 100 µl of rabbit anti-CICP antibody was then added to each well, followed by another incubation period of 45 minutes at 25°C. After this, the wells were washed three times again. The next step involved the addition of 100 µl of lyophilized goat anti-rabbit IgG antibody conjugated to alkaline phosphatase (ALP) to each well. The plate was then incubated for 45 minutes at 25°C. Following three more washes, 100 µl of working substrate (pNPP dissolved in a diethanolamine and magnesium chloride solution) was added to each well and incubated for 30 minutes at 25°C.The reaction was then halted by adding 50 µl of stop solution to each well. The optical density at 405 nm was measured using a microplate reader within 15 minutes of adding the stop solution. The results were analyzed using the 4-parameter logistic (4-PL) curve method: y = (A-D)/(1+(x/C)^B)+D, and the concentrations of samples and controls were determined based on the standard curve generated from this analysis. This method allowed for the precise quantification of CICP levels in the samples.

2.2.6.2 Collagen 2 Synthesis Assessment

For measuring the synthesis of collagen 2, the Collagen 2 Synthesis ELISA kit from IBEX, Montréal, QC, Canada, was employed to quantify the concentration of Type II C-terminal collagen propeptide (CIICP).

The procedure began with pipetting 50 µl of the sample into a polypropylene mix plate. For each plate, 50 µl of the antibody was diluted in 6 ml of assay buffer, and then 50 µl of this diluted CP II antibody was added to each well. The plate was then incubated at room temperature with shaking at 600-700 rpm. Subsequently, 80 µl of each sample was transferred onto the ELISA plate. The ELISA plate, covered, was incubated for 120 minutes at room temperature with continuous shaking at 600-700 rpm. Following this, the wells were washed six times with the wash buffer. For the next step, 50 µl of GAR-HRP (Goat Anti-Rabbit Horseradish Peroxidase) was diluted in 11 ml of buffer III, and 100 µl of this diluted solution was added to each well. The plate, once again covered, was incubated at room temperature for 30 minutes. Post-incubation, the wells were washed six times. After the washing step, 100 µl of TMB (Tetramethylbenzidine) substrate was added to each well. The ELISA plate, covered, was incubated for up to 30 minutes at room temperature. To conclude the reaction, 100 µl of stop solution was

added to each well. The optical density at 450 nm was then read using a microplate reader within 10 minutes of adding the stop solution. This process allowed for the accurate assessment of CIICP levels in the samples.

2.2.6.3 Total Protein Normalization

The protein data collected in the study were normalized to the total protein content to ensure accuracy and consistency. This normalization process was conducted using the Qubit® Protein Assay Kit provided by Thermo Fisher Scientific Inc, Waltham, MA, United States. The method involves labeling proteins with a specific fluorescent dye, a process integral to the quantification of protein concentration. Once the proteins were labeled, their fluorescence levels were quantified using the Qubit Fluorometer, also from Thermo Fisher Scientific Inc, Waltham, MA, United States.

The key to this quantification method lies in its reliance on a standard curve. This standard curve is generated based on standards provided within the assay kit. By following the manufacturer's detailed instructions, these standards are prepared and their fluorescence is measured to create a reference curve. The fluorescence readings of the experimental samples are then compared against this standard curve. This comparison allows for the determination of the protein concentrations in the samples based on their fluorescence intensity relative to that of the known standards. This step of normalizing against the total protein content is crucial, as it ensures that the protein data are accurately reflective of the actual protein levels in the samples, free from the influence of sample-to-sample variations in protein concentration.

2.2.7 Cellular Metabolic Activity Assessment

To ascertain the metabolic activity of chondrocytes, the water-soluble tetrazolium salt (WST-1) assay (Roche GmbH, Grenzach-Wyhlen, Germany) was executed. Mitochondrial dehydrogenase promotes the reduction of the tetrazolium salt to formazan, changing the color from orange to yellow. After removing the medium, 500 µL of a 10% dilution of WST-1 reagent with DMEM was added into each well. Following an incubation period of 1 hour at 37°C, 100 µL from each well was transferred into a 96-well plate, maintaining duplicates. The absorption at a wavelength of 450 nm (reference wavelength of 630 nm) was measured deducted to a blank using the multimode plate reader Infinite 200 pro (Tecan Group Ltd., Maennedorf, Switzerland).

2.2.8 Data Illustration and Statistical Analysis

The results of the cell experiments were presented graphically using scatter plots created with GraphPad Prism 9.5.1 (GraphPad Software Inc., San Diego, CA, United States). The scatterplots depict all values, accompanied by essential statistical parameters, including mean values and standard deviation. All of the statistical

analyses were conducted using GraphPad Prism 9.5.1. Data were assessed for normality using the Shapiro-Wilk test. All comparisons between groups were made separately using a two-sample test. For comparisons without sex-based distinction and within same sex, paired t-tests (for normally distributed data) and Wilcoxon matched-pairs signed rank tests (for non-normally distributed data) were used. For comparison between both sexes, unpaired t-tests (for normally distributed data) and Mann-Whitney tests (for non-normally distributed data) were used. A p-value < 0.05 indicated statistical significance, while a p-value between 0.05 and 0.1 suggested a statistical trend.

3. Results

3.1 Verification of the Accuracy of Constructed Simulation Model

3.1.1 Comparison between Simulated and Measured Local Voltages

The simulated and measured local voltages within the stimulation chamber are depicted in Figure 10. The absolute differences and relative differences between them are illustrated in Figures 11 and 12, respectively.

1) **At 60 kHz:** the measured local voltages show a remarkable conformity with the simulated data (Figure 10). At this frequency, with an output voltage of 1.4 V_{RMS}, the absolute differences between the measured and simulated voltages at most measurement points are below 0.08 V (Figure 11a), with the relative differences below 15% (Figure 12a). With an output voltage of 0.2 V_{RMS}, the absolute differences at most measurement points are below 0.01 V (Figure 11b), with the relative difference being less than 10% (Figure 12b).
2) **At 1 kHz:** the conformity between the measured and simulated local voltages decreased (Figure 10). At this frequency, with an output voltage of 1.4 V_{RMS}, the absolute difference between the measured and simulated voltages at most measurement points is below 0.3 V (Figure 11a), and the relative difference is under 70% (Figure 12a). When the output voltage is 0.2 V_{RMS}, the absolute difference at most measurement points is below 0.06 V (Figure 11b), with the relative difference being less than 80% (Figure 12b).
3) **At 20 Hz:** virtually, the conformity between the measured and simulated voltages is exceedingly low at this frequency (Figure 10). At this frequency, with an output voltage of 1.4 V_{RMS}, the absolute difference between the measured and simulated voltages at most measurement points exceeds 0.24 V (Figure 11a), with the relative difference exceeding 50%, and reaching up to 160% at certain points (Figure 12a). When the output voltage is 0.2 V_{RMS}, the absolute difference at most measurement points exceeds 0.05 V (Figure 11b), with the relative difference surpassing 50%, and reaching up to 130% at certain points (Figure 12b). At this frequency, the voltage drop across the medium is virtually imperceptible (Figure 10) and it can be predicted that the calculated electric field strength at this frequency will be significantly lower than the simulated values.

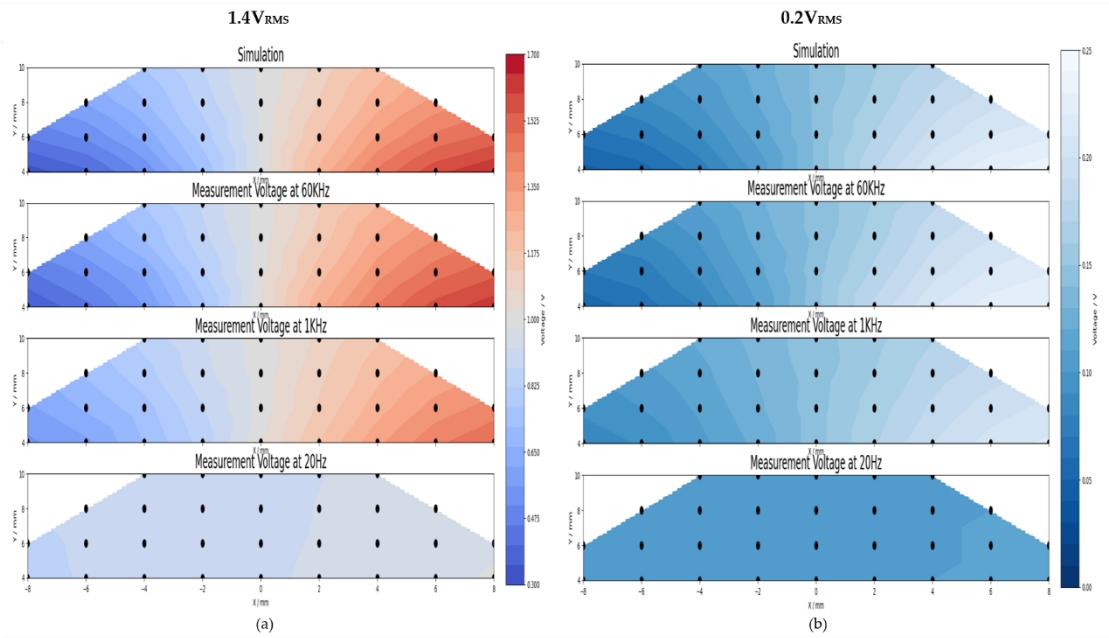

Figure 10. With input voltage of (a) 1.4 V_{RMS} and (b) 0.2 V_{RMS}, the simulated local voltages and measured local voltages at 60 kHz, 1 kHz and 20 Hz on the grid. The measurement points are represented by black dots. The simulated and measured voltages were interpolated to produce a heatmap. The absolute and relative difference between the measured and simulated values is depicted in Figure 11 and Figure 12.

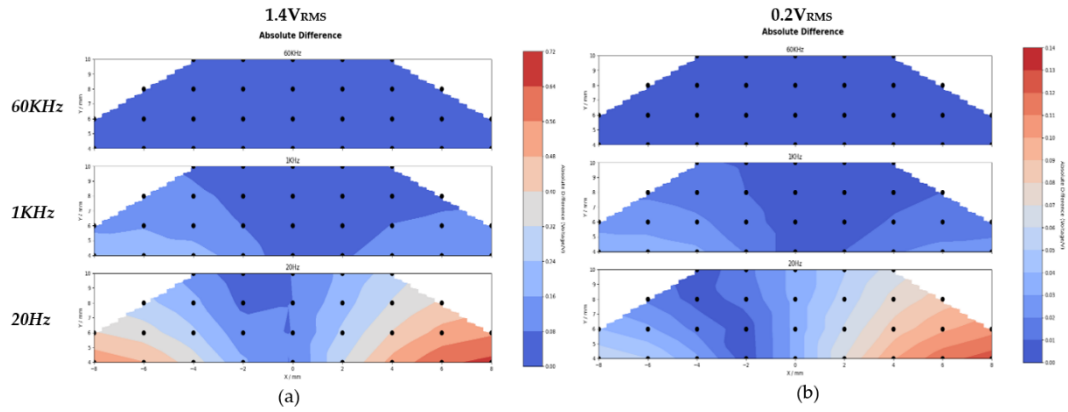

Figure 11. With input voltage of (a) 1.4 V_{RMS} and (b) 0.2 V_{RMS}., the absolute differences between the measured and simulated local voltages at 60 kHz, 1 kHz and 20 Hz on the grid.

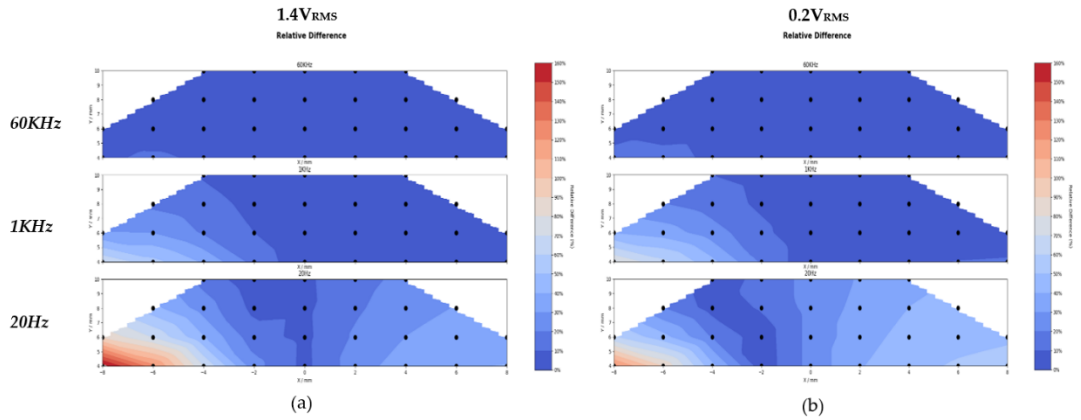

Figure 12. With input voltage of (a) 1.4 V_{RMS} and (b) 0.2 V_{RMS}, the relative differences between the measured and simulated local voltages at 60 kHz, 1 kHz and 20 Hz on the grid.

3.1.2 Electric Field Strengths

The simulated and measured electric field strengths determined by calculating the gradient of simulated and measured local voltages, separately, is shown in Figure 13. At 60 kHz, the calculated and simulated field strengths closely match with each other. At 1 kHz, the calculated electric field strengths decrease, resulting in reduced conformity with the simulated electric field. At 20 Hz, the decrease in electric field strength is much more pronounced, with the field strength being much weaker than the simulated electric field. In other words, at the same input voltage, as the frequency decreases, the electric field strength also decreases, leading to a reduced conformity with the simulated field strength.

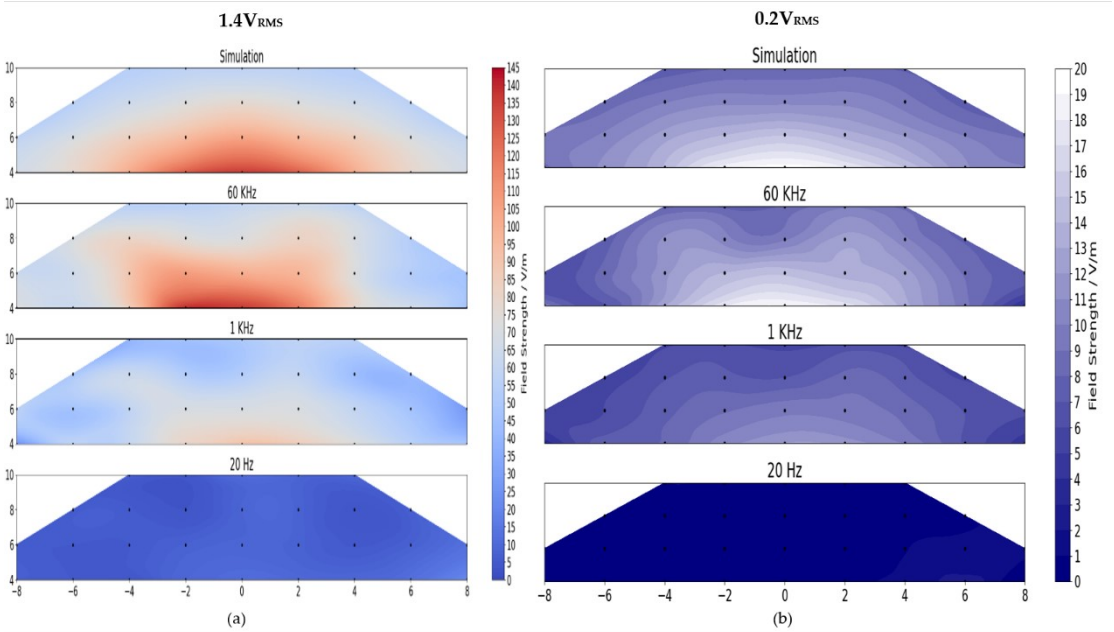

Figure 13. With input voltage of (a) 1.4 V_{RMS} and (b) 0.2 V_{RMS}, the simulated and measured field strengths at 60 kHz, 1 kHz and 20 Hz. The simulated and measured field strengths were determined by calculating the gradient of simulated and measured local voltages, separately.

3.2. Assessment of the Influence of Varying Generators and Electrodes during In Vitro Stimulation

3.2.1 Comparison between Different Used Stimulation Electrodes

The electric fields generated by the stimulation electrodes of different usage status are shown in figure 14. It can be observed that the electric fields generated by two electrodes are quite similar. The absolute and relative differences between the measured local voltages are depicted in Figure 15. With an input voltage of 1.4 V_{RMS}, the absolute differences at most measurement points are below 0.14 V, with relative differences below 18%. With an input voltage of 0.2 V_{RMS}, the absolute differences at most measurement points are below 0.025 V, with relative differences below 18.5%. Furthermore, it is noteworthy that, under both input voltage, there are greater discrepancies at 20 Hz compared to 60 kHz and 1 kHz.

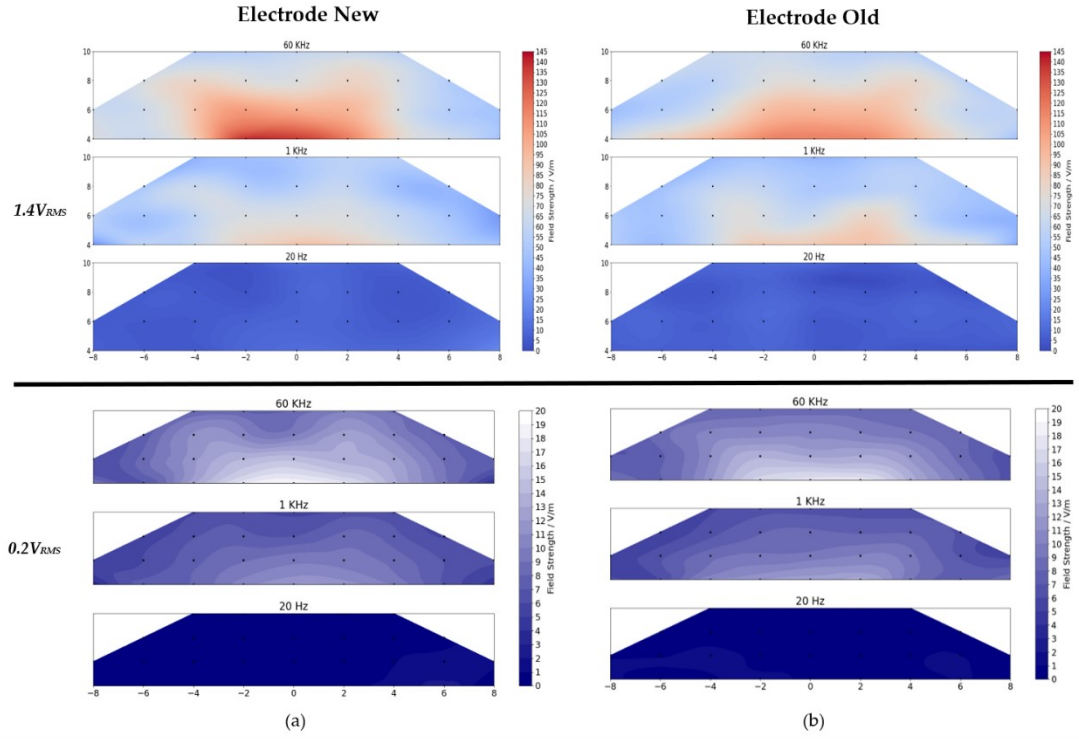

Figure 14. With input voltage of 1.4 V_{RMS} (Upper Panel) and 0.2 V_{RMS} (Lower Panel), electric fields generated by (**a**) new electrode;(**b**) electrode used for 1 year at 60 kHz, 1 kHz and 20 Hz. The electric field strengths were determined by calculating the gradient of measured local voltages.

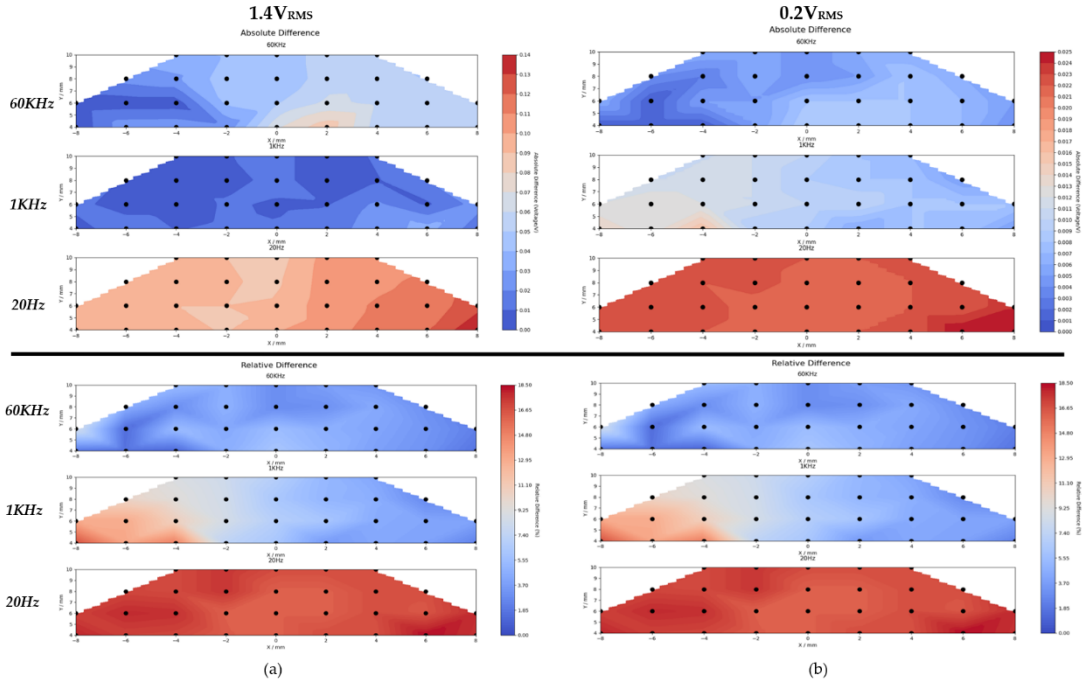

Figure 15. With input voltage (a) 1.4 V_{RMS} and (b) 0.2 V_{RMS}, the absolute (Upper Panel) and relative differences (Lower Panel) of the measured local voltages between two electrodes at 60 kHz, 1 kHz and 20 Hz.

3.2.2 Comparison between Different Used Generators

The electric fields generated by two different generators are shown in Figure 16. It is shown that the electric fields generated by the two generators look similar, yet differences still could be noted. The absolute and relative differences of the measured local voltages between two generators are depicted in Figure 17. With an input voltage of 1.4V_{RMS}, the absolute differences between most measurement points are below 0.09 V, with relative differences below 17%. With an input voltage of 0.2V_{RMS}, the absolute differences between all measurement points are below 0.03 V, with relative differences below 16%.

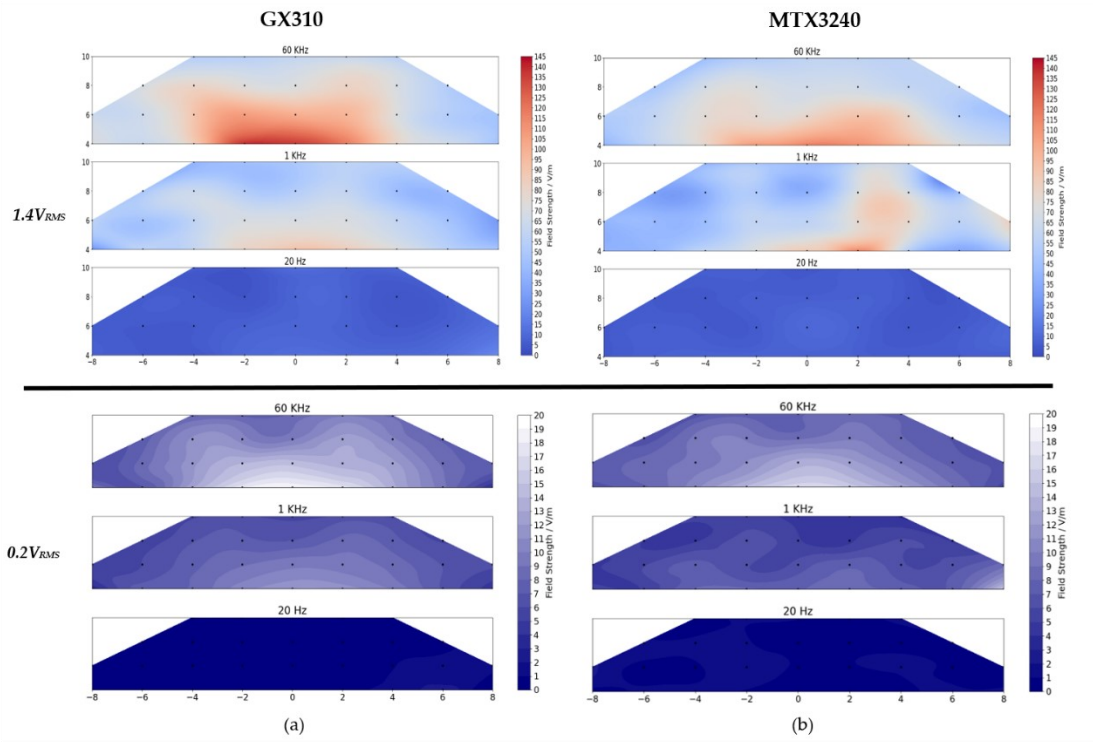

Figure 16. With input voltage of 1.4 V_{RMS} (Upper Panel) and 0.2 V_{RMS} (Lower Panel), electric fields generated by (a) Metrix GX310; (b) Metrix MTX 3240 at 60 kHz, 1 kHz and 20 Hz. The electric field strengths were determined by calculating the gradient of measured local voltages.

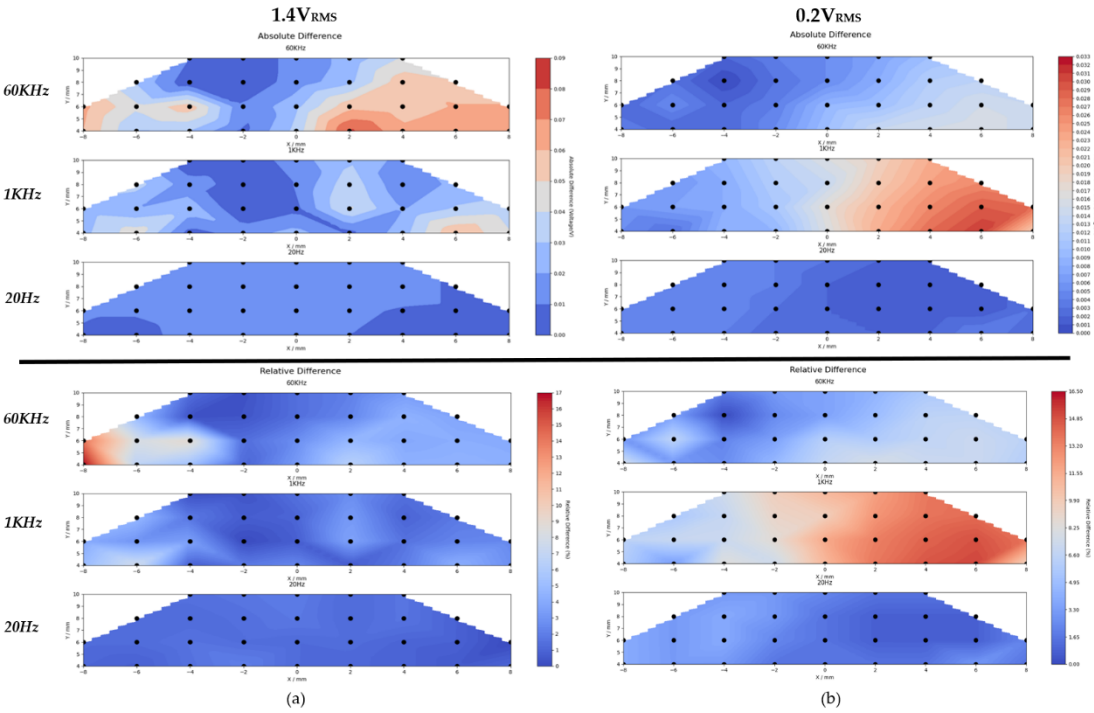

Figure 17. With input voltage (a) 1.4 V_{RMS} and (b) 0.2 V_{RMS}, the absolute (Upper Panel) and relative differences (Lower Panel) of the measured local voltages between two generators at 60 kHz, 1 kHz and 20 Hz.

3.3 Electrical Cell Stimulation In Vitro

3.3.1 Image Analysis

In total, 19,824 chondrocytes (male (n=9958): female (n=9866)) were analyzed. Statistical evaluation revealed that the form factor distribution for all identified chondrocytes spanned from a 25th percentile of 0.5901 to a 75th percentile of 0.8063, with a median value of 0.7064. Therefore, form factor of 0.7 was chosen as the threshold for chondrocytes shape classification in current experiment. This means that chondrocytes with a form factor above 0.7 were classified as rounded, whereas those with a form factor below 0.7 were classified as elongated. For a more intuitive comparison, the form factor of a rectangle with an aspect ratio of 2:1 is 0.698.

The ratio of rounded chondrocytes to elongated chondrocytes is presented in Figure 18. Analysis indicates that there was a significant increase (p=0.0374) in the ratio of rounded to elongated chondrocytes following stimulation at 15-20 V/m (mean ± SD ,1.353 ± 0.6) compared to the control group (1.06 ± 0.463) (Figure 18a). In contrast, no statistically significant changes were observed following stimulation at 0.8-1.2 V/m and 100-140 V/m. A sex-related difference was observed. Although not statistically significant, a higher ratio of rounded chondrocytes in male donors compared to female donors was noted (Figure 18b).

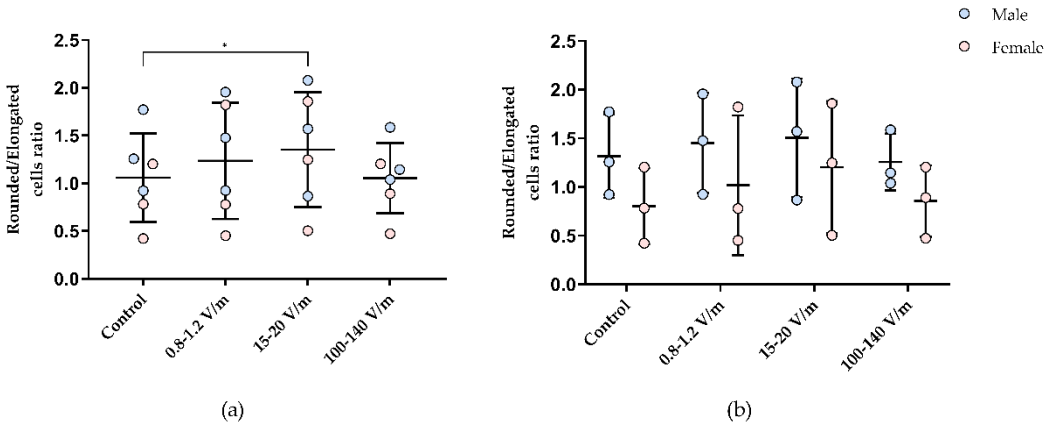

Figure 18. Human chondrocytes were exposed to electric fields of 0.8-1.2 V/m, 15-20 V/m, and 100-140 V/m for three days. Subsequently, cells were stained using Calcein AM and images were captured. The images were analyzed using CellProfiler and cells were classified into rounded and elongated cells with form factor as criteria. The ratio of rounded to elongated chondrocytes were then calculated for each group. (**a**) Comparison of Rounded/Elongated cell ratios between different groups without sex-based distinction; (**b**) Comparison of Rounded/Elongated cell ratios both within and between chondrocytes from male and female donors. Data were presented as scatter plots. The intermediary horizontal lines signify the mean values, while the upper and lower horizontal demarcations represent one standard deviation above and below the mean, respectively. Statistical analysis was conducted by (**a**) Paired t-test and (**b**) Paired t-test (Comparison within the same sex) and Unpaired t-test (Comparison between both sexes). * $p \leq 0.05$.

3.3.2 Synthesis of Collagen 2, Collagen 1 and Collagen 2/Collagen 1 Ratio

The quantification of collagen 1 and collagen 2 in the supernatant was conducted to determine the synthesis of ECM proteins following electrical stimulation (Figure 19). In comparison to the control group, electrical stimulation groups exhibited the following changes.

1) **0.8-1.2 V/m**: No significant changes were observed in the synthesis of collagen 1 and collagen 2, as well as the Col2/Col1 ratio.
2) **15-20 V/m**: No alterations were noted in collagen 2 and collagen 1 synthesis. However, an ascending trend (p=0.0897) in the Col2/Col1 synthesis ratio in this group (1.788 ± 0.622) was observed compared to the control group (1.572 ± 0.639) (Figure 19c)
3) **100-140 V/m**: A significant reduction in collagen 1 (0.144 ± 0.05 ng/µg, p = 0.0493) (Figure 19b) and collagen 2 (0.175 ± 0.062 ng/µg, p = 0.0180) (Figure 19a) was observed compared to the control group (0.17 ± 0.044 ng/µg; 0.245 ± 0.036 ng/µg, respectively). The Col2/Col1 synthesis ratio (1.401 ± 0.755) showed a decreasing trend (p=0.0824) compared to the control group (1.572 ± 0.639) (Figure 19c).

Additionally, comparison between electrical stimulation groups revealed that the Col2/Col1 synthesis ratio following 15-20 V/m stimulation (1.788 ± 0.622) was significantly higher (p = 0.0489) than that at 100-140 V/m (1.401 ± 0.755) (Figure 19c).

Furthermore, comparisons were made both within and between chondrocytes from male and female donors (Figure 20). Comparison within same sex revealed that in chondrocytes from male donors, an elevated (p = 0.0444) collagen 2 synthesis following stimulation at 0.8-1.2 V/m (0.249 ± 0.029 ng/µg) compared to 100-140 V/m (0.178 ± 0.053 ng/µg) (Figure 20a). Moreover, comparisons between both sexes showed that following stimulation at 0.8-1.2 V/m (0.293 ± 0.12 ng/µg) and 15-20 V/m (0.181 ± 0.055 ng/µg), chondrocytes from female donors exhibited a higher trend (p=0.0615; p=0.0630, respectively) of collagen 1 synthesis compared to chondrocytes from male donors (0.113 ± 0.013 ng/µg; 0.093 ± 0.024 ng/µg, respectively) (Figure 20b). Conversely, there were no significant differences in collagen 2 synthesis between chondrocytes from male and female donors. Consequently, following stimulation at 0.8-1.2 V/m, chondrocytes from female donors exhibited a significantly lower Col2/Col1 ratio (1.019 ± 0.324, p = 0.0185) compared to chondrocytes from male donors (2.234 ± 0.442). Meanwhile, following stimulation at 15-20 V/m, a decreasing trend (p=0.0689) of Col2/Col1 ratio in chondrocytes from female donors (1.347 ± 0.473) compared to chondrocytes from male donors (2.23 ± 0.399) was also observed (Figure 20c).

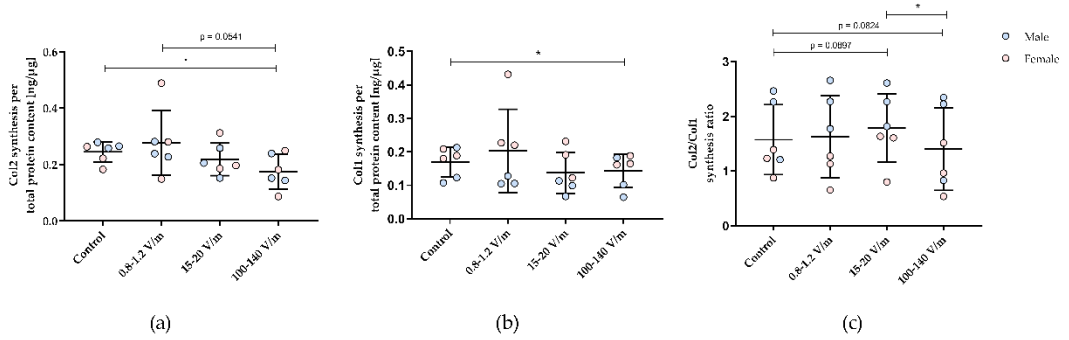

Figure 19. Human chondrocytes were exposed to electric fields of 0.8-1.2 V/m, 15-20 V/m, and 100-140 V/m for three days. Subsequently, the synthesis of collagen 2 and collagen 1 was assessed in the supernatant and normalized to total protein content. (**a**) Comparison of collagen 2 synthesis between different groups. (**b**) Comparison of collagen 1 synthesis between different groups; (**c**) Col2/Col1 ratio was calculated and compared between different groups. Data is presented as scatter plots. The intermediary horizontal lines signify the mean values, while the upper and lower horizontal demarcations represent one standard deviation above and below the mean, respectively. Statistical analysis was conducted using Paired t-test. * $p \leq 0.05$.

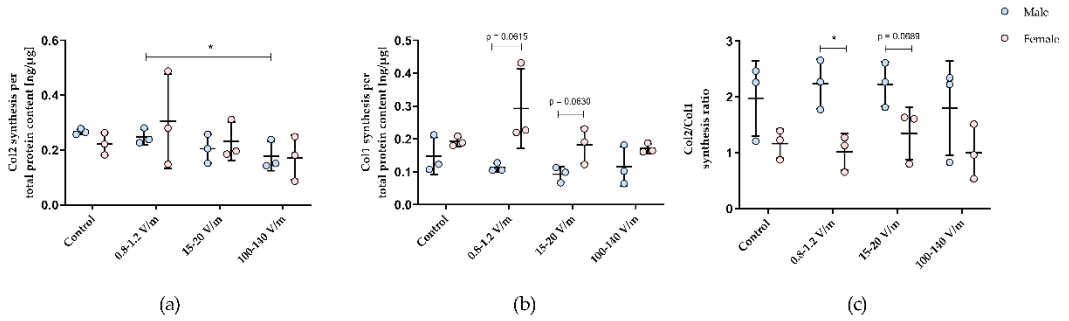

Figure 20. Human chondrocytes were exposed to electric fields of 0.8-1.2 V/m, 15-20 V/m, and 100-140 V/m for three days. Subsequently, the synthesis of collagen 2 and collagen 1 was assessed in the supernatant and normalized to total protein content. (**a**) Comparison of Collagen 2 synthesis both within and between chondrocytes from male and female donors. (**b**) Comparison of Collagen 1 synthesis both within and between chondrocytes from male and female donors. (**c**) The Col2/Col1 ratio was calculated separately for male and female, and then compared both within and between chondrocytes from male and female donors. Data is presented as scatter plots. The intermediary horizontal lines signify the mean values, while the upper and lower horizontal demarcations represent one standard deviation above and below the mean, respectively. Statistical analysis was conducted using Paired t-test for comparison within the same sex and unpaired t-test for comparison between both sexes. * $p \leq 0.05$.

3.3.3 Cellular Metabolic Activity

Metabolic activity of human chondrocytes was measured by water-soluble tetrazolium salt (WST-1) assay, whereby a high optical density (OD) correlates with a high metabolic activity of the cells. As shown in Figure 21a, following electrical stimulation

at 0.8-1.2 V/m and 15-20 V/m, the OD values (0.14 ± 0.042; 0.152 ± 0.026, respectively) exhibited a decreasing trend (p=0.0915; p=0.0830, respectively) compared to the control group (0.203 ± 0.076), indicating a decreasing trend in cell metabolic activity. Comparisons within and between chondrocytes from male and female donors revealed no differences in cell metabolic activity.

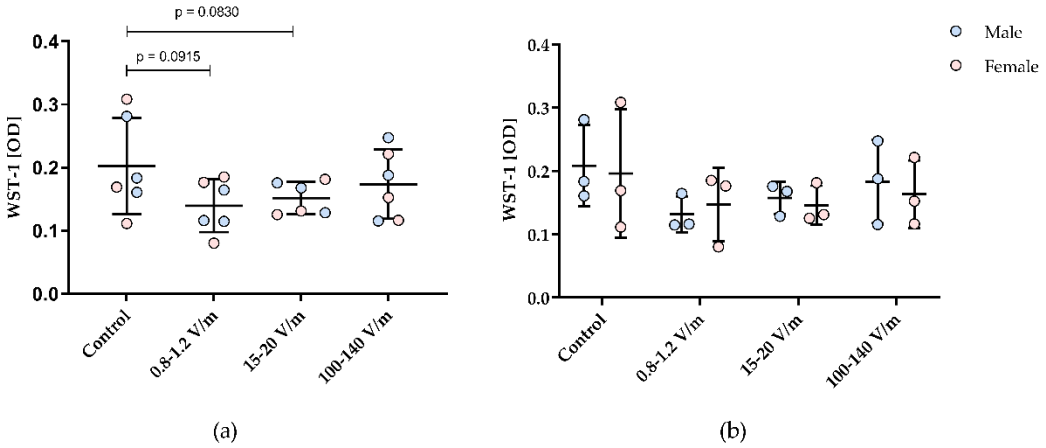

Figure 21. Metabolic activity of human chondrocytes subsequent to electrical stimulation with electric fields ranging from 0.8-1.2 V/m, 15-20 V/m, to 100-140 V/m for three days. (a) Comparison of cell metabolic activity between different groups without sex-based distinction; (b) Comparison of cell metabolic activity both within and between chondrocytes from male and female donors. The OD data is presented as scatter plots, where the scattered points indicate all values. The intermediary horizontal lines signify the mean values, while the upper and lower horizontal demarcations represent one standard deviation above and below the mean, respectively. Statistical analysis was conducted using (a) Paired t-test and (b) Wilcoxon matched-pairs signed rank test (Comparison within the same sex) and Mann-Whitney test (Comparison between chondrocytes from male and female donors). * $p \leq 0.05$.

4. Discussion

The treatment of articular cartilage defects remains a significant challenge in orthopedic surgery. One of the main challenges in cell-based therapies, such as autologous chondrocyte implantation (ACI) and matrix-assisted autologous chondrocyte implantation (MACI), is the tendency of chondrocytes to de-differentiate during in vitro expansion. This de-differentiation often results in the formation of fibrocartilage tissue, which is functionally and biomechanically inferior to hyaline cartilage, following re-implantation [29, 58, 71].

To address the de-differentiation of cartilaginous cells, electrical stimulation emerges as a promising and effective strategy [111, 190, 191]. Despite years of research and promising results, determining the optimal parameters for the electrical stimulation of chondrocytes remains a challenge. Vaca-González et al. [192] investigated the influence of various parameters including stimulation time, output frequencies, voltages and EF strength. The literature reaches a consensus on the use of sinusoidal alternating current with a frequency of 60 kHz [140, 157, 159, 164]. In current experiment, a frequency of 20 Hz was also used, which was rarely applied in human chondrocyte cultures in vitro but has shown good results in promoting bone regeneration [163, 175]. At the same time, investigations into electric stimulation encompass a wide range of field strengths, from as low as 5.2 x 10^{-6} V/m [161] to as high as 35 V/m [7]. A significant discrepancy exists in the use of electric field strength, with different studies varying in their stating about the optimal value. The most common field strength of 2 V/m, used by Brighton et al. [110, 112, 164], was reported to increase the production of collagen 2 and proteoglycans, as well as the upregulation of their mRNA expression. In contrast, Vaca-González et al. [157] suggested that the field strength should range between 0.4 V/cm and 0.8 V/m. What's more, electric field strengths of 20-35 V/m have been used on human chondrocytes and mesenchymal stem cells, resulting in increased synthesis of collagen 2 under hypoxic conditions [7]. Higher field strengths, such as 80-90 V/m, have not yet been reported for in vitro stimulation of chondrocytes, but have been used for in vitro cultures of osteoblasts and bacteria [163].

In the current work, the cell stimulation setup was based upon an established in vitro direct-coupled AC electrical stimulation setup [7]. Stimulation parameters, including the form of the sinusoidal signal and the duration of stimulation were selected based on the previous investigations by our working group [7, 163, 193]. The decision to use AC stimulation over DC was aimed at minimizing the potential adverse electrochemical reactions associated with DC stimulation [7]. These reactions, which can include shifts in pH, the formation of hydrogen peroxide, and the generation of reactive oxygen

species, can be detrimental to cell health and viability [194]. By oscillating the current, AC stimulation avoids the continuous unidirectional flow of electrons characteristic of DC, thereby reducing the likelihood of the aforementioned adverse reactions. Therefore, in contrast to DC, AC stimulation tends to produce less drastic electrochemical changes, making it a safer and more effective option for stimulating cells in biological experiments and therapeutic applications [7]. The study's preference for direct coupling over capacitive coupling in electrical stimulation was informed by practical considerations regarding energy efficiency and effectiveness. Compared to direct coupling, capacitive coupling typically requires much higher energy input to achieve the desired electric field strengths for effective stimulation. This increased energy requirement can pose limitations in terms of accessibility and feasibility of achieving specific electric field strengths needed for optimal cell stimulation.

In the current stimulation setup, the cylindrical electrodes and the dielectric irregularities of DMEM contribute to the relative inhomogeneity of its electric field. To determine the field strength within this setup through simulation , J. Zimmermann et al. [171] has constructed the latest simulation model for this electric field. The primary objective of this study is to verify the accuracy of the established simulation model by comparing the measured and simulated local voltages on the grid. In this process, the electric field strength can be determined by calculating the gradient of measured local voltages. Additionally, influence of electrodes and generators were also assessed by comparing the measured local voltages.

4.1 Method for Electric Field Strength Measurement

In 1985, Gundersen and Greenebaum presented three methodologies for measuring the strength of electric fields: the voltage-slope method, the current density-conductivity method, and the dipole method [169]. The voltage-slope method involves scanning the local voltage distribution within the stimulation chamber. The current density-conductivity method necessitates the measurement of the applied voltage, resulting current, and conductivity of the stimulated sample. The dipole method employs two measurement electrodes to determine the voltage difference between them. When assessing relatively homogeneous electric fields, these three methods exhibited less than a 3% variance in their electric field strength estimates [169]. For the comparatively inhomogeneous electric field in our experiment, we opted for the voltage-slope method. This measurement procedure was based on the research by Zimmermann et al [171], where some enhancements were made to the original voltage-slope method. Specifically, in a homogeneous electric field, the measured voltage is linearly related to the distance from the chamber, allowing estimation of the field strength based on the slope of this line. However, in a non-uniform electric field,

although the electric voltage gradient still represents the field strength, the relationship between the measured voltage and the distance from the chamber is no longer linear. Therefore, in this experiment, we upgraded to measuring the voltages at grid coordinate points. By calculating the voltage gradient on this grid, the electric field strength can be determined.

To determine the actual electric field strengths during electrical stimulation, it is crucial to replicate the environment within the incubator. Initially, a redlight lamp was used to heat the area surrounding the culture solution (Figure 22). The lamp's distance was adjusted based on the temperature inside the culture solution to achieve the desired 37 °C. However, this method presented significant drawbacks. Firstly, maintaining a constant temperature was challenging as the heating effect was difficult to stabilize. Secondly, it failed to mimic the closed environment of an incubator. Most critically, the lamp's irradiation accelerated the evaporation of the medium. To overcome these limitations, a box was constructed using acrylic board and polystyrene foam, effectively replicated the incubator's environment. The sealed box simulates the incubator's closed environment, while a hot water bath alongside with the controller ensures stable temperature control at 37±0.5 °C. Additionally, the chamber's top was made of a relatively thin acrylic plate to optimize visibility during the measurements. Hence, the constructed measurement environment fulfilled temperature-controlled, and ensured sufficient space and visibility.

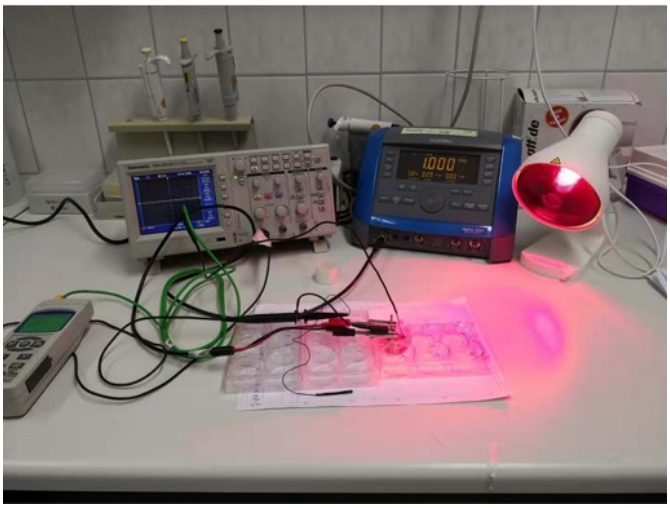

Figure 22. Initial version of the measurement environment construction: utilizing infrared lamp for heating up. This method was replaced by the temperature control box due to its difficulty in controlling temperature and its tendency to accelerate medium evaporation.

The choice of probes has also evolved. In the beginning, an uninsulated cannula was used as a probe, however, the tip of this probe was not fine enough to place precisely at the coordinate points. Moreover, a noteworthy phenomenon was observed when

using this probe. If the cannula was not kept straight, the measurement value changed [171]. Therefore, it was switched to the Ag/AgCl probe insulated with plastic skin and nail polish. By insulating the shaft of the probe, the deviation of the measured voltage from the expected voltage value was significantly reduced. However, during the measurement process, the nail polish used for insulation tends to peel off. Moreover, due to the softness of the probe material, bending often occurs during measurements, which impeded the measurement process. Eventually, a platinum-iridium probe from "MicroProbes" was chosen as the measurement probe. This probe has a better electrochemical stability, a thinner tip for more precise measurements and a higher bending strength, which is perfectly suited to our measurement requirements. Further, the measurement probe should be widely insulated to minimize the effect of probe. Keeping the probe in a vertical position is required to give the most accurate measurement results.

4.2. Verification of Electrical Simulation Model and Assessment of the Influence of Varying Generators and Electrodes

The measured local electric voltages and field strengths at 60 kHz exhibit a remarkable conformity with the simulated data. However, as the frequency decreases, this conformity diminishes. At 20 Hz, the electric field strength is less than 10% of the simulated field strength. This disparity is attributed to the relationship between impedance and frequency. In circuits, the impedance of capacitors and inductors varies with signal frequency. To be specific, the impedance of inductors is directly proportional to frequency, while the impedance of capacitors is inversely proportional to frequency [195]. The electrode-electrolyte interface resembles a double-layer capacitor, with impedance inversely proportional to frequency [196]. Therefore, at higher frequencies, the impedance of the electrode–electrolyte interface (EEI) is quite low, making its effect negligible and leading to a remarkable conformity between simulation and measurement results. However, at lower frequencies, increased impedance of EEI leads to reduced charge transfer within the electrolyte, resulting in a much smaller voltage drop than expected [171]. The calculated electric field strength confirms this theory. At a frequency of 20 Hz, the voltage drop across the medium is only a few millivolts. In conclusion, at high frequencies (60kHz and higher), the simulation model could accurately predict the electric field distribution and strength. However, at lower frequencies, the inaccuracy decreases due to the enhanced impedance of EEI. In the future, obtaining the impedance-frequency curve of EEI through measurements at different frequencies and incorporating this curve into the simulation model may enable more precise simulation of the electric field across a wider frequency range.

In stimulation experiments involving multiple electrodes, the consistency and

interchangeability of these electrodes are crucial. In our visualization analysis, slight differences were observed when comparing the electric fields generated by two electrodes of varying usage status. However, this difference is within an acceptable range. At frequencies of 60 kHz and 1 kHz, the relative differences at most measurement points remain within 10%. At a frequency of 20 Hz, the differences increase but still remain within 18%. Rather than manufacturing errors, this difference is more likely a result of material accumulation on the conductive metal surfaces, a common consequence of the electrical stimulation procedure [171]. Studies have shown that titanium implants can corrode in aqueous environments, forming calcium phosphate in electrolyte solutions [197, 198]. This process may be accentuated by active electrical stimulation [199]. Despite cleaning with 10% acetic acid and ultrasound, stubborn deposits might still persist. This highlights the importance of cleaning all electrodes with ascorbic acid and ultrasound and ensuring that they have similar electrode surface conditions before each cell experiment. Differences have also been observed between different generators. However, due to the complexity of the internal structures of generators, understanding the reasons for these differences is challenging. Therefore, in electrical stimulation experiments, we recommend using generators of the same model to minimize potential discrepancies.

4.3 Cell Stimulation Experiments

The aim of this work was to investigate the impact of various electric field strengths on human chondrocytes expanded in vitro with respect to possible sex differences. This involves three aspects: changes in cell morphology, the synthesis of extracellular matrix (ECM) components (specifically collagen 1 and collagen 2), and cell metabolic activity. To achieve this, chondrocytes were exposed to electric fields of varying strengths for a period of three days. Following exposure, morphological changes in chondrocytes were analyzed using CellProfiler following staining, the synthesis of collagen 1 and 2 in chondrocytes were determined by enzyme-linked immunosorbent assay (ELISA) and cell metabolic activity was assessed by water soluble tetrazolium (WST-1) test.

4.3.1 Cell Morphology

It is widely recognized that de-differentiated chondrocytes, as they shift from synthesizing collagen 2, 9, 11, and aggrecan to collagen 1 and 3, undergo a significant morphological transformation. They lose their characteristic rounded appearance and change to elongated appearance [72, 75]. In current experiment, we used form factor as the shape descriptor for chondrocytes. Research has demonstrated that during the process of chondrocyte de-differentiation, the form factor of chondrocytes decreases [200, 201], while inhibiting de-differentiation can restore chondrocytes to a rounded

shape [202]. In our experiment, we observed an increase in the proportion of rounded chondrocytes following 15-20 V/m electrical stimulation. This trend aligns with the increase in the Col2/Col1 ratio, indicating that 15-20 V/m EF might promote the re-differentiation of chondrocytes. Furthermore, studies indicate that when chondrocytes were maintained in rounded morphology, their replicative capacity as well as the quality and quantity of in vitro cartilage formation were improved [203]. This suggests that maintaining the rounded morphology of chondrocytes may also help for the generation of hyaline cartilage during autologous chondrocyte implantation.

4.3.2 ECM Synthesis

Assessment on chondrocyte ECM synthesis has yielded observations. Among the three experimental groups, a reduction in collagen 1 and collagen 2 synthesis was only observed following stimulation at 100-140 V/m, with no significant changes observed in the other two experimental groups. However, compared to the isolated analysis of collagen 1 and collagen 2, analyzing the ratio of collagen 2 (Col2)/ collagen 1 (Col1) provides a deeper understanding of chondrocyte de-differentiation or re-differentiation. Previous studies have indicated that in monolayer cultures, the Col2/Col1 ratio significantly decreases from over 15-fold to over 1800-fold within a mere 10 days, indicating cellular de-differentiation [83, 84]. In our current experiment, following stimulation of 15-20 V/m EF, an upward trend in the Col2/Col1 ratio was observed. This observation is consistent with cell morphology observation, suggesting that an electric field of 15-20 V/m might promote chondrocyte re-differentiation. Conversely, 100-140 V/m stimulation led to a downward trend in the Col2/Col1 ratio, indicating an EF of 100-140 V/m might inhibit chondrocyte re-differentiation. In a previous study by Hiemer et al. [7], electrical stimulation was applied to human chondrocytes, bone marrow mesenchymal stem cells (BM-MSCs), and co-cultures of chondrocytes and BM-MSCs under hypoxic and normoxic conditions. In their study, the electric field strength used was 20-35 V/m, which was close to the 15-20 V/m electric field strength in our study. Their results indicated that under normal hypoxic conditions, there was no significant change in neither collagen 1 and collagen 2 synthesis after electrical stimulation. However, under hypoxic conditions, an increase in the Col2/Col1 ratio was observed. Although in their study, the increase in the Col2/Col1 ratio was primarily attributed to an increase in Col2 synthesis - a phenomenon not observed in our research - the results of both studies suggest that EF field within a similar range may have the effect of inhibiting chondrocyte de-differentiation and promoting chondrocyte re-differentiation.

4.3.3 Cellular Metabolic Activity

Human chondrocytes following electrical stimulation at 0.8-1.2 V/m and 15-20 V/m

showed slightly diminishing trend in cell metabolic activity. This tends to be attributed to the direct contact between the electrodes and the electrolyte, which can lead to electrochemical reactions such as pH changes and the formation of hydrogen peroxide or reactive oxygen species in electrical stimulation that are harmful to the exposed cells [151]. However, in previous study which also used direct coupling to deliver 20-35 V/m electric field on human chondrocytes and mesenchymal stem cells, no changes in cell metabolic activity were observed [7]. Theoretically, changing the direct coupling to capacitive coupling can prevent negative effects of electrochemical reaction by avoiding direct contact of electrodes and electrolyte [151, 204]. However, a decrease in metabolic activity of human chondrocytes was observed by Krueger et al. [161] when using capacitive coupling, with increased synthesis rates of collagen 2 and glycosaminoglycans noted simultaneously. Therefore, the decrease in metabolic activity of chondrocytes may be attributed to other reasons other than electrochemical changes. It has been reported that that during the initial phase of de-differentiation, chondrocytes exhibit a glycolytic phenotype with heightened expression of metabolic and antioxidant-related genes, leading to increased cellular activity [205]. This leads us to hypothesize that the observed decrease in cellular activity may be attributed to a weakening of chondrocyte de-differentiation. Upon comprehensive observation of the OD values and Col2/Col1 ratio of electrical stimulation groups, a certain inverse relationship is observed. Specifically, the only electrical stimulation group that didn't show reduced cellular metabolic activity, which is 100-140 V/m, exhibited a decrease in the Col2/Col1 ratio. Meanwhile, a decrease in the Col2/Col1 ratio implies an enhancement in the trend of de-differentiation [83, 84].

4.3.4 Sex Difference on Chondrocyte Re-differentiation

Comparison between chondrocytes from male and female revealed significantly higher collagen 1 synthesis and lower Col2/Col1 ratios in cells from female donors, especially after electrical stimulation with the lower electric fields. At the same time, these cells display a higher proportion of elongated chondrocytes following in vitro culture. Despite the average age of female donors being 7.4 years higher than that of male donors, the comparison among donors did not reveal any relationship between age and collagen synthesis. Moreover, literature suggests that the synthesis of extracellular matrix macromolecules does not depend on age [206]. Therefore, we are inclined to attribute these differences to sexes. Other studies revealed further that chondrocytes from female patients showed significantly lower gene expression and protein synthesis of SOX9 compared to chondrocytes from male donors [207]. Similar sex disparities were also observed in bovine chondrocytes [208] . Meanwhile, literature indicates that SOX9 plays a role in inhibiting the de-differentiation of chondrocytes [209] and SOX9 transduction can significantly reduce the expression of collagen 1 [210]. This might

explain the higher levels of collagen 1 synthesis observed in chondrocytes from female donors in our study, suggesting that these cells have a higher tendency towards de-differentiation compared to male. Besides chondrocytes, similar sex differences were also reported in human MSCs derived from vBMA clots [211]. In addition to higher expression levels of specific growth factors involved in bone regeneration and defined osteogenic markers in male MSCs, F. Salamanna et al [211].also observed higher SOX9 expression, suggesting not only greater osteogenic but also greater chondrogenic differentiation capacity in male MSCs. This is consistent with the higher chondrogenic differentiation capacity observed in chondrocytes from male donors. Meanwhile, the higher tendency to de-differentiate implies a greater likelihood of producing fibrocartilage with inferior mechanical properties during in vitro expansion for ACI [78]. Therefore, this observation led to hypothesize whether the postoperative out-comes of ACI might be less favorable in females compared to males. Consulting the literature on the differences between the sexes in ACI outcomes, Filardo et al. [212] evaluated 250 knees treated with matrix-assisted autologous chondrocyte implantation (MACI) at 1, 2, and minimum 5 years of follow-up. This evaluation demonstrated superior subjective International Knee Documentation Committee (IKDC) scores in male patients compared to male patients at all follow-up intervals. Similarly, Kreuz et al. [63] followed up 52 patients who underwent ACI at 6, 12, and 48 months postoperatively, observing significantly better KOOS (Knee Injury and Osteoarthritis Outcome) scores and stronger strength values in male patients during the follow-up period. These follow-up results, which show consistency with our hypothesis, implies that difference in de-differentiation tendency between chondrocytes from male and female donors during in vitro expansion might be one of the reasons for the differing postoperative outcomes of ACI between sexes.

4.4 Outlook

Articular cartilage, due to its unique structural composition and functional attributes, is highly susceptible to degradation and wear. In addressing cartilage repair, ACI has become an increasingly viable and promising method. The critical challenge in ACI lies in promoting the re-differentiation of chondrocytes during the process of expansion in vitro. Electrical stimulation has emerged as a novel and effective approach to encourage this process. To ascertain the electric field strengths of the established stimulation setup, which delivers alternating current electric field by direct coupling, we developed a simulation model and subjected it to verification.

Our verification work demonstrated that the simulation model can accurately simulate the electric fields at high frequencies (60kHz and above), with this accuracy diminishing at lower frequencies. In the future, obtaining the impedance-frequency

curve of EEI through measurements at different frequencies and incorporating it into the simulation model might enable precise field strength simulation at low frequencies. Furthermore, through comparisons of electrodes of varying usage duration and generators of different models, it was found that electrodes with varying usage durations could influence the electric field, but remain within acceptable range, and different models of generators exhibit a similar effect. This highlights the importance of ensuring that all electrodes have similar surface conditions before each cell experiment. Meanwhile, generators of the same model were used in the subsequent electrical stimulation experiments to avoid potential influences.

The results of the electrical stimulation experiments indicate a positive impact of the 15-20 V/m EF on the re-differentiation of chondrocytes, whereas 100-140 V/m had an inhibitory effect on chondrocyte re-differentiation. Moreover, the comparisons between sexes suggest that chondrocytes from female donors are more prone to de-differentiate in vitro compared to those from female donors. However, this study showed limitations. Due to the limited number of donors, only three groups of chondrocytes from each sex were stimulated and assessed. Future studies will include more samples of chondrocytes from male and female donors to further validate the observed gender differences. In addition, this study only assessed collagen 2 and collagen 1 as markers of chondrocyte re-differentiation and de-differentiation. In future experiments, more re-differentiation markers such as Aggrecan and SOX9, as well as the dedifferentiation markers such as Matrix Metalloproteinase-13, will be evaluated to more comprehensively analyze the regulatory effects of the electrical stimulation on the differentiation of human chondrocytes. What's more, in addition to inherent differences in re-differentiation capacity based on sex, it was observed that electrical stimulation exhibited a more significant re-differentiation-promoting effect on chondrocytes derived from male donors. In future experiments, the stimulation period will be extended to verify whether there still exists a difference in the response of chondrocytes from male and female donors to electrical stimulation.

5. Summary

Human articular cartilage is crucial for the smooth functioning of joints, providing a smooth, well-lubricated surface that minimizes friction and cushions external forces during movement. Throughout this process, it endures stress and friction. However, human articular cartilage is characterized by the absence of blood and lymphatic vessels, the lack of innervation, and a low chondrocyte-to-matrix volume ratio. These properties result in a limited capacity for self-repair and regeneration. The unique structural composition and function of human articular cartilage make it particularly susceptible to substantial degradation and wear. Trauma-induced cartilage lesions and age-related cartilage degeneration are two prevalent factors that lead to impaired joint function, pain, and ultimately arthritis. In the field of cartilage repair, autologous chondrocyte implantation (ACI) has emerged as an increasingly viable and promising approach. The critical challenge of ACI lies in promoting chondrocyte re-differentiation during in vitro expansion. Electrical stimulation has emerged as a novel and effective method to facilitate this process. In current study, direct coupling method was used to submit alternating current electric fields to chondrocytes cultured in vitro. Prior to this, a simulation model for this stimulation setup was constructed to simulate its field distribution. The accuracy of this model was verified by measuring the local voltages and subsequently comparing with simulated values. The validation results proved that the simulation model can accurately simulate the electric field at high frequencies but exhibited reduced accuracy at lower frequencies. During this process, the electric field strengths were determined by calculating the gradient of measured local voltages. Meanwhile, considering our cell electrostimulation experiments require the simultaneous use of multiple electrodes and generators, an assessment was conducted on the influences of used electrodes and generators. The results demonstrate that electrodes with varying usage durations have an influence on electric field, but remain within acceptable range, and different models of generators exhibit a similar effect. The difference in electrodes might be due to material accumulation on the conductive metal surfaces. This underscores the importance of ensuring that all electrodes have similar surface conditions before cell experiment. Meanwhile, to avoid potential influence of generator, generators of the same model were used in the subsequent electrical stimulation experiments. Three electric field strengths of 0.8-1.2 V/m, 15-20 V/m, and 100-140 V/m were used for human chondrocyte stimulation. Chondrocytes isolated from the articular cartilage of male and female donors undergoing total knee replacement surgery were exposed to electric fields for three days. Subsequent cell morphology analysis revealed an increased proportion of rounded, chondrocyte-like cells following stimulation at 15-20 V/m. Simultaneously, there was an upward trend in the Collagen 2 / Collagen 1 ratio following stimulation at

15-20 V/m. Conversely, a downward trend in the Collagen 2 / Collagen 1 ratio was noted following stimulation at 100-140 V/m. These findings suggest that electric field of 15-20 V/m might has a promoting effect on chondrocyte re-differentiation, while a field of 100-140 V/m might have an inhibitory effect. Cell metabolic activity indicated a reduction trend following electrical stimulation at 0.8-1.2 V/m and 15-20 V/m. This might be due to inhibited cell de-differentiation. Furthermore, comparative analysis between sexes revealed that chondrocytes from female donors exhibited higher collagen 1 synthesis, decreased Collagen 2/Collagen1 ratio and a greater proportion of elongated, fibroblast-like cells compared to males. These observations suggest that chondrocytes from male donors might have a higher chondrogenic differentiation capacity compared to chondrocytes from female donors, while chondrocytes from female donors are more prone to de-differentiation when cultured in vitro.

6. References

[1] Y. Krishnan, A.J. Grodzinsky, Cartilage diseases, Matrix biology : journal of the International Society for Matrix Biology 71-72 **(2018)** 51-69. https://doi.org/10.1016/j.matbio.2018.05.005

[2] A.M. Bhosale, J.B. Richardson, Articular cartilage: structure, injuries and review of management, British medical bulletin 87 **(2008)** 77-95. https://doi.org/10.1093/bmb/ldn025

[3] J.P. Halloran, S. Sibole, C.C. van Donkelaar, M.C. van Turnhout, C.W. Oomens, J.A. Weiss, F. Guilak, A. Erdemir, Multiscale mechanics of articular cartilage: potentials and challenges of coupling musculoskeletal, joint, and microscale computational models, Annals of biomedical engineering 40(11) **(2012)** 2456-74. https://doi.org/10.1007/s10439-012-0598-0

[4] J.E. Lafont, Lack of oxygen in articular cartilage: consequences for chondrocyte biology, International journal of experimental pathology 91(2) **(2010)** 99-106. https://doi.org/10.1111/j.1365-2613.2010.00707.x

[5] N.P. Cohen, R.J. Foster, V.C. Mow, Composition and dynamics of articular cartilage: structure, function, and maintaining healthy state, The Journal of orthopaedic and sports physical therapy 28(4) **(1998)** 203-15. https://doi.org/10.2519/jospt.1998.28.4.203

[6] A.J. Sophia Fox, A. Bedi, S.A. Rodeo, The basic science of articular cartilage: structure, composition, and function, Sports health 1(6) **(2009)** 461-8. https://doi.org/10.1177/1941738109350438

[7] B. Hiemer, M. Krogull, T. Bender, J. Ziebart, S. Krueger, R. Bader, A. Jonitz-Heincke, Effect of electric stimulation on human chondrocytes and mesenchymal stem cells under normoxia and hypoxia, Mol Med Rep 18(2) **(2018)** 2133-2141. https://doi.org/10.3892/mmr.2018.9174

[8] V.C. Mow, A. Ratcliffe, A.R. Poole, Cartilage and diarthrodial joints as paradigms for hierarchical materials and structures, Biomaterials 13(2) **(1992)** 67-97. https://doi.org/10.1016/0142-9612(92)90001-5

[9] R. Karuppal, Current concepts in the articular cartilage repair and regeneration, Journal of orthopaedics 14(2) **(2017)** A1-a3. https://doi.org/10.1016/j.jor.2017.05.001

[10] K. Zhang, J. Guo, Z. Ge, J. Zhang, Nanosecond pulsed electric fields (nsPEFs) regulate phenotypes of chondrocytes through Wnt/β-catenin signaling pathway, Scientific reports 4 **(2014)** 5836. https://doi.org/10.1038/srep05836

[11] E. Charlier, C. Deroyer, F. Ciregia, O. Malaise, S. Neuville, Z. Plener, M. Malaise, D. de Seny, Chondrocyte dedifferentiation and osteoarthritis (OA), Biochemical pharmacology 165 **(2019)** 49-65. https://doi.org/10.1016/j.bcp.2019.02.036

[12] E.M. Darling, S. Zauscher, F. Guilak, Viscoelastic properties of zonal articular chondrocytes measured by atomic force microscopy, Osteoarthritis and cartilage 14(6) **(2006)** 571-9. https://doi.org/10.1016/j.joca.2005.12.003

[13] F. Guilak, A. Ratcliffe, V.C. Mow, Chondrocyte deformation and local tissue strain in articular cartilage: a confocal microscopy study, Journal of orthopaedic research : official publication of the Orthopaedic Research Society 13(3) **(1995)** 410-21. https://doi.org/10.1002/jor.1100130315

[14] M. Wong, P. Wuethrich, P. Eggli, E. Hunziker, Zone-specific cell biosynthetic activity in mature bovine articular cartilage: A new method using confocal microscopic stereology and quantitative autoradiography, 14(3) **(1996)** 424-432. https://doi.org/10.1002/jor.1100140313

[15] A.J. Freemont, V. Hampson, R. Tilman, P. Goupille, Y. Taiwo, J.A. Hoyland, Gene expression of matrix metalloproteinases 1, 3, and 9 by chondrocytes in osteoarthritic human knee articular cartilage is zone and grade specific, Annals of the rheumatic diseases 56(9) **(1997)** 542-9. https://doi.org/10.1136/ard.56.9.542

[16] D.A. Lee, T. Noguchi, M.M. Knight, L. O'donnell, G. Bentley, D.L. Bader, Response of chondrocyte subpopulations cultured within unloaded and loaded agarose, 16(6) **(1998)** 726-733. https://doi.org/10.1002/jor.1100160615

[17] I. Youn, J.B. Choi, L. Cao, L.A. Setton, F. Guilak, Zonal variations in the three-dimensional morphology of the chondron measured in situ using confocal microscopy, Osteoarthritis and cartilage 14(9) **(2006)** 889-97. https://doi.org/10.1016/j.joca.2006.02.017

[18] A.R. Poole, T. Kojima, T. Yasuda, F. Mwale, M. Kobayashi, S. Laverty, Composition and structure of articular cartilage: a template for tissue repair, Clinical orthopaedics and related research (391 Suppl) **(2001)** S26-33. https://doi.org/10.1097/00003086-200110001-00004

[19] A.F. Steinert, S.C. Ghivizzani, A. Rethwilm, R.S. Tuan, C.H. Evans, U. Noth, Major biological obstacles for persistent cell-based regeneration of articular cartilage, Arthritis research & therapy 9(3) **(2007)** 213. https://doi.org/10.1186/ar2195

[20] S. Camarero-Espinosa, B. Rothen-Rutishauser, E.J. Foster, C. Weder, Articular cartilage: from formation to tissue engineering, Biomaterials Science 4(5) **(2016)** 734-767. https://doi.org/10.1039/C6BM00068A

[21] O.S. Schindler, Current concepts of articular cartilage repair, Acta orthopaedica Belgica 77(6) **(2011)** 709-26.

[22] L. Roseti, G. Desando, C. Cavallo, M. Petretta, B. Grigolo, Articular Cartilage Regeneration in Osteoarthritis, Cells 8(11) **(2019)**. https://doi.org/10.3390/cells8111305

[23] L.J. Sandell, T. Aigner, Articular cartilage and changes in arthritis. An introduction: cell biology of osteoarthritis, Arthritis research 3(2) **(2001)** 107-13. https://doi.org/10.1186/ar148

[24] M.B. Goldring, Chondrogenesis, chondrocyte differentiation, and articular cartilage metabolism in health and osteoarthritis, Therapeutic advances in musculoskeletal disease 4(4) **(2012)** 269-85. https://doi.org/10.1177/1759720x12448454

[25] L.J. Sandell, A.M. Nalin, R.A. Reife, Alternative splice form of type II procollagen mRNA (IIA) is predominant in skeletal precursors and non-cartilaginous tissues during early mouse development, Developmental dynamics : an official publication of the American Association of Anatomists 199(2) **(1994)** 129-40. https://doi.org/10.1002/aja.1001990206

[26] D. Eyre, Collagen of articular cartilage, Arthritis research 4(1) **(2002)** 30-35. https://doi.org/10.1186/ar380

[27] E. Reichenberger, T. Aigner, K. von der Mark, H. Stöss, W. Bertling, In situ hybridization studies on the expression of type X collagen in fetal human cartilage, Developmental biology 148(2) **(1991)** 562-72. https://doi.org/10.1016/0012-1606(91)90274-7

[28] T. Kirsch, B. Swoboda, K. von der Mark, Ascorbate independent differentiation of human chondrocytes in vitro: simultaneous expression of types I and X collagen and matrix mineralization, Differentiation; research in biological diversity 52(1) **(1992)** 89-100. https://doi.org/10.1111/j.1432-0436.1992.tb00503.x

[29] P.D. Benya, J.D. Shaffer, Dedifferentiated chondrocytes reexpress the differentiated collagen phenotype when cultured in agarose gels, Cell 30(1) **(1982)** 215-24.

[30] T. Aigner, J. Stove, Collagens--major component of the physiological cartilage matrix, major target of cartilage degeneration, major tool in cartilage repair, Advanced drug delivery reviews 55(12) **(2003)** 1569-93. https://doi.org/10.1016/j.addr.2003.08.009

[31] Y.M. Bastiaansen-Jenniskens, W. Koevoet, A.C. de Bart, J.C. van der Linden, A.M. Zuurmond, H. Weinans, J.A. Verhaar, G.J. van Osch, J. Degroot, Contribution of collagen network features to functional properties of engineered cartilage, Osteoarthritis and cartilage 16(3) **(2008)** 359-66. https://doi.org/10.1016/j.joca.2007.07.003

[32] T.A. Ahmed, M.T. Hincke, Strategies for articular cartilage lesion repair and functional restoration, Tissue engineering. Part B, Reviews 16(3) **(2010)** 305-29. https://doi.org/10.1089/ten.TEB.2009.0590

[33] S. Giovannini, J. Diaz-Romero, T. Aigner, P. Heini, P. Mainil-Varlet, D. Nesic, Micromass co-culture of human articular chondrocytes and human bone marrow mesenchymal stem cells to investigate stable neocartilage tissue formation in vitro, European cells & materials 20 **(2010)** 245-59. https://doi.org/10.22203/ecm.v020a20

[34] F. McCormick, A. Yanke, M.T. Provencher, B.J. Cole, Minced articular cartilage--basic science, surgical technique, and clinical application, Sports medicine and arthroscopy review 16(4) **(2008)** 217-20. https://doi.org/10.1097/JSA.0b013e31818e0e4a

[35] R. Zehbe, J. Libera, U. Gross, H. Schubert, Short-term human chondrocyte culturing on oriented collagen coated gelatine scaffolds for cartilage replacement, Bio-medical materials and engineering 15(6) **(2005)** 445-54.

[36] K. Lewandrowski, A. Ekkernkamp, A. David, G. Muhr, G.J.T.A.j.o.k.s. Schollmeier, Classification of articular cartilage lesions of the knee at arthroscopy, 9(3) **(1996)** 121-128.

[37] R.E. Outerbridge, The etiology of chondromalacia patellae, The Journal of bone and joint surgery. British volume 43-b **(1961)** 752-7. https://doi.org/10.1302/0301-620x.43b4.752

[38] M. Brittberg, A. Lindahl, A. Nilsson, C. Ohlsson, O. Isaksson, L. Peterson, Treatment of Deep Cartilage Defects in the Knee with Autologous Chondrocyte Transplantation, 331(14) **(1994)** 889-895. https://doi.org/10.1056/nejm199410063311401

[39] J.S. Temenoff, A.G. Mikos, Review: tissue engineering for regeneration of articular cartilage, Biomaterials 21(5) **(2000)** 431-40. https://doi.org/10.1016/s0142-9612(99)00213-6

[40] T.A. Ahmed, M. Griffith, M. Hincke, Characterization and inhibition of fibrin hydrogel-degrading enzymes during development of tissue engineering scaffolds, Tissue engineering 13(7) **(2007)** 1469-77. https://doi.org/10.1089/ten.2006.0354

[41] B.C. Fleming, B.L. Proffen, P. Vavken, M.R. Shalvoy, J.T. Machan, M.M. Murray, Increased platelet concentration does not improve functional graft healing in bio-enhanced ACL reconstruction, Knee Surgery, Sports Traumatology, Arthroscopy 23(4) **(2015)** 1161-1170. https://doi.org/10.1007/s00167-014-2932-6

[42] R. Yoshida, M. Cheng, M.M. Murray, Increasing platelet concentration in platelet-rich plasma inhibits anterior cruciate ligament cell function in three-dimensional culture, 32(2) **(2014)** 291-295. https://doi.org/10.1002/jor.22493

[43] D. Dallari, C. Stagni, N. Rani, G. Sabbioni, P. Pelotti, P. Torricelli, M. Tschon, G. Giavaresi, Ultrasound-Guided Injection of Platelet-Rich Plasma and Hyaluronic Acid, Separately and in Combination, for Hip Osteoarthritis:A Randomized Controlled Study, 44(3) **(2016)** 664-671. https://doi.org/10.1177/0363546515620383

[44] M. Battaglia, F. Guaraldi, F. Vannini, G. Rossi, A. Timoncini, R. Buda, S. Giannini, Efficacy of ultrasound-guided intra-articular injections of platelet-rich plasma versus hyaluronic acid for hip osteoarthritis, Orthopedics 36(12) **(2013)** e1501-8. https://doi.org/10.3928/01477447-20131120-13

[45] G. Milano, L. Deriu, E.S. Passino, G. Masala, M. Saccomanno, R. Postacchini, C. Fabbriciani, The Effect of Autologous Conditioned Plasma on the Treatment of Focal Chondral Defects of the Knee. An Experimental Study, 24(1_suppl2) **(2011)** 117-124. https://doi.org/10.1177/03946320110241s222

[46] Y.H. Chang, H.W. Liu, K.C. Wu, D.C. Ding, Mesenchymal Stem Cells and Their Clinical Applications in Osteoarthritis, Cell transplantation 25(5) **(2016)** 937-50. https://doi.org/10.3727/096368915x690288

[47] J.P. Zlotnicki, A.G. Geeslin, I.R. Murray, F.A. Petrigliano, R.F. LaPrade, B.J. Mann, V. Musahl, Biologic Treatments for Sports Injuries II Think Tank-Current

Concepts, Future Research, and Barriers to Advancement, Part 3: Articular Cartilage, Orthop J Sports Med 4(4) **(2016)** 2325967116642433. https://doi.org/10.1177/2325967116642433

[48] A. Xie, L. Nie, G. Shen, Z. Cui, P. Xu, H. Ge, Q. Tan, The application of autologous platelet‐rich plasma gel in cartilage regeneration, Molecular medicine reports 10(3) **(2014)** 1642-8. https://doi.org/10.3892/mmr.2014.2358

[49] J. Lana, L.F. da Fonseca, R.D.R. Macedo, T. Mosaner, W. Murrell, A. Kumar, J. Purita, M.A.P. de Andrade, Platelet-rich plasma vs bone marrow aspirate concentrate: An overview of mechanisms of action and orthobiologic synergistic effects, World journal of stem cells 13(2) **(2021)** 155-167. https://doi.org/10.4252/wjsc.v13.i2.155

[50] R.A. Hauser, A. Orlofsky, Regenerative injection therapy with whole bone marrow aspirate for degenerative joint disease: a case series, Clinical medicine insights. Arthritis and musculoskeletal disorders 6 **(2013)** 65-72. https://doi.org/10.4137/cmamd.S10951

[51] X. Li, A. Shah, P. Franklin, R. Merolli, J. Bradley, B. Busconi, Arthroscopic debridement of the osteoarthritic knee combined with hyaluronic acid (Orthovisc) treatment: a case series and review of the literature, Journal of orthopaedic surgery and research 3 **(2008)** 43. https://doi.org/10.1186/1749-799x-3-43

[52] A.J. Krych, D.B.F. Saris, M.J. Stuart, B. Hacken, Cartilage Injury in the Knee: Assessment and Treatment Options, The Journal of the American Academy of Orthopaedic Surgeons 28(22) **(2020)** 914-922. https://doi.org/10.5435/jaaos-d-20-00266

[53] G. Versier, F. Dubrana, Treatment of knee cartilage defect in 2010, Orthopaedics & traumatology, surgery & research : OTSR 97(8 Suppl) **(2011)** S140-53. https://doi.org/10.1016/j.otsr.2011.09.007

[54] D.L. Richter, J.A. Tanksley, M.D. Miller, Osteochondral Autograft Transplantation: A Review of the Surgical Technique and Outcomes, 24(2) **(2016)** 74-78. https://doi.org/10.1097/jsa.0000000000000099

[55] W.D. Bugbee, F. Richard Convery, OSTEOCHONDRAL ALLOGRAFT TRANSPLANTATION, Clinics in Sports Medicine 18(1) **(1999)** 67-75. https://doi.org/https://doi.org/10.1016/S0278-5919(05)70130-7

[56] J.M. Lopez-Alcorocho, L. Aboli, I. Guillen-Vicente, E. Rodriguez-Inigo, M. Guillen-Vicente, T.F. Fernandez-Jaen, S. Arauz, S. Abelow, P. Guillen-Garcia, Cartilage Defect Treatment Using High-Density Autologous Chondrocyte Implantation: Two-Year Follow-up, Cartilage 9(4) **(2018)** 363-369. https://doi.org/10.1177/1947603517693045

[57] M. Hevesi, A.J. Krych, D.B.F. Saris, Treatment of Cartilage Defects With the Matrix-Induced Autologous Chondrocyte Implantation Cookie Cutter Technique, Arthroscopy Techniques 8(6) **(2019)** E591-E596. https://doi.org/10.1016/j.eats.2019.01.022

[58] R.L. Davies, N.J. Kuiper, Regenerative Medicine: A Review of the Evolution of Autologous Chondrocyte Implantation (ACI) Therapy, Bioengineering (Basel, Switzerland) 6(1) **(2019)**. https://doi.org/10.3390/bioengineering6010022

[59] T.M. Southworth, N.B. Naveen, B.U. Nwachukwu, B.J. Cole, R.M. Frank, Orthobiologics for Focal Articular Cartilage Defects, Clinics in sports medicine 38(1) **(2019)** 109-122. https://doi.org/10.1016/j.csm.2018.09.001

[60] M.I. Kennedy, K. Whitney, T. Evans, R.F. LaPrade, Platelet-Rich Plasma and Cartilage Repair, Current reviews in musculoskeletal medicine 11(4) **(2018)** 573-582. https://doi.org/10.1007/s12178-018-9516-x

[61] M. Brittberg, Autologous chondrocyte implantation--technique and long-term follow-up, Injury 39 Suppl 1 **(2008)** S40-9. https://doi.org/10.1016/j.injury.2008.01.040

[62] H.S. McCarthy, S. Roberts, A histological comparison of the repair tissue formed when using either Chondrogide® or periosteum during autologous chondrocyte implantation, Osteoarthritis and Cartilage 21(12) **(2013)** 2048-2057. https://doi.org/https://doi.org/10.1016/j.joca.2013.10.004

[63] P.C. Kreuz, S. Müller, C. Erggelet, A. von Keudell, T. Tischer, C. Kaps, P. Niemeyer, A. Hirschmüller, Is gender influencing the biomechanical results after autologous chondrocyte implantation?, Knee Surgery, Sports Traumatology, Arthroscopy 22(1) **(2014)** 72-79. https://doi.org/10.1007/s00167-012-2280-3

[64] J. Gille, P. Behrens, A.P. Schulz, R. Oheim, B. Kienast, Matrix-Associated Autologous Chondrocyte Implantation:A Clinical Follow-Up at 15 Years, 7(4) **(2016)** 309-315. https://doi.org/10.1177/1947603516638901

[65] E. Basad, F.R. Wissing, P. Fehrenbach, M. Rickert, J. Steinmeyer, B.J.K.S. Ishaque, Sports Traumatology, Arthroscopy, Matrix-induced autologous chondrocyte implantation (MACI) in the knee: clinical outcomes and challenges, 23(12) **(2015)** 3729-3735. https://doi.org/10.1007/s00167-014-3295-8

[66] T. Ogura, B.A. Mosier, T. Bryant, T. Minas, A 20-Year Follow-up After First-Generation Autologous Chondrocyte Implantation, 45(12) **(2017)** 2751-2761. https://doi.org/10.1177/0363546517716631

[67] M.E. Al-Masawa, W. Zaman, K.H. Chua, Biosafety evaluation of culture-expanded human chondrocytes with growth factor cocktail: a preclinical study, Scientific Reports 10(1) **(2020)**. https://doi.org/10.1038/s41598-020-78395-y

[68] D.L. Bader, M.M. Knight, 4 - Measuring the biomechanical properties of cartilage cells, in: C. Archer, J. Ralphs (Eds.), Regenerative Medicine and Biomaterials for the Repair of Connective Tissues, Woodhead Publishing2010, pp. 106-136.

[69] H.C. Anderson, S. Chacko, J. Abbott, H. Holtzer, The loss of phenotypic traits by differentiated cells in vitro. VII. Effects of 5-bromodeoxyuridine and prolonged culturing on fine structure of chondrocytes, The American journal of pathology 60(2) **(1970)** 289-312.

[70] K. von der Mark, V. Gauss, H. von der Mark, P. Muller, Relationship between cell shape and type of collagen synthesised as chondrocytes lose their cartilage

phenotype in culture, Nature 267(5611) **(1977)** 531-2. https://doi.org/10.1038/267531a0

[71] Z. Lin, J.B. Fitzgerald, J. Xu, C. Willers, D. Wood, A.J. Grodzinsky, M.H. Zheng, Gene expression profiles of human chondrocytes during passaged monolayer cultivation, Journal of orthopaedic research : official publication of the Orthopaedic Research Society 26(9) **(2008)** 1230-7. https://doi.org/10.1002/jor.20523

[72] L. Duan, B. Ma, Y. Liang, J. Chen, W. Zhu, M. Li, D. Wang, Cytokine networking of chondrocyte dedifferentiation in vitro and its implications for cell-based cartilage therapy, American journal of translational research 7(2) **(2015)** 194-208.

[73] J. Diaz-Romero, J.P. Gaillard, S.P. Grogan, D. Nesic, T. Trub, P. Mainil-Varlet, Immunophenotypic analysis of human articular chondrocytes: Changes in surface markers associated with cell expansion in monolayer culture, Journal of Cellular Physiology 202(3) **(2005)** 731-742. https://doi.org/10.1002/jcp.20164

[74] U.R. Goessler, P. Bugert, K. Bieback, H. Sadick, A. Baisch, K. Hormann, F. Riedel, In vitro analysis of differential expression of collagens, integrins, and growth factors in cultured human chondrocytes, Otolaryngology-Head and Neck Surgery 134(3) **(2006)** 510-515. https://doi.org/10.1016/j.otohns.2005.10.026

[75] B. Ma, J.C.H. Leijten, L. Wu, M. Kip, C.A. van Blitterswijk, J.N. Post, M. Karperien, Gene expression profiling of dedifferentiated human articular chondrocytes in monolayer culture, Osteoarthritis and cartilage 21(4) **(2013)** 599-603. https://doi.org/10.1016/j.joca.2013.01.014

[76] M. Schnabel, S. Marlovits, G. Eckhoff, I. Fichtel, L. Gotzen, V. Vécsei, J. Schlegel, Dedifferentiation-associated changes in morphology and gene expression in primary human articular chondrocytes in cell culture, Osteoarthritis and cartilage 10(1) **(2002)** 62-70. https://doi.org/10.1053/joca.2001.0482

[77] D. Moulin, V. Salone, M. Koufany, T. Clément, I. Behm-Ansmant, C. Branlant, B. Charpentier, J.Y. Jouzeau, MicroRNA-29b Contributes to Collagens Imbalance in Human Osteoarthritic and Dedifferentiated Articular Chondrocytes, Biomed Research International 2017 **(2017)**. https://doi.org/10.1155/2017/9792512

[78] K.L. Caldwell, J. Wang, Cell-based articular cartilage repair: the link between development and regeneration, Osteoarthritis and cartilage 23(3) **(2015)** 351-62. https://doi.org/10.1016/j.joca.2014.11.004

[79] H. Shafaei, H. Bagernezhad, H. Bagernajad, Importance of Floating Chondrons in Cartilage Tissue Engineering, World journal of plastic surgery 6(1) **(2017)** 62-67.

[80] Y.Y. Luo, D. Sinkeviciute, Y. He, M. Karsdal, Y. Henrotin, A. Mobasheri, P. Önnerfjord, A. Bay-Jensen, The minor collagens in articular cartilage, Protein & Cell 8(8) **(2017)** 560-572. https://doi.org/10.1007/s13238-017-0377-7

[81] S. Gay, P.K. Müller, C. Lemmen, K. Remberger, K. Matzen, K. Kühn, Immunohistological study on collagen in cartilage-bone metamorphosis and

degenerative osteoarthrosis, Klinische Wochenschrift 54(20) **(1976)** 969-76. https://doi.org/10.1007/bf01468947

[82] P.D. Benya, S.R. Padilla, M.E. Nimni, Independent regulation of collagen types by chondrocytes during the loss of differentiated function in culture, Cell 15(4) **(1978)** 1313-21. https://doi.org/10.1016/0092-8674(78)90056-9

[83] S. Marlovits, M. Hombauer, M. Truppe, V. Vècsei, W. Schlegel, Changes in the ratio of type-I and type-II collagen expression during monolayer culture of human chondrocytes, Journal of Bone and Joint Surgery-British Volume 86B(2) **(2004)** 286-295. https://doi.org/10.1302/0301-620x.86b2.14918

[84] A. Barlic, M. Drobnic, E. Malicev, N. Kregar-Velikonja, Quantitative analysis of gene expression in human articular chondrocytes assigned for autologous implantation, Journal of Orthopaedic Research 26(6) **(2008)** 847-853. https://doi.org/10.1002/jor.20559

[85] S.P. Nukavarapu, D.L. Dorcemus, Osteochondral tissue engineering: current strategies and challenges, Biotechnology advances 31(5) **(2013)** 706-21. https://doi.org/10.1016/j.biotechadv.2012.11.004

[86] M.M. Caron, P.J. Emans, M.M. Coolsen, L. Voss, D.A. Surtel, A. Cremers, L.W. van Rhijn, T.J. Welting, Redifferentiation of dedifferentiated human articular chondrocytes: comparison of 2D and 3D cultures, Osteoarthritis and cartilage 20(10) **(2012)** 1170-8. https://doi.org/10.1016/j.joca.2012.06.016

[87] M.M.G. Sun, F. Beier, Chondrocyte hypertrophy in skeletal development, growth, and disease, Birth Defects Research Part C-Embryo Today-Reviews 102(1) **(2014)** 74-82. https://doi.org/10.1002/bdrc.21062

[88] A.A. Pitsillides, F. Beier, Cartilage biology in osteoarthritis-lessons from developmental biology, Nature Reviews Rheumatology 7(11) **(2011)** 654-663. https://doi.org/10.1038/nrrheum.2011.129

[89] F.M. Watt, Effect of seeding density on stability of the differentiated phenotype of pig articular chondrocytes in culture, Journal of cell science 89 (Pt 3) **(1988)** 373-8. https://doi.org/10.1242/jcs.89.3.373

[90] D.H. Rosenzweig, M. Matmati, G. Khayat, S. Chaudhry, B. Hinz, T.M. Quinn, Culture of Primary Bovine Chondrocytes on a Continuously Expanding Surface Inhibits Dedifferentiation, Tissue Engineering Part A 18(23-24) **(2012)** 2466-2476. https://doi.org/10.1089/ten.tea.2012.0215

[91] R.J. Egli, J.D. Bastian, R. Ganz, W. Hofstetter, M. Leunig, Hypoxic expansion promotes the chondrogenic potential of articular chondrocytes, Journal of Orthopaedic Research 26(7) **(2008)** 977-985. https://doi.org/10.1002/jor.20603

[92] B. Bachmann, S. Spitz, B. Schädl, A.H. Teuschl, H. Redl, S. Nürnberger, P. Ertl, Stiffness Matters: Fine-Tuned Hydrogel Elasticity Alters Chondrogenic Redifferentiation, Frontiers in bioengineering and biotechnology 8 **(2020)** 373. https://doi.org/10.3389/fbioe.2020.00373

[93] E. Costa, C. González-García, J.L.G. Ribelles, M. Salmerón-Sánchez, Maintenance of chondrocyte phenotype during expansion on PLLA

microtopographies, Journal of Tissue Engineering 9 **(2018)**. https://doi.org/10.1177/2041731418789829

[94] K.H. Chua, B.S. Aminuddin, N.H. Fuzina, B.H. Ruszymah, Insulin-transferrin-selenium prevent human chondrocyte dedifferentiation and promote the formation of high quality tissue engineered human hyaline cartilage, European cells & materials 9 **(2005)** 58-67; discussion 67. https://doi.org/10.22203/ecm.v009a08

[95] C. Mennan, J. Garcia, H. McCarthy, S. Owen, J. Perry, K. Wright, R. Banerjee, J.B. Richardson, S. Roberts, Human Articular Chondrocytes Retain Their Phenotype in Sustained Hypoxia While Normoxia Promotes Their Immunomodulatory Potential, Cartilage 10(4) **(2019)** 467-479. https://doi.org/10.1177/1947603518769714

[96] N.J. Gunja, K.A. Athanasiou, Passage and reversal effects on gene expression of bovine meniscal fibrochondrocytes, Arthritis research & therapy 9(5) **(2007)**. https://doi.org/10.1186/ar2293

[97] M. Angelozzi, L. Penolazzi, S. Mazzitelli, E. Lambertini, A. Lolli, R. Piva, C. Nastruzzi, Dedifferentiated Chondrocytes in Composite Microfibers As Tool for Cartilage Repair, Frontiers in bioengineering and biotechnology 5 **(2017)** 35. https://doi.org/10.3389/fbioe.2017.00035

[98] M.M.J. Caron, P.J. Emans, M.M.E. Coolsen, L. Voss, D.A.M. Surtel, A. Cremers, L.W. van Rhijn, T.J.M. Welting, Redifferentiation of dedifferentiated human articular chondrocytes: comparison of 2D and 3D cultures, Osteoarthritis and cartilage 20(10) **(2012)** 1170-1178. https://doi.org/10.1016/j.joca.2012.06.016

[99] A.M. Freyria, F. Mallein-Gerin, Chondrocytes or adult stem cells for cartilage repair: the indisputable role of growth factors, Injury 43(3) **(2012)** 259-65. https://doi.org/10.1016/j.injury.2011.05.035

[100] M. Jakob, O. Demarteau, D. Schafer, B. Hintermann, W. Dick, M. Heberer, I. Martin, Specific growth factors during the expansion and redifferentiation of adult human articular chondrocytes enhance chondrogenesis and cartilaginous tissue formation in vitro, Journal of cellular biochemistry 81(2) **(2001)** 368-77. https://doi.org/10.1002/1097-4644(20010501)81:2<368::aid-jcb1051>3.0.co;2-j

[101] A. Barbero, S. Grogan, D. Schafer, M. Heberer, P. Mainil-Varlet, I. Martin, Age related changes in human articular chondrocyte yield, proliferation and post-expansion chondrogenic capacity, Osteoarthritis and cartilage 12(6) **(2004)** 476-84. https://doi.org/10.1016/j.joca.2004.02.010

[102] A. Barbero, S. Ploegert, M. Heberer, I. Martin, Plasticity of clonal populations of dedifferentiated adult human articular chondrocytes, Arthritis and rheumatism 48(5) **(2003)** 1315-25. https://doi.org/10.1002/art.10950

[103] G. Liu, H. Kawaguchi, T. Ogasawara, Y. Asawa, J. Kishimoto, T. Takahashi, U.I. Chung, H. Yamaoka, H. Asato, K. Nakamura, T. Takato, K. Hoshi, Optimal combination of soluble factors for tissue engineering of permanent cartilage from cultured human chondrocytes, Journal of Biological Chemistry 282(28) **(2007)** 20407-20415. https://doi.org/10.1074/jbc.M608383200

[104] V. Jeyakumar, E. Niculescu-Morzsa, C. Bauer, Z. Lacza, S. Nehrer, Platelet-rich Plasma supports Proliferation and redifferentiation of chondrocytes during In Vitro expansion, Frontiers in Bioengineering and Biotechnology 5 **(2017)**. https://doi.org/10.3389/fbioe.2017.00075

[105] V. Jeyakumar, E. Niculescu-Morzsa, C. Bauer, Z. Lacza, S. Nehrer, Redifferentiation of Articular Chondrocytes by Hyperacute Serum and Platelet Rich Plasma in Collagen Type I Hydrogels, International journal of molecular sciences 20(2) **(2019)**. https://doi.org/10.3390/ijms20020316

[106] C.L. Murphy, J.M. Polak, Control of human articular chondrocyte differentiation by reduced oxygen tension, Journal of Cellular Physiology 199(3) **(2004)** 451-459. https://doi.org/10.1002/jcp.10481

[107] B.D. Markway, H. Cho, B. Johnstone, Hypoxia promotes redifferentiation and suppresses markers of hypertrophy and degeneration in both healthy and osteoarthritic chondrocytes, Arthritis research & therapy 15(4) **(2013)**. https://doi.org/10.1186/ar4272

[108] X.L. Ouyang, Y.F. Xie, G.H. Wang, Mechanical stimulation promotes the proliferation and the cartilage phenotype of mesenchymal stem cells and chondrocytes co-cultured in vitro, Biomedicine & Pharmacotherapy 117 **(2019)**. https://doi.org/10.1016/j.biopha.2019.109146

[109] J.A.A. Hendriks, R.L. Miclea, R. Schotel, E. de Bruijn, L. Moroni, M. Karperien, J. Riesle, C.A. van Blitterswijk, Primary chondrocytes enhance cartilage tissue formation upon co-culture with a range of cell types, Soft Matter 6(20) **(2010)** 5080-5088. https://doi.org/10.1039/c0sm00266f

[110] C.T. Brighton, W. Wang, C.C. Clark, The effect of electrical fields on gene and protein expression in human osteoarthritic cartilage explants, J Bone Joint Surg Am 90(4) **(2008)** 833-48. https://doi.org/10.2106/JBJS.F.01437

[111] J.J. Vaca-González, J.M. Guevara, M.A. Moncayo, H. Castro-Abril, Y. Hata, D.A. Garzón-Alvarado, Biophysical Stimuli: A Review of Electrical and Mechanical Stimulation in Hyaline Cartilage, Cartilage 10(2) **(2019)** 157-172. https://doi.org/10.1177/1947603517730637

[112] C.T. Brighton, W. Wang, C.C. Clark, Up-regulation of matrix in bovine articular cartilage explants by electric fields, Biochemical and biophysical research communications 342(2) **(2006)** 556-61. https://doi.org/10.1016/j.bbrc.2006.01.171

[113] W. Wang, Z. Wang, G. Zhang, C.C. Clark, C.T. Brighton, Up-regulation of chondrocyte matrix genes and products by electric fields, Clinical orthopaedics and related research (427 Suppl) **(2004)** S163-73.

[114] H. Muir, P. Bullough, A.J.T.J.o.B. Maroudas, J.S.B. Volume, The distribution of collagen in human articular cartilage with some of its physiological implications, 52(3) **(1970)** 554-563.

[115] L.A. Setton, W. Zhu, V.C. Mow, The biphasic poroviscoelastic behavior of articular cartilage: role of the surface zone in governing the compressive

behavior, Journal of biomechanics 26(4-5) **(1993)** 581-92. https://doi.org/10.1016/0021-9290(93)90019-b

[116] J.M. Clark, VARIATION OF COLLAGEN FIBER ALIGNMENT IN A JOINT SURFACE - A SCANNING ELECTRON-MICROSCOPE STUDY OF THE TIBIAL PLATEAU IN DOG, RABBIT, AND MAN, Journal of Orthopaedic Research 9(2) **(1991)** 246-257. https://doi.org/10.1002/jor.1100090213

[117] I. Redler, V.C. Mow, M.L. Zimny, J. Mansell, The ultrastructure and biomechanical significance of the tidemark of articular cartilage, Clin Orthop Relat Res (112) **(1975)** 357-62.

[118] L.A. Setton, H. Tohyama, V.C. Mow, Swelling and curling behaviors of articular cartilage, Journal of Biomechanical Engineering-Transactions of the Asme 120(3) **(1998)** 355-361. https://doi.org/10.1115/1.2798002

[119] J.M. Clark, P.T. Simonian, Scanning electron microscopy of "fibrillated" and "malacic" human articular cartilage: technical considerations, Microscopy research and technique 37(4) **(1997)** 299-313. https://doi.org/10.1002/(sici)1097-0029(19970515)37:4<299::Aid-jemt5>3.0.Co;2-g

[120] A.I. Maroudas, Balance between swelling pressure and collagen tension in normal and degenerate cartilage, Nature 260(5554) **(1976)** 808-9. https://doi.org/10.1038/260808a0

[121] V.C. Mow, G.A. Ateshian, R.L. Spilker, Biomechanics of diarthrodial joints: a review of twenty years of progress, Journal of biomechanical engineering 115(4b) **(1993)** 460-7. https://doi.org/10.1115/1.2895525

[122] V.C. Mow, A. Ratcliffe, Structure and function of articular cartilage and meniscus, 1997.

[123] V. Mow, X.E. Guo, Mechano-electrochemical properties of articular cartilage: Their inhomogeneities and anisotropies, Annual Review of Biomedical Engineering 4 **(2002)** 175-209. https://doi.org/10.1146/annurev.bioeng.4.110701.120309

[124] T. Hodgkinson, D.C. Kelly, C.M. Curtin, F.J. O'Brien, Mechanosignalling in cartilage: an emerging target for the treatment of osteoarthritis, Nature Reviews Rheumatology 18(2) **(2022)** 67-84. https://doi.org/10.1038/s41584-021-00724-w

[125] C.D. McCaig, B. Song, A.M. Rajnicek, Electrical dimensions in cell science, 122(23) **(2009)** 4267-4276. https://doi.org/10.1242/jcs.023564 %J Journal of Cell Science

[126] M.A. Messerli, D.M. Graham, Extracellular Electrical Fields Direct Wound Healing and Regeneration, 221(1) **(2011)** 79-92. https://doi.org/10.1086/BBLv221n1p79

[127] M. Levin, Molecular bioelectricity: How endogenous voltage potentials control cell behavior and instruct pattern regulation in vivo, Molecular Biology of the Cell 25(24) **(2014)** 3835-3850. https://doi.org/10.1091/mbc.E13-12-0708

[128] L.S. Jenkins, B.S. Duerstock, R.B. Borgens, Reduction of the current of injury leaving the amputation inhibits limb regeneration in the red spotted newt, Developmental biology 178(2) **(1996)** 251-62. https://doi.org/10.1006/dbio.1996.0216

[129] W.M. Lai, D.D. Sun, G.A. Ateshian, X.E. Guo, V.C. Mow, Electrical signals for chondrocytes in cartilage, Biorheology 39(1-2) **(2002)** 39-45.

[130] V.C. Mow, C.C. Wang, C.T. Hung, The extracellular matrix, interstitial fluid and ions as a mechanical signal transducer in articular cartilage, Osteoarthritis and cartilage 7(1) **(1999)** 41-58. https://doi.org/10.1053/joca.1998.0161

[131] B. Baker, J. Spadaro, A. Marino, R.O. Becker, Electrical stimulation of articular cartilage regeneration, Annals of the New York Academy of Sciences 238 **(1974)** 491-9. https://doi.org/10.1111/j.1749-6632.1974.tb26815.x

[132] P.H. Chao, R. Roy, R.L. Mauck, W. Liu, W.B. Valhmu, C.T. Hung, Chondrocyte translocation response to direct current electric fields, Journal of biomechanical engineering 122(3) **(2000)** 261-7. https://doi.org/10.1115/1.429661

[133] D.M. Ciombor, G. Lester, R.K. Aaron, P. Neame, B. Caterson, Low frequency EMF regulates chondrocyte differentiation and expression of matrix proteins, Journal of orthopaedic research : official publication of the Orthopaedic Research Society 20(1) **(2002)** 40-50. https://doi.org/10.1016/s0736-0266(01)00071-7

[134] S. Mayer-Wagner, A. Passberger, B. Sievers, J. Aigner, B. Summer, T.S. Schiergens, V. Jansson, P.E. Muller, Effects of low frequency electromagnetic fields on the chondrogenic differentiation of human mesenchymal stem cells, Bioelectromagnetics 32(4) **(2011)** 283-90. https://doi.org/10.1002/bem.20633

[135] A. Fioravanti, F. Nerucci, G. Collodel, R. Markoll, R.J.A.o.t.r.d. Marcolongo, Biochemical and morphological study of human articular chondrocytes cultivated in the presence of pulsed signal therapy, 61(11) **(2002)** 1032-1033.

[136] D.M. Ciombor, R.K. Aaron, S. Wang, B. Simon, Modification of osteoarthritis by pulsed electromagnetic field--a morphological study, Osteoarthritis and cartilage 11(6) **(2003)** 455-62.

[137] M.E. Jahns, E. Lou, N.G. Durdle, K. Bagnall, V.J. Raso, D. Cinats, R.D. Barley, J. Cinats, N.M. Jomha, The effect of pulsed electromagnetic fields on chondrocyte morphology, Medical & biological engineering & computing 45(10) **(2007)** 917-25. https://doi.org/10.1007/s11517-007-0216-8

[138] M. De Mattei, A. Caruso, F. Pezzetti, A. Pellati, G. Stabellini, V. Sollazzo, G.C. Traina, Effects of pulsed electromagnetic fields on human articular chondrocyte proliferation, Connect Tissue Res 42(4) **(2001)** 269-79. https://doi.org/10.3109/03008200109016841

[139] C.T. Brighton, P.F. Townsend, Increased cAMP production after short-term capacitively coupled stimulation in bovine growth plate chondrocytes, Journal of orthopaedic research : official publication of the Orthopaedic Research Society 6(4) **(1988)** 552-8. https://doi.org/10.1002/jor.1100060412

[140] C.T. Brighton, L. Jensen, S.R. Pollack, B.S. Tolin, C.C. Clark, Proliferative and synthetic response of bovine growth plate chondrocytes to various capacitively coupled electrical fields, Journal of orthopaedic research : official publication of the Orthopaedic Research Society 7(5) **(1989)** 759-65. https://doi.org/10.1002/jor.1100070519

[141] P. Sadoghi, A. Leithner, R. Dorotka, P. Vavken, Effect of pulsed electromagnetic fields on the bioactivity of human osteoarthritic chondrocytes, Orthopedics 36(3) **(2013)** e360-5. https://doi.org/10.3928/01477447-20130222-27

[142] B. Cecen, L. Kozaci, T. Boylu, N. Kurt, D. Erdemli, M. Yuksel, H. Havitçioğlu, Effects Of Electromagnetic Fields On Chondrocytes Cells Of Human Seeded Onto 3d Collagen-Plla Scaffolds And Chondro-Gide Membrane, SAÜ Fen Bilimleri Enstitüsü Dergisi 16 **(2012)** 213-220. https://doi.org/10.5505/saufbe.2012.27247

[143] M. De Mattei, A. Pellati, M. Pasello, A. Ongaro, S. Setti, L. Massari, D. Gemmati, A. Caruso, Effects of physical stimulation with electromagnetic field and insulin growth factor-I treatment on proteoglycan synthesis of bovine articular cartilage, Osteoarthritis and cartilage 12(10) **(2004)** 793-800. https://doi.org/10.1016/j.joca.2004.06.012

[144] B. Schmidt-Rohlfing, J. Silny, S. Woodruff, K. Gavenis, Effects of pulsed and sinusoid electromagnetic fields on human chondrocytes cultivated in a collagen matrix, Rheumatology international 28(10) **(2008)** 971-7. https://doi.org/10.1007/s00296-008-0565-0

[145] V. Nicolin, C. Ponti, G. Baldini, D. Gibellini, R. Bortul, M. Zweyer, B. Martinelli, P. Narducci, In vitro exposure of human chondrocytes to pulsed electromagnetic fields, European journal of histochemistry : EJH 51(3) **(2007)** 203-12.

[146] N. Szasz, H. Hung, S. Sen, A. Grodzinsky, Electric field regulation of chondrocyte biosynthesis in agarose gel constructs, 49th Annual Meeting of the Orthopaedic Research Society, 2003, p. 1.

[147] O.O. Akanji, D.A. Lee, D.A. Bader, The effects of direct current stimulation on isolated chondrocytes seeded in 3D agarose constructs, Biorheology 45(3-4) **(2008)** 229-43.

[148] L.A. MacGinitie, Y.A. Gluzband, A.J. Grodzinsky, Electric field stimulation can increase protein synthesis in articular cartilage explants, Journal of orthopaedic research : official publication of the Orthopaedic Research Society 12(2) **(1994)** 151-60. https://doi.org/10.1002/jor.1100120202

[149] A. Ongaro, A. Pellati, F.F. Masieri, A. Caruso, S. Setti, R. Cadossi, R. Biscione, L. Massari, M. Fini, M. De Mattei, Chondroprotective effects of pulsed electromagnetic fields on human cartilage explants, Bioelectromagnetics 32(7) **(2011)** 543-51. https://doi.org/10.1002/bem.20663

[150] F.M. Hilz, P. Ahrens, S. Grad, M.J. Stoddart, C. Dahmani, F.L. Wilken, M. Sauerschnig, P. Niemeyer, J. Zwingmann, R. Burgkart, R. von Eisenhart-Rothe, N.P. Südkamp, T. Weyh, A.B. Imhoff, M. Alini, G.M. Salzmann, Influence of extremely low frequency, low energy electromagnetic fields and combined

mechanical stimulation on chondrocytes in 3-D constructs for cartilage tissue engineering, Bioelectromagnetics 35(2) **(2014)** 116-28. https://doi.org/10.1002/bem.21822

[151] G. Thrivikraman, S.K. Boda, B. Basu, Unraveling the mechanistic effects of electric field stimulation towards directing stem cell fate and function: A tissue engineering perspective, Biomaterials 150 **(2018)** 60-86. https://doi.org/10.1016/j.biomaterials.2017.10.003

[152] M. Korpan, I. Chekman, S. Magomedov, O. Burjanov, V.J.P.M. Fialka-Moser, Rehabilitationsmedizin, Kurortmedizin, Influence of Direct Current on the Cartilaginous Metabolism in vivo, 21(01) **(2011)** 45-51.

[153] H. Okihana, Y. Shimomura, Effect of direct current on cultured growth cartilage cells in vitro, 6(5) **(1988)** 690-694. https://doi.org/https://doi.org/10.1002/jor.1100060511

[154] J. Farr, M.A. Mont, D. Garland, J.R. Caldwell, T.M. Zizic, Pulsed electrical stimulation in patients with osteoarthritis of the knee: follow up in 288 patients who had failed non-operative therapy, Surgical technology international 15 **(2006)** 227-33.

[155] L. Lippiello, D. Chakkalakal, J.F. Connolly, Pulsing direct current-induced repair of articular cartilage in rabbit osteochondral defects, Journal of orthopaedic research : official publication of the Orthopaedic Research Society 8(2) **(1990)** 266-75. https://doi.org/10.1002/jor.1100080216

[156] P.F. Armstrong, C.T. Brighton, A.M. Star, Capacitively coupled electrical stimulation of bovine growth plate chondrocytes grown in pellet form, Journal of orthopaedic research : official publication of the Orthopaedic Research Society 6(2) **(1988)** 265-71. https://doi.org/10.1002/jor.1100060214

[157] J.J. Vaca-González, J.M. Guevara, J.F. Vega, D.A.J.C. Garzón-Alvarado, M. Bioengineering, An In Vitro Chondrocyte Electrical Stimulation Framework: A Methodology to Calculate Electric Fields and Modulate Proliferation, Cell Death and Glycosaminoglycan Synthesis, 9(1) **(2016)** 116-126. https://doi.org/10.1007/s12195-015-0419-2

[158] S. Nakasuji, Y. Morita, K. Tanaka, T. Tanaka, E. Nakamachi, Effect of pulse electric field stimulation on chondrocytes, Asian Pacific Conference for Materials and Mechanics, 2009, pp. 1-4.

[159] C.T. Brighton, A.S. Unger, J.L. Stambough, In vitro growth of bovine articular cartilage chondrocytes in various capacitively coupled electrical fields, Journal of orthopaedic research : official publication of the Orthopaedic Research Society 2(1) **(1984)** 15-22. https://doi.org/10.1002/jor.1100020104

[160] S. Krueger, A. Riess, A. Jonitz-Heincke, A. Weizel, A. Seyfarth, H. Seitz, R. Bader, Establishment of a New Device for Electrical Stimulation of Non-Degenerative Cartilage Cells In Vitro, International journal of molecular sciences 22(1) **(2021)**. https://doi.org/10.3390/ijms22010394

[161] S. Krueger, S. Achilles, J. Zimmermann, T. Tischer, R. Bader, A. Jonitz-Heincke, Re-Differentiation Capacity of Human Chondrocytes in Vitro Following Electrical

Stimulation with Capacitively Coupled Fields, Journal of Clinical Medicine 8(11) **(2019)**. https://doi.org/10.3390/jcm8111771

[162] H. Samadian, S.S. Zakariaee, M. Adabi, H. Mobasheri, M. Azami, R. Faridi-Majidi, Effective parameters on conductivity of mineralized carbon nanofibers: an investigation using artificial neural networks, RSC Advances 6(113) **(2016)** 111908-111918. https://doi.org/10.1039/C6RA21596C

[163] T.J. Dauben, J. Ziebart, T. Bender, S. Zaatreh, B. Kreikemeyer, R. Bader, A Novel In Vitro System for Comparative Analyses of Bone Cells and Bacteria under Electrical Stimulation, BioMed research international 2016 **(2016)** 5178640. https://doi.org/10.1155/2016/5178640

[164] W. Wang, Z.Y. Wang, G.H. Zhang, C.C. Clark, C.T. Brighton, Up-regulation of chondrocyte matrix genes and products by electric fields, Clinical Orthopaedics and Related Research (427) **(2004)** S163-S173. https://doi.org/10.1097/01.blo.0000143837.53434.5c

[165] P.J. Nicksic, D.T. Donnelly, N. Verma, A.J. Setiz, A.J. Shoffstall, K.A. Ludwig, A.M. Dingle, S.O. Poore, Electrical Stimulation of Acute Fractures: A Narrative Review of Stimulation Protocols and Device Specifications, Frontiers in Bioengineering and Biotechnology 10 **(2022)**. https://doi.org/10.3389/fbioe.2022.879187

[166] K. Budde, J. Zimmermann, E. Neuhaus, M. Schroder, A.M. Uhrmacher, U. van Rienen, Requirements for Documenting Electrical Cell Stimulation Experiments for Replicability and Numerical Modeling(∗), Annual International Conference of the IEEE Engineering in Medicine and Biology Society. IEEE Engineering in Medicine and Biology Society. Annual International Conference 2019 **(2019)** 1082-1088. https://doi.org/10.1109/embc.2019.8856863

[167] L.P. da Silva, S.C. Kundu, R.L. Reis, V.M. Correlo, Electric Phenomenon: A Disregarded Tool in Tissue Engineering and Regenerative Medicine, Trends in Biotechnology 38(1) **(2020)** 24-49. https://doi.org/10.1016/j.tibtech.2019.07.002

[168] L.A. Portelli, K. Falldorf, G. Thuróczy, J. Cuppen, Retrospective estimation of the electric and magnetic field exposure conditions in in vitro experimental reports reveal considerable potential for uncertainty, Bioelectromagnetics 39(3) **(2018)** 231-243. https://doi.org/10.1002/bem.22099

[169] R. Gundersen, B. Greenebaum, Low-voltage ELF electric field measurements in ionic media, Bioelectromagnetics 6(2) **(1985)** 157-68. https://doi.org/10.1002/bem.2250060207

[170] L. Scott, K. Elídóttir, K. Jeevaratnam, I. Jurewicz, R. Lewis, Electrical stimulation through conductive scaffolds for cardiomyocyte tissue engineering: Systematic review and narrative synthesis, Annals of the New York Academy of Sciences 1515(1) **(2022)** 105-119. https://doi.org/10.1111/nyas.14812

[171] J. Zimmermann, F. Sahm, N. Arbeiter, H. Bathel, Z. Song, R. Bader, A. Jonitz-Heincke, U. van Rienen, Experimental and numerical methods to ensure comprehensible and replicable alternating current electrical stimulation

experiments, Bioelectrochemistry (Amsterdam, Netherlands) 151 **(2023)** 108395. https://doi.org/10.1016/j.bioelechem.2023.108395

[172] J.J.I.f.a. Schöberl, V.U.o.T. scientific computing, C++ 11 implementation of finite elements in NGSolve, 30 **(2014)**.

[173] J. Schöberl, NETGEN An advancing front 2D/3D-mesh generator based on abstract rules, Computing and Visualization in Science 1(1) **(1997)** 41-52. https://doi.org/10.1007/s007910050004

[174] D.R. Cantrell, S. Inayat, A. Taflove, R.S. Ruoff, J.B. Troy, Incorporation of the electrode–electrolyte interface into finite-element models of metal microelectrodes, Journal of Neural Engineering 5(1) **(2008)** 54. https://doi.org/10.1088/1741-2560/5/1/006

[175] H. Raben, P.W. Kämmerer, R. Bader, U. van Rienen, Establishment of a Numerical Model to Design an Electro-Stimulating System for a Porcine Mandibular Critical Size Defect, Applied Sciences-Basel 9(10) **(2019)**. https://doi.org/10.3390/app9102160

[176] T. Ning, K. Zhang, B.C. Heng, Z. Ge, Diverse effects of pulsed electrical stimulation on cells - with a focus on chondrocytes and cartilage regeneration, European cells & materials 38 **(2019)** 79-93. https://doi.org/10.22203/eCM.v038a07

[177] R. Vaiciuleviciute, I. Uzieliene, P. Bernotas, V. Novickij, A. Alaburda, E. Bernotiene, Electrical Stimulation in Cartilage Tissue Engineering, Bioengineering (Basel, Switzerland) 10(4) **(2023)**. https://doi.org/10.3390/bioengineering10040454

[178] M. Hronik-Tupaj, W.L. Rice, M. Cronin-Golomb, D.L. Kaplan, I. Georgakoudi, Osteoblastic differentiation and stress response of human mesenchymal stem cells exposed to alternating current electric fields, Biomedical Engineering Online 10 **(2011)**. https://doi.org/10.1186/1475-925x-10-9

[179] E. Pettersen, Promoting osseointegration in titanium implants using pulsed electrical stimulation, **(2020)**.

[180] J.M. Olivereau, J.F. Lambert, A. Truong-Ngoc, Influence of air ions on brain activity induced by electrical stimulation in the rat, International journal of biometeorology 25(1) **(1981)** 63-9. https://doi.org/10.1007/bf02184440

[181] J.D. Hunter, Matplotlib: A 2D Graphics Environment, Computing in Science & Engineering 9(3) **(2007)** 90-95. https://doi.org/10.1109/MCSE.2007.55

[182] S.J. Pelletier, M. Lagacé, I. St-Amour, D. Arsenault, G. Cisbani, A. Chabrat, S. Fecteau, M. Lévesque, F. Cicchetti, The Morphological and Molecular Changes of Brain Cells Exposed to Direct Current Electric Field Stimulation, International Journal of Neuropsychopharmacology 18(5) **(2015)**. https://doi.org/10.1093/ijnp/pyu090

[183] Y. Su, R. Souffrant, D. Klüß, M. Ellenrieder, H. Ewald, W. Mittelmeier, R. Bader, Electro-Stimulating Implants for Bone Regeneration: Parameter Analysis on

Design and Implant Position, 2011 COMSOL Conference. COMSOL, Incorporated, Stuttgart, Germany, 2011.

[184] H. Ye, Mechanic stress generated by a time-varying electromagnetic field on bone surface, Medical & biological engineering & computing 56(10) **(2018)** 1793-1805. https://doi.org/10.1007/s11517-018-1814-3

[185] V.P. Shastri, N. Rahman, I. Martin, R. Langer, Application of Conductive Polymers in Bone Regeneration, MRS Proceedings 550 **(1998)** 215. https://doi.org/10.1557/PROC-550-215

[186] C.T. Brighton, G.B. Pfeffer, S.R. Pollack, In vivo growth plate stimulation in various capacitively coupled electrical fields, Journal of orthopaedic research : official publication of the Orthopaedic Research Society 1(1) **(1983)** 42-9. https://doi.org/10.1002/jor.1100010106

[187] C.-Y. Qu, S.-W. Yu, The damage and healing of bone in the disuse state under mechanical and electro-magnetic loadings, Procedia Engineering 10 **(2011)** 171-176. https://doi.org/https://doi.org/10.1016/j.proeng.2011.04.031

[188] S. Séguier, G. Godeau, M. Leborgne, G. Pivert, N. Brousse, Quantitative morphological analysis of Langerhans cells in healthy and diseased human gingiva, Archives of Oral Biology 45(12) **(2000)** 1073-1081. https://doi.org/https://doi.org/10.1016/S0003-9969(00)00069-8

[189] I.M. Tolić-Nørrelykke, N. Wang, Traction in smooth muscle cells varies with cell spreading, Journal of Biomechanics 38(7) **(2005)** 1405-1412. https://doi.org/https://doi.org/10.1016/j.jbiomech.2004.06.027

[190] H. Jahr, C. Matta, A. Mobasheri, Physicochemical and Biomechanical Stimuli in Cell-Based Articular Cartilage Repair, Current Rheumatology Reports 17(3) **(2015)**. https://doi.org/10.1007/s11926-014-0493-9

[191] X.B. Huang, R. Das, A. Patel, T.D. Nguyen, Physical Stimulations for Bone and Cartilage Regeneration, Regenerative Engineering and Translational Medicine 4(4) **(2018)** 216-237. https://doi.org/10.1007/s40883-018-0064-0

[192] J.J. Vaca-González, J.M. Guevara, M.A. Moncayo, H. Castro-Abril, Y. Hata, D.A.J.C. Garzón-Alvarado, Biophysical stimuli: a review of electrical and mechanical stimulation in hyaline cartilage, 10(2) **(2019)** 157-172.

[193] A. Jonitz-Heincke, A. Klinder, D. Boy, A. Salamon, D. Hansmann, J. Pasold, A. Buettner, R. Bader, In Vitro Analysis of the Differentiation Capacity of Postmortally Isolated Human Chondrocytes Influenced by Different Growth Factors and Oxygen Levels, Cartilage 10(1) **(2019)** 111-119. https://doi.org/10.1177/1947603517719318

[194] C. Windisch, W. Kolb, E. Rohner, M. Wagner, A. Roth, G. Matziolis, A. Wagner, Invasive electromagnetic field treatment in osteonecrosis of the femoral head: a prospective cohort study, The open orthopaedics journal 8 **(2014)** 125-9. https://doi.org/10.2174/1874325020140515001

[195] D.D. Traficante, Impedance: What it is, and why it must be matched, 1(2) **(1989)** 73-92. https://doi.org/https://doi.org/10.1002/cmr.1820010205

[196] P. Sharma, T.S. Bhatti, A review on electrochemical double-layer capacitors, Energy Conversion and Management 51(12) **(2010)** 2901-2912. https://doi.org/https://doi.org/10.1016/j.enconman.2010.06.031

[197] R.A. Gittens, R. Olivares-Navarrete, R. Tannenbaum, B.D. Boyan, Z. Schwartz, Electrical Implications of Corrosion for Osseointegration of Titanium Implants, Journal of Dental Research 90(12) **(2011)** 1389-1397. https://doi.org/10.1177/0022034511408428

[198] T. Hanawa, M. Ota, CALCIUM-PHOSPHATE NATURALLY FORMED ON TITANIUM IN ELECTROLYTE SOLUTION, Biomaterials 12(8) **(1991)** 767-774. https://doi.org/10.1016/0142-9612(91)90028-9

[199] R. Narayanan, S.K. Seshadri, T.Y. Kwon, K.H. Kim, Calcium phosphate-based coatings on titanium and its alloys, Journal of Biomedical Materials Research Part B-Applied Biomaterials 85B(1) **(2008)** 279-299. https://doi.org/10.1002/jbm.b.30932

[200] N. N'Dre, P. Lecor, A. Assoumou, M.J.J.N.P. Blohoua, Evaluation of chondrocyte dedifferentiation mechanisms using confocal Raman microscopy, 5(1) **(2024)** 1-8.

[201] J. Parreno, M. Nabavi Niaki, K. Andrejevic, A. Jiang, P.H. Wu, R.A. Kandel, Interplay between cytoskeletal polymerization and the chondrogenic phenotype in chondrocytes passaged in monolayer culture, Journal of anatomy 230(2) **(2017)** 234-248. https://doi.org/10.1111/joa.12554

[202] J. Parreno, S. Raju, P.-h. Wu, R.A. Kandel, MRTF-A signaling regulates the acquisition of the contractile phenotype in dedifferentiated chondrocytes, Matrix Biology 62 **(2017)** 3-14. https://doi.org/https://doi.org/10.1016/j.matbio.2016.10.004

[203] H. Shen, Y. He, N. Wang, M.R. Fritch, X. Li, H. Lin, R.S. Tuan, Enhancing the potential of aged human articular chondrocytes for high-quality cartilage regeneration, FASEB journal : official publication of the Federation of American Societies for Experimental Biology 35(3) **(2021)** e21410. https://doi.org/10.1096/fj.202002386R

[204] S. Krueger, S. Achilles, J. Zimmermann, T. Tischer, R. Bader, A. Jonitz-Heincke, Re-Differentiation Capacity of Human Chondrocytes in Vitro Following Electrical Stimulation with Capacitively Coupled Fields, J Clin Med 8(11) **(2019)**. https://doi.org/10.3390/jcm8111771

[205] Y. Chen, Y. Yu, Y. Wen, J. Chen, J. Lin, Z. Sheng, W. Zhou, H. Sun, C. An, J. Chen, W. Wu, C. Teng, W. Wei, H. Ouyang, A high-resolution route map reveals distinct stages of chondrocyte dedifferentiation for cartilage regeneration, Bone Research 10(1) **(2022)** 38. https://doi.org/10.1038/s41413-022-00209-w

[206] K. Bobacz, L. Erlacher, J. Smolen, A. Soleiman, W.B. Graninger, Chondrocyte number and proteoglycan synthesis in the aging and osteoarthritic human articular cartilage, Annals of the Rheumatic Diseases 63(12) **(2004)** 1618. https://doi.org/10.1136/ard.2002.002162

[207] L. Jain, C.A. Jardim, R. Yulo, S.M. Bolam, A.P. Monk, J.T. Munro, R. Pitto, J. Tamatea, N. Dalbeth, R.C. Poulsen, Phenotype and energy metabolism differ between osteoarthritic chondrocytes from male compared to female patients: Implications for sexual dimorphism in osteoarthritis development?, Osteoarthritis and cartilage **(2023)**. https://doi.org/https://doi.org/10.1016/j.joca.2023.09.013

[208] P.A. Hernandez, M. Moreno, Z. Barati, C. Hutcherson, A.A. Sathe, C. Xing, J. Wright, T. Welch, Y. Dhaher, Sexual Dimorphism in the Extracellular and Pericellular Matrix of Articular Cartilage, CARTILAGE 13(3) **(2022)** 19476035221121792. https://doi.org/10.1177/19476035221121792

[209] A. Haseeb, R. Kc, M. Angelozzi, C. de Charleroy, D. Rux, R.J. Tower, L. Yao, R. Pellegrino da Silva, M. Pacifici, L. Qin, V. Lefebvre, SOX9 keeps growth plates and articular cartilage healthy by inhibiting chondrocyte dedifferentiation/osteoblastic redifferentiation, 118(8) **(2021)** e2019152118. https://doi.org/doi:10.1073/pnas.2019152118

[210] S.R. Tew, P.D. Clegg, C.J. Brew, C.M. Redmond, T.E. Hardingham, SOX9 transduction of a human chondrocytic cell line identifies novel genes regulated in primary human chondrocytes and in osteoarthritis, Arthritis Research & Therapy 9(5) **(2007)** R107. https://doi.org/10.1186/ar2311

[211] F. Salamanna, D. Contartese, V. Borsari, S. Pagani, M. Sartori, M. Tschon, C. Griffoni, G. Giavaresi, G. Tedesco, G. Barbanti Brodano, A. Gasbarrini, M. Fini, Gender-Specific Differences in Human Vertebral Bone Marrow Clot, International journal of molecular sciences 24(14) **(2023)**. https://doi.org/10.3390/ijms241411856

[212] G. Filardo, E. Kon, L. Andriolo, F. Vannini, R. Buda, A. Ferruzzi, S. Giannini, M. Marcacci, Does Patient Sex Influence Cartilage Surgery Outcome?: Analysis of Results at 5-Year Follow-up in a Large Cohort of Patients Treated With Matrix-Assisted Autologous Chondrocyte Transplantation, The American Journal of Sports Medicine 41(8) **(2013)** 1827-1834. https://doi.org/10.1177/0363546513480780

[1] https://github.com/j-zimmermann/PyVISAScope/tree/master/examples/

Appendix

List of Abbreviations

AC	Alternating current
ACI	autologous chondrocyte implantation
ADAMTS-5	A Disintegrin and Metalloproteinase with Thrombospondin motifs 5
Ag/AgCl	silver/silver chloride
BMAC	bone marrow aspirate concentration
BM-MSC	mesenchymal stem cells derived from bone marrow
BMP	bone morphogenetic protein
CAD	computer aid design
CICP	Type I C-terminal collagen propeptide
CIICP	Type II C-terminal collagen propeptide
Col1	Collagen 1
Col2	Collagen 2
DC	direct current
ECM	extracellular matrix
EDTA	Ethylenediaminetetraacetic acid
EEI	impedance of the electrode–electrolyte interface
EF	electric field
EGF	epidermal growth factor
ELISA	enzyme-linked immunosorbent assay
EMF	electromagnetic fields
ES	electrical stimulation
FCS	fetal calf serum
FEM	finite element method
FGF	fibroblast growth factors
GAG	glycosaminoglycan

GAR-HRP	Goat Anti-Rabbit Horseradish Peroxidase
hESC	human embryonic stem cells
ICRS	International Cartilage Repair Society
IGF	insulin-like growth factor
IKDC	International Knee Documentation Committee
IL	Interleukin
ITS	Insulin-Transferrin-Selen
KOOS	Knee Injury and Osteoarthritis Outcome
MACI	matrix-induced autologous chondrocyte implantation
MMP	matrix metalloproteinase
MSC	mesenchymal stem cells
OA	osteoarthritis
PBS	phosphate-buffered saline
PCM	pericellular matrix
PDGF	platelet derived growth factor
PEEK	polyetherether ketone
PES	pulsing electrical stimulation
PEMF	pulsing electromagnetic field
PRP	platelet-rich plasma
TGF	transforming growth factor
TKA	total knee arthroplasty
TMB	Tetramethylbenzidine
TNF	tumor necrosis factor
VEGF	vascular endothelial growth factor
V_{RMS}	voltage root mean square
WST	water soluble tetrazolium
3D	three-dimensional

List of Figures

List of Tables

Materials

Table S1: Cell culture media and supplements

Product	**Supplier**
DMEM	Gibco®, Thermo Fisher Scientific Inc., Waltham, MA, United States
FCS	Pan Biotech, Aidenbach, Germany
Penicillin/streptomycin	Thermo Scientific, Waltham, MA, United States
Amphotericin B	Biochrom GmbH, Berlin, Germany
Ascorbic acid	Sigma-Aldrich, Merck KGaA, Darmstadt, Germany
ITS	BD Biosciences, Franklin Lakes, NJ, United States
dexamethasone	Sigma-Aldrich, Merck KGaA, Darmstadt, Germany

Table S2: Assay kits and reagents

Product	**Supplier**
PBS	PAA, Cölbe, Germany
Trypsin/EDTA	Gibco® Invitrogen, Darmstadt, Germany
collagenase A	Roche, Mannheim, Germany
WST-1 assay	Roche GmbH, Grenzach-Wyhlen, Germany
CICP ELISA kit	Quidel, San Diego, CA, United States
CIICP ELISA kit	IBEX, Montréal, QC, Canada
Qubit® Protein Assay Kit	Thermo Fisher Scientific Inc, Waltham, MA, United States
Calcein AM	Thermo Fisher Scientific, Inc., Waltham, MA, United States

Table S3: Instruments and facilities

Product	Supplier
JUMO eTRON M controller	JUMO GmbH & Co. KG Fulda, Germany
PCE-T390 thermometer	PCE Germany GmbH, Meschede, Germany
Acrifix 1S 0116	Röhm GmbH, United States
Solvex® 37-900 chemical protective gloves	Ansell Gmbh, Brussels, Belgium
Metrix GX310	Chauvin Arnoux, Annecy, France
Metrix MTX 3240	Chauvin Arnoux, Annecy, France
F30PV linear amplifier	Datatec Gmbh, FLC, Gothenburg, Sweden
F10A linear amplifier	Datatec Gmbh, FLC, Gothenburg, Sweden
Agilent 33502a linear amplifier	Keysight Gmbh, Santa Clara, CA, United States
Rigol MSO5104Ω oscilloscope	Batronix GmbH, Preetz, Germany
platinum-iridium microelectrode	Microprobes, Gaithersburg, MD, United States
Nikon Eclipse 120 fluorescence microscope	Nikon Instruments, Tokyo, Japan

Table S4: Software

SOLIDWORKS 2023 SP5	SolidWorks Corporation, 175 Wyman Street, Waltham, MA, United States, available at https://www.salome-platform.org/
Python 3.7	——
GraphPad Prism 9.5.1	GraphPad Software Inc., San Diego, CA, United States
ImageJ 1.53	National Institutes of Health, Bethesda, MD, United States, available at https://imagej.net/ij/
CellProfiler 4.2.1	Broad Institute, Cambridge, MA, United States, available at https://cellprofiler.org/citations

Supplement Figures

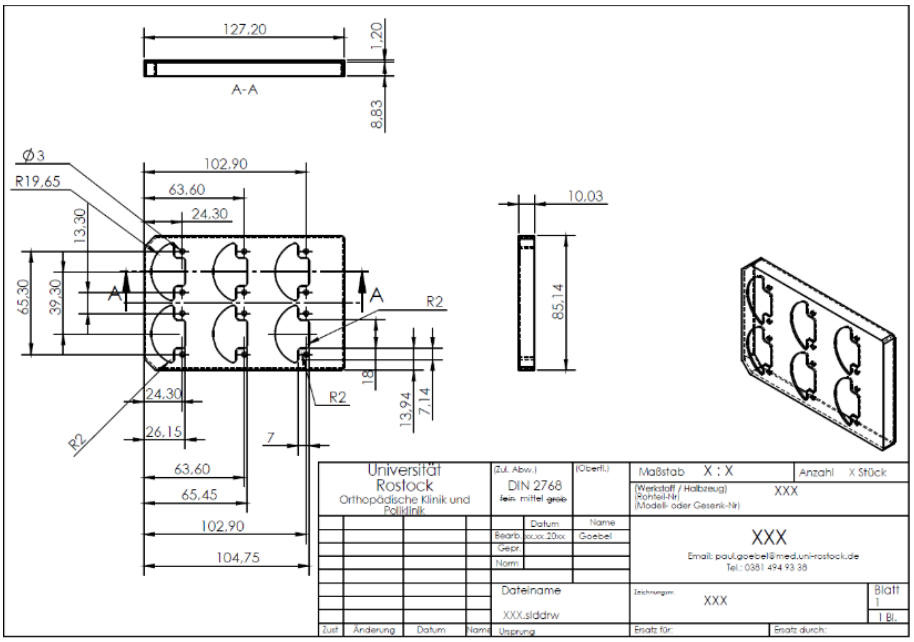

Figure S1. Detailed dimensional illustration of the lid.

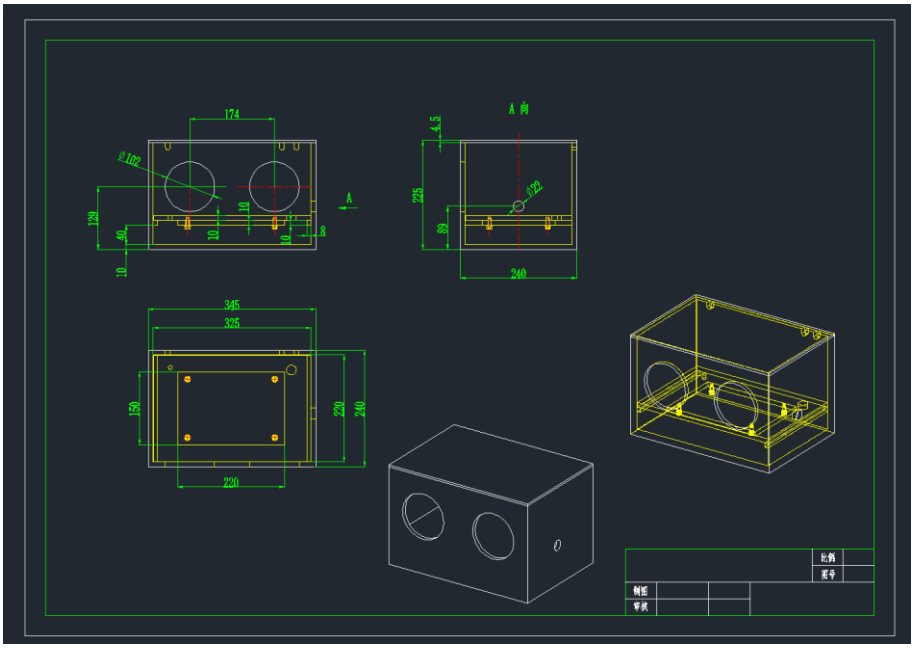

Figure S2. Detailed dimensional illustration of the temperature control box.

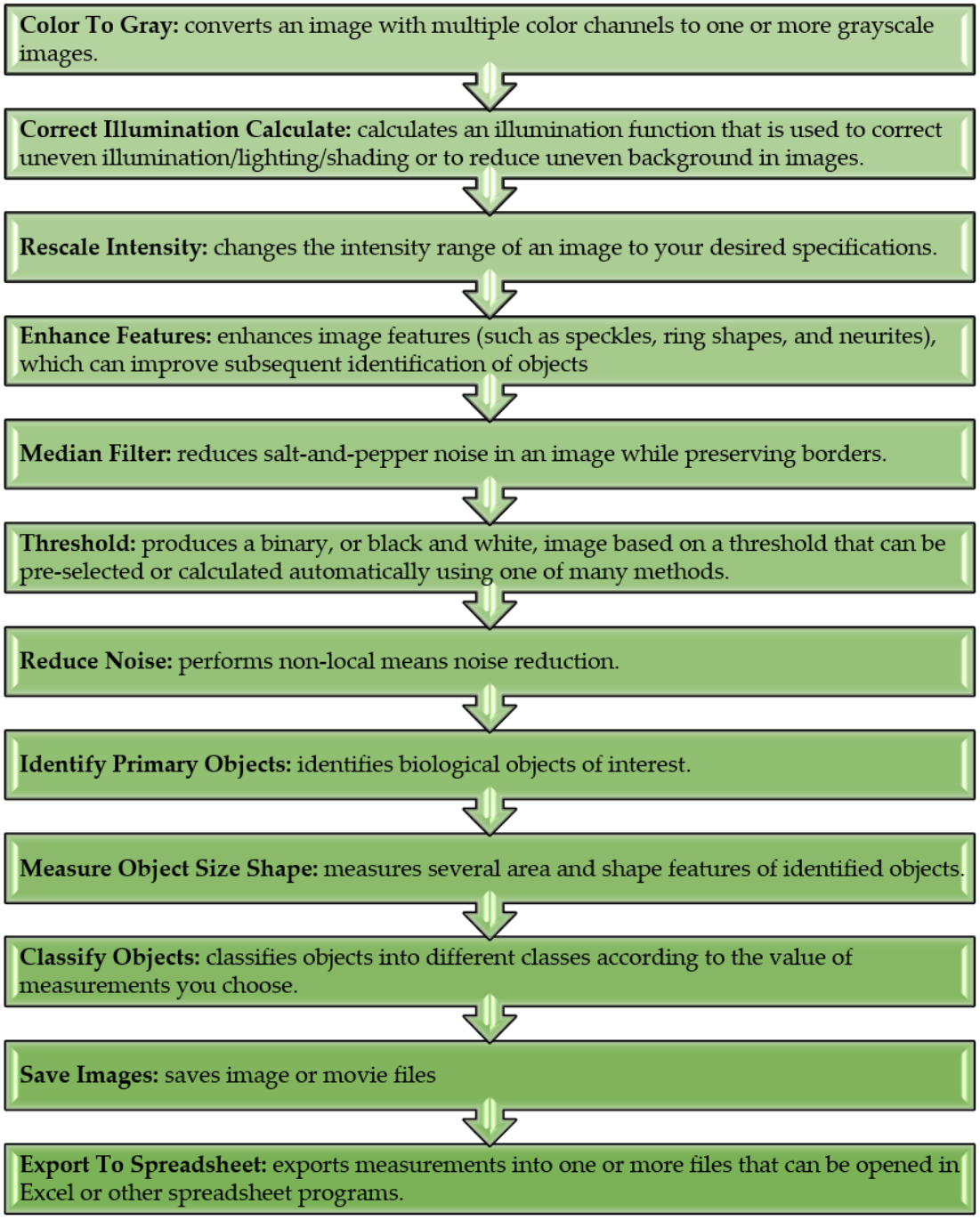

Figure S3. Pipeline for CellProfiler image analysis. This pipeline was constructed using modules provided by CellProfiler, version 4.2.1.

Acknowledgments

Throughout the writing of this dissertation, I have received a great deal of support and assistance. I would first like to express my deepest appreciation to my supervisors, Prof. Dr. Rainer Bader, working with him was a real pleasure as I learned a lot from him. Despite his busy agenda, he was there for me whenever I needed his advice on both research and personal matters. Daniel's supervision was very invaluable to me, and without his guidance and persistent help, this dissertation would not have been possible.

I want to give thanks to my great colleagues at the Biomechanics and Implant Technology Research Laboratory (Department of Orthopaedics) for the wonderful work environment. Special thanks to Dr. Anika Jonitz-Heincke for her guidance, inspiration and professional supports. I would like to extend my acknowledgements to my dear co-workers, Vivica Freiin Grote, M.Sc, Mario Jackszis, Doris Hansmann, Dr. Franziska Sahm ,Dr. Julius Zimmermann and Dr. Janine Waletzko-Hellwig for their support over these years. This project would never have been finished without your generous help.

A very special gratitude goes out to some amazing people without whom I would not be able to complete this work:

My parents, Ying Song and Baohong Song, for believing in me and for their unconditional support and sympathetic ear. They have always been proud of me for my academic achievement and I am now indescribably delighted to make them feel this way again by accomplishing my doctorate degree.

Curriculum Vitae

Name: Zezhong Song
Birth date: 13. 12, 1989
Birth place: Shandong, China

Academic education

09/2007-06/2012
Bachelor of Human Medicine.
Shandong University, Shandong, China
Major: Clinical Medicine

09/ 2012-07/ 2015
Master of Human Medicine
Shandong University, Shandong, China
Major: Orthopedics
Thesis: “Analysis of factors influencing tissue-engineered bone formation by detecting the expression levels of osteogenetic markers”

Pulications

[1] Z. Song, V. Freiin Grote, F. Sahm, J. Zimmermann, C. Lutter, A. Jonitz-Heincke, R. Bader, Exploring the role of directly coupled alternating electric fields on chondrocyte morphology and redifferentiation capacity with a focus on sex differences, Journal of Experimental Orthopaedics12(2) (2025) e70261.

[2] J. Zimmermann, F. Sahm, N. Arbeiter, H. Bathel, Z. Song, R. Bader, A. Jonitz-Heincke, U. van Rienen, Experimental and numerical methods to ensure comprehensible and replicable alternating current electrical stimulation experiments, Bioelectrochemistry 151 (2023) 108395.

[3] C. Wu, Z. Song, H. Liu, J. Pan, H. Jiang, C. Liu, Z. Yan, H. Feng, S. Sun, Inhibition of furin results in increased growth, invasiveness and cytokine production of synoviocytes from patients with rheumatoid arthritis, Joint Bone Spine 84(4) (2017) 433-439.

[4] Song, Z., C. Wu, S. Sun, et al., Quantitative analysis of factors influencing tissue-engineered bone formation by detecting the expression levels of alkaline phosphatase and boneγ-carboxyglutamate protein 2. Experimental and Therapeutic Medicine, 2015, 9(4): p. 1097-1102.

Erklärung

Ich erkläre, dass ich die eingereichte Dissertation selbständig und ohne fremde Hilfe verfasst, andere als die von mir angegebenen Quellen und Hilfsmittel nicht benutzt und die den benutzten Werken wörtlich oder inhaltlich entnommenen Stellen als solche kenntlich gemacht habe.

Rostock, Juni 2024

Zezhong Song

Erklärung

Hiermit erkläre ich, dass ich mich bisher noch keinem Promotionsverfahren unterzogen oder um eine Zulassung zu solchem beworben habe. Die eingereichte Schrift wurde an keiner anderen Hochschule vorgelegt.

Rostock, Juni 2024

Zezhong Song